Nanocarrier Encapsulated Recombinant IκBα as Potential Therapeutic Agent

Thesis submitted by

Subhamoy Banerjee

Roll No. 08610614

For the award of the degree of

Doctor of Philosophy

Department of Biotechnology

Indian Institute of Technology Guwahati

Guwahati 781039, Assam, India

Dedicated to my parents for their love, encouragement and support

DECLARATION

I, hereby, declare that the matter embodied in this thesis entitled "***Nanocarrier Encapsulated Recombinant IκBα as Potential Therapeutic Agent***" is the result of investigations carried out by me under the supervision of Prof. Siddhartha Sankar Ghosh, Department of Biotechnology, Indian Institute of Technology Guwahati, India for the award of degree of Doctor of Philosophy. This work has not been submitted elsewhere for any degree, diploma, associateship or membership etc. of any institute or university to the best of my knowledge and belief.

IIT Guwahati

January, 2014

Subhamoy Banerjee

Roll No.-08610614

INDIAN INSTITUTE OF TECHNOLOGY GUWAHATI
DEPARTMENT OF BIOTECHNOLOGY

CERTIFICATE

This is to certify that the thesis entitled **"*Nanocarrier Encapsulated Recombinant IκBα as Potential Therapeutic Agent*"** being submitted to the **Indian Institute of Technology Guwahati** by **SUBHAMOY BANERJEE** for the award of the degree of **Doctor of Philosophy** in **Biotechnology**, is a bonafide record of research work carried out by him. The contents of this thesis have not been submitted to any other University or Institute for the award of any degree or diploma.

Prof. Siddhartha Sankar Ghosh
(Supervisor)

Acknowledgement

PhD is a long journey in one's academic life. This journey cannot be completed without the help of other people. It gives me a deep sense of satisfaction to have an opportunity to pay my gratitude to all those people who have helped me directly and indirectly during my stay in IIT Guwahati for the degree of Doctor of Philosophy. During this period, they have played a big role in my growth and evolution both on personal as well as professional front. Thank you all.

First of all, I would like to express my deepest gratitude to my reverent thesis supervisor Prof. Siddhartha Sankar Ghosh for channelizing my potential to the desired end. It was under his constant guidance and motivation at every step of my research endeavor that I could take ventures in the field of this research work and successfully complete them. Throughout this period, he always encouraged me to explore new ideas and gave me ample freedom to work. I am deeply indebted to him for his unending support, understanding, care and concern. Thank you very much Sir. I am blessed to have you as my mentor.

Next to him, it was the doctoral committee comprising of Dr. Biplab Bose, Dr. Ajai B Kunnumakkara and Dr. Bhubaneswar Mandal which evaluated my performance from time to time and underscored the gaps where I had to work hard. I sincerely thank them for their critical comments and valuable suggestions which helped me to gain insight in the work I had undertaken. I would also like to thank Prof. Arun Chattopadhyay and my former doctoral committee member Prof. Lingaraj Sahoo. I also owe my gratitude to the Department of Biotechnology, Centre for Nanotechnology, and Central Instrument Facility, IIT Guwahati for providing me all supports and necessary facilities. Here I would like to thank their respective staff members also.

During the PhD tenure, as lab becomes the second home, the lab members play a very important role in successful research. I would like to take this opportunity to acknowledge my lab members-

Amaresh, Nidhi, Chockalingam, Kohila, Archita, Sharmila, Asif, Neha, Upashi, Bandhan and Deepanjali. A very special thanks to them for the wonderful experiences during the PhD especially to Archita, Sharmila, Asif and Neha. Also, I must acknowledge my former lab members Vinod, Pallab, Amit and Shilpa in this opportunity.

I would like to sincerely mention many other friends for sharing memorable moments with me. To name a few- Asim, Supriyo, Pojul, Ashok, Sagarika, Manab, Sudip, Sandipan, Mitun, Seraj, Tushar, Rishi, Sadhu, Rumi, Rama, Palash….

Last but not the least, I would like to acknowledge my parents who have been constantly keeping my spirits high with their deep understanding, concern, patience and support in difficult moments of this five years of my career. I thank them for their endless love, affection and care. I would wish to thank my relatives and some other people (Proma and her family) who are very special to me. Above all, my thanks to Almighty for giving me an opportunity to carry out research in a prestigious institute with His loving manifestations around me.

SUBHAMOY BANERJEE

CONTENTS

Abbreviations

5-FU- 5-Fluorouracil

AO- Acridine orange

Apo-BrDU TUNEL- Apo bromolated deoxyuridine triphosphates terminal deoxy nucleotidyltransferase dUTP nick end label

Bcl-xL- B cell lymphoma extra large

BSA- Bovine serum albumin

C/EBPβ- CCAAT-enhancer-binding proteins β

CD- Circular dichroism

c-IAP2- Cellular inhibitor of apoptosis

c-Myc- Cellular myc

Cox-2- Cyclooxygenase 2

CXCR-4- CXC chemokine receptor-4

DAB- 3, 3'-diaminobenzidine tetrahydrochloride

DEPC- Diethyl pyrocarbonate

DNA- Deoxyribo nucleic acid

dNTPs- Deoxyneucleotide triphosphate

EB- Ethidium bromide

FACS- Fluorescence activated cell sorting

FDA- US food and drug administration

FGF- Fibroblast growth factor

FITC- Fluorescein isothiocyanate

GST- Glutathione S transferase

HIF- Hypoxia inducible factor

HRP- Horse radish peroxidase

HSP-70- Heat shock protein-70

IKK- IκB kinase

IPTG- Isopropyl-1-thio-β-D galactopyranoside

IκBα- Nuclear factor of kappa light polypeptide gene enhancer in B-cells inhibitor, alpha

MALDI-TOF- Matrix assisted laser desorption ionization- time of flight

MCP-1- Monocyte chemotactic protein-1

MDR- Multidrug resistant

MMP-9- Matrix metalloproteinase 9

MTT- 3-(4, 5-dimethylthiazol-2-yl)-2, 5-diphenyltetrazolium bromide

NCs- Nanocarriers

NFκB- Nuclear factor κ light chain enhancer of activated B cells

NPs-Nanoparticles

NSAID- Nonsteroidal anti-inflammatory drugs

PCR- Polymerase chain reaction

PDGF- Platelet derived growth factor

PI- Propidium iodide

PLL- poly L-Lysine

PVA- Poly vinyl alcohol

PVP- Poly vinyl pyrrolidone

RHD- Rel homology domain

RNA- Ribonucleic acid

SDS-PAGE- Sodium dodecyl sulphate-polyacrylamide gel electrophoresis

SR-IκBα- Super repressor IκBα

TGF-β- Tumor growth factor β

TNFα- Tumor Necrosis Factor α

TNFαR- Tumor Necrosis Factor α receptor

VEGF- Vascular endothelial growth factor

X-gal- 5-bromo-4-chloro-3-indolyl-β-D-galactopyranoside

XTT- 2, 3-bis-(2-methoxy-4-nitro-5-sulfophenyl)-2H-tetrazolium-5-carboxanilide

ABSTRACT

Protein therapeutics has been established as a potential weapon in anticancer armamentarium. The limitations of conventional chemo and radiotherapy, including poor response and undesired toxicity, have led researchers to contrive new ways to combat cancer. This quest has generated a whole array of new generation therapy, starting from gene therapy and encompassing protein as well as nanoparticle mediated therapy. Every approach has its own shortcoming, e.g. proteins have a very limited half-life and lose their active conformations if added from outside by conventional routes, thus confining their medical applications. Thus, a new strategy has been devised to deliver the therapeutic protein through nanocarrier based systems to protect its native conformation and burst or sustained release or both as per the requirement. Different types of nanocarriers have been tested as a suitable mode for delivery of therapeutic proteins.

The current thesis explores the potential of recombinant IκBα as a therapeutic protein when delivered via polymeric nanocarriers. This thesis contains an **Introduction** about the importance of nanocarrier mediated recombinant IκBα delivery to cancer cells and the relevance of using recombinant IκBα as a therapeutic molecule. The **Review of Literature** contains the scholastic insights into the role of IκBα and previous work done in the field of therapeutic protein delivery and combination therapy, primarily focusing on 5-fluorouracil (5-FU) and curcumin. In **Materials and Methods** section, the chemicals, enzymes, bacterial strains, cancer cell lines, primers, antibodies etc. and the detailed protocol for each experiment have been elaborated. The **Results and Discussions** section starts with cloning of IκBα using cDNA obtained from mammalian cells, followed by purification as a bacterially expressed GST tagged recombinant protein and functional delivery via biodegradable polymeric hydrogel nanocarriers to the cervical carcinoma (HeLa) and glioblastoma (U87MG) cells. Then based on the result, the efficacy of recombinant IκBα has further been augmented by using it with poly L Lysine coated curcumin nanoparticles as a protein curcumin nanoformulation. Next, to understand molecular effects, IκBα transfected stable glioblastoma (U87-IκBα) cell line was established and its response to common chemotherapeutic agent 5-Fluorouracil (5-FU) was enumerated through cell viability assay, cell cycle and doubling time analysis by flow cytometry and real time PCR for the expression of cyclins. Finally, in the **Conclusions**

and Future aspects section, the anticancer effects of recombinant IκBα delivered via nanocarriers and its potential application as a therapeutic molecule have been discussed.

1

INTRODUCTION

INTRODUCTION 1

The clinical trial of aminopterin, a folate antagonist for treating lymphoblastic leukemia in late 1947 by Sydney Farber was the harbinger of modern day chemotherapeutics. The initial success of various types of chemical agents in cancer treatment raised the hope for eradicating cancer. But with the severe side effects and recurrence of cancer, this hope of complete eradication was soon faded away. Since then, the war against cancer by mankind is continuing with designing of varieties of strategies. The intensive research on cancer for many years has yielded ample information about the nature of cancer in terms of genetics, molecular biology and immunology. This information has shed light on the genetic instability, drug resistance and immunosuppressive nature of cancer. The strategy to fight cancer has been devised accordingly ranging from small molecule drugs to recombinant antibodies. Beside the recombinant antibody based therapy, of late the recombinant protein therapeutics is gaining attention. The endless potential of naturally occurring proteins as therapeutic agent is attracting both scientific community and industries. Using the recombinant cytokines like interferons (IFN-γ, IFN-α2), granulocyte macrophage colony stimulating factor (G-MCSF), interleukin-2 (IL-2) etc. are already in market, and many are in clinical trials. But one hindering factor of cytokines as therapeutic agent is their ambivalent nature. Many times, cytokines act as a double edged sword in tumor microenvironment, thus leaving lot of questions about its safe application to the patients. These promise and limitations together open up another avenue in protein therapeutics. The inhibitors of key regulatory pathways of oncogenesis may be attractive agents for cancer therapeutics.

The NFκB (nuclear factor κ light chain enhancer of activated B cells) an inducible transcription factor, which acts in response to a large number of external stimuli, is one such key regulatory protein responsible for a variety of oncogenic signatures e.g. - inflammation, proliferation, angiogenesis and drug resistance. Its cellular inhibitor IκBα blocks its translocation from cytoplasm to nucleus and eventually induces cell cycle arrest and apoptosis. Thus, IκBα may hold the prospective to become a candidate in the regiment of therapeutic proteins to fight cancer. In this present study, the potential of IκBα as a therapeutic agent has been studied in two ways- i) as recombinant GST tagged

IκBα produced by *Escherichia coli* BL21 strain and ii) over expressing it in human glioblastoma cell line (U87MG) and sensitizing the recombinant cells with chemotherapeutic agents (5-Fluorouracil and curcumin) used in this study.

As the protein is a macromolecule whose function largely depends on its structural integrity, functional delivery of cytoplasmic proteins into the cell is also a challenging domain. To address this issue, hydrogel nanoparticles have been found to play an effective role to deliver proteins in its functional form. In the present study, poly vinyl pyrrolidone (PVP) and poly vinyl alcohol (PVA) based nontoxic hydrogel was synthesized by oil based green synthesis method. The purified recombinant GST tagged IκBα was encapsulated in the hydrogel. The protein encapsulated hydrogel nanocarrier was characterized via transmission electron microscopy (TEM), field emission scanning electron microscopy (FESEM), dynamic light scattering (DLS) and zeta potential, Fourier transformed Infrared spectroscopy (FT-IR) etc. to study its particle nature, hydrodynamic diameter, charge and the presence of protein in this module. The release of GST tagged IκBα was recorded at two different pH. Then it was delivered to human cervical carcinoma (HeLa) and glioblastoma (U87MG) cell lines to examine its efficacy. Cytotoxicity study, flowcytometry fluorescence microscopy and western blotting were used to study the effect of functional delivery of recombinant GST tagged IκBα. Further, IκBα encapsulated hydrogel was tested in combination with another common anti-cancer drug 5-Fluorouracil (5-FU) on U87MG cell line and its higher efficacy was checked by cytotoxicity assay.

Based on the result of hydrogel mediated recombinant GST tagged IκBα on the cells, the recombinant IκBα based combination therapy was further augmented by using another common bioactive molecule, curcumin. Curcumin is also a natural NFκB inhibitor. In this study, PVP stabilized water soluble curcumin nanoparticle was synthesized and recombinant GST tagged IκBα was attached with it via positively charged homopolymer poly L-Lysine in physiological pH. The synthesized nanoparticles were characterized by fluorescence and UV-Vis spectrophotometer, TEM, DLS and zeta potential to enumerate its fluorescence property, particle nature, hydrodynamic diameter and net charge upon it. Then the combination module was administered on HeLa and U87MG cells. The cells

were found to be more sensitized. Thus the role of IκBα as a therapeutic protein was further substantiated.

The IκBα cloned in pCINeo plasmid (mammalian expression vector) was transfected in U87MG cells and stable transfected cell line was established by selection with G418 sulphate. Thus, the expression of IκBα was made homogenous across the cell line. The cells were treated with 5-FU and BSA conjugated curcumin NPs. The combined effects of BSA loaded curcumin NPs and 5-FU in presence of IκBα in sensitization of U87MG is the goal of this section. Transfected U87MG was found to be more sensitive towards 5-FU and curcumin NPs as compared to normal U87MG by cytotoxicity assay. Further its role in cell cycle was elucidated by flow cytometry and real time PCR. In flowcytometry, DNA binding dye propidium iodide (PI) was used to analyze cell cycle. Expression of different cyclin genes were checked by Realtime PCR. Also, cell division rate was measured by CFSE dye based flowcytometry. Finally, cells were treated with different combinations of 5-FU and curcumin NPs to establish combination effect.

The thesis outline is as follows-

Part 1→ Isolation of RNA and synthesis of c-DNA from mammalian cells

↓

PCR amplification of IκBα with gene specific primer and cloning of IκBα into pGEM T Easy vector

↓

Sub-cloning of IκBα into pGEX4T2 vector and traformation into *E.coli* cells

↓

Expression and purification of GST tagged recombinant IκBα by affinity chromatography

↓

Characterization of recombinant IκBα protein by CD, MALDI-TOF, Western blotting

↓

Synthesis of PVA/PVP hydrogel and encapsulation of recombinant IκBα

↓

Characterization of hydrogels by TEM, FESEM, DLS, FT-IR etc.

↓

Hydrogel mediated functional delivery of recombinant IκBα to the cancer cells

↓

Anticancer effect checked by cell viability assay, fluorescence microscopy, flowcytometry etc.

Part 2→ Synthesis of PVP stabilized curcumin nanoparticles

↓

Loading of recombinant IκBα onto curcumin nanoparticles via PLL

↓

Characterization of hydrogels by fluorescence and UV-Vis spectroscopy, TEM, FESEM, DLS, zeta potential etc.

↓

Delivery of recombinant IκBα loaded curcumin NPs to the cancer cells

↓

Anticancer effect studied by cell viability assay, fluorescence microscopy, different flowcytometry assay (PI based cell cycle analysis, ROS generation, apoptosis study) and gene expression analysis by semi-quantitative RT PCR.

Part 3→ Cloning of IκBα into pCINeo mammalian expression vector

↓

Transfection of pCINeo-IκBα into U87MG and establishment of IκBα over-expressing stable cell line by G418 selection

↓

Over-expression of IκBα measured by semi-quantitative PCR, real time PCR, Western blotting

↓

Study of the effect of 5-FU on U87MG and U87-IκBα by cell viability assay, flow cytometry (PI based cell cycle assay and CFSE based cell proliferation assay)

↓

Study of the effect of BSA loaded curcumin NPs on U87MG and U87-IκBα cells by cell viability assay, fluorescence microscopy, flowcytometry ((PI based cell cycle analysis, ROS generation, apoptosis study by FITC-Annexin V and PI double staining and Caspase-3 assay)

↓

Study of the combined effect of BSA laoded curcumin NPs and 5-FU on U87MG and U87-IκBα cells

Thus, the thesis entitled "Nanocarrier encapsulated recombinant IκBα as potential therapeutic agent" is organized in the following manner-

Section 1. **Introduction**

Section 2. **Review of literature**

Section 3. **Materials and Methods**

Section 4. **Results and Discussions**

The section 4 is further subdivided into 3 parts-

Part 1. *Functional delivery of hydrogel nanocarriers encapsulated recombinant IκBα to the cancer cells.*

Part 2. *Effect of IκBα loaded curcumin nanoparticles on cancer cells*.

Part 3. *Effect of 5-Fluorouracil and curcumin nanoparticles on IκBα over expressing glioblastoma.*

Section 5. **Conclusions and future aspects**

2

REVIEW OF LITERATURE

IκBα is a cytoplasmic protein, which binds to p50/p65 heterodimer of NFκB system (Baeuerle and Baltimore, 1988; Malek *et al*, 2003) in resting cells. It is a family member of NFκB inhibitor protein which consists of five archetypal proteins viz. IκBα, IκBβ, IκBε, p100 and p105 (Hatada et al, 1992). Also, two atypical members are Bcl-3 (Bours *et al*, 1990; Ohno *et al*, 1990) and IκBζ (Trinh *et al*, 2008), which are induced by external stimuli. In common, their function is to interact with dimers of NFκB system and inhibit their nuclear translocation.

1. NFκB transcription factor family- The cells have to interact with varieties of external stimuli throughout their lifespan. The inducible transcription factors are the key to determine the cellular behavior towards the external stimuli. One such important inducible transcriptional regulator is nuclear factor-κB. It was first discovered in mid of 1980s, in B lymphocytes (Sen and Baltimore, 1986; Singh *et al*, 1986). Later, it was found that this transcription factor is almost ubiquitous. This transcription factor family consists of five subunits- p65 (also called RelA), RelB, c-Rel, p105/p50 and p100/p52 (Hayden and Ghosh, 2004; Hayden and Ghosh 2008). They share a conserved amino terminal rel homology domain (RHD, 300 amino acids long) in common (Baldwin, 1996; Ghosh *et al*, 1998). This site contains major functional sites e.g. - dimerization domain (DD), DNA binding domain (DBD), interaction with its inhibitor IκBs and nuclear translocation signals (Grumont and Gerondakis, 1989; Kieran *et al*, 1990; Rushlow and Warrior, 1992; Leeman *et al*, 2008). The diagrammatic representation of the NFκB subunits are shown in figure 1.

The five subunits can make 15 possible combinations of homo or hetero dimers, although, all possible combinations have not been found yet. It is found that p50/p65 heterodimer is most prevalent among all the cell types. The other dimeric complexes till date documented are p65/p65, p65/c-Rel, p65/p52, c-Rel/c-Rel, p50/c-Rel, p52/c-Rel, RelB/p50, p50/p50 and RelB/p52 (Hayden and Ghosh, 2004; Hoffman and Baltimore, 2006), although, many of them are limited to specific cell types (Sen, 2006; Ouazz *et al*, 2002; Gerondakis *et al*, 2006; Gerondakis and Siebenlist, 2010). The crystal structure of DNA bound p50 homo dimer and p50/p65 hetero dimer revealed specific DNA sequence (5'-GGGPuNNPyPyCC-

3') present in the regulatory regions of NFκB target genes (Ghosh *et al*, 1995; Muller *et al*, 1995; Chen *et al*, 1998; Sengchanthalangsy *et al*, 1999) and the interaction is mediated by amino terminal part of RHD.

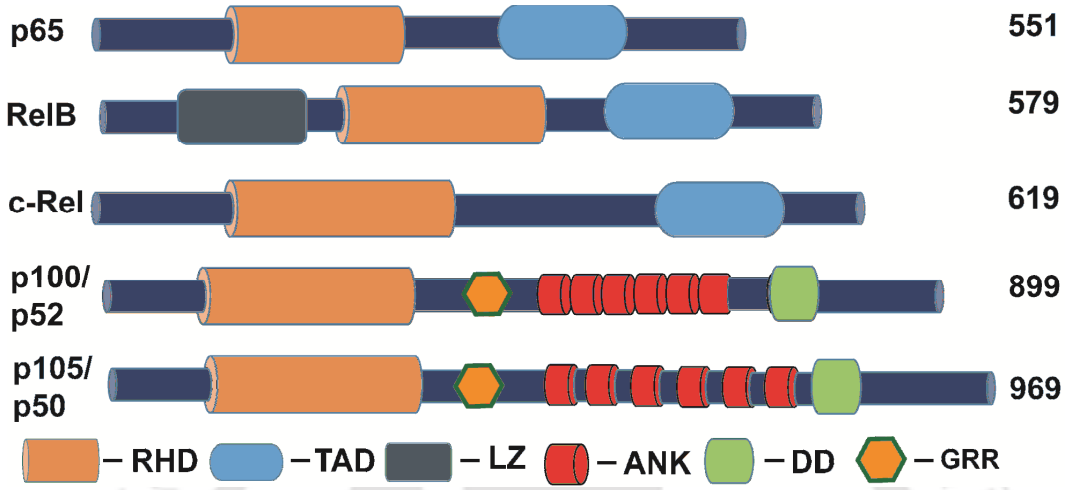

Figure 1. Different subunits of NFκB transcription factor. RHD-Rel Homology Domain, TAD-Trans Activation Domain, LZ- Leucine Zipper Domain, ANK-Ankyrine repeat domain, DD-Death Domain, GRR-Glycine rich region. The numbers represent the length of each subunit in terms of amino acids.

Another family member of NF-κB is their inhibitors which localize them in the cytoplasm in resting cells (Baeuerle and Baltimore, 1988; Nolan *et al*, 1991). As mentioned before, there are six family members of IκB proteins, which tightly regulate the activity of NFκB. The IκB proteins share ankyrin repeats in common; IκBα and IκBβ contains C terminal PEST sequence, which is rich in proline (P), glutamic acid (E), serine (S) and threonine (T) (Chen *et al*, 1995; Traenckner *et al*, 1995). The PEST region in IκBα also requires the disruption of DNA: NFκB complexes (Ernst *et al*, 1995; Rottjakob *et al*, 1996). IκBα also contains a functional nuclear export sequence, which plays crucial role in shuttling the p50/p65 heterodimer out of nucleus (Huang *et al*, 2000; Luque and Gélinas, 1998; Tam *et al*, 2001; Arenzana-Seisdedos *et al*, 1997). Diagrammatic representation of the IκB proteins are shown in figure 2.

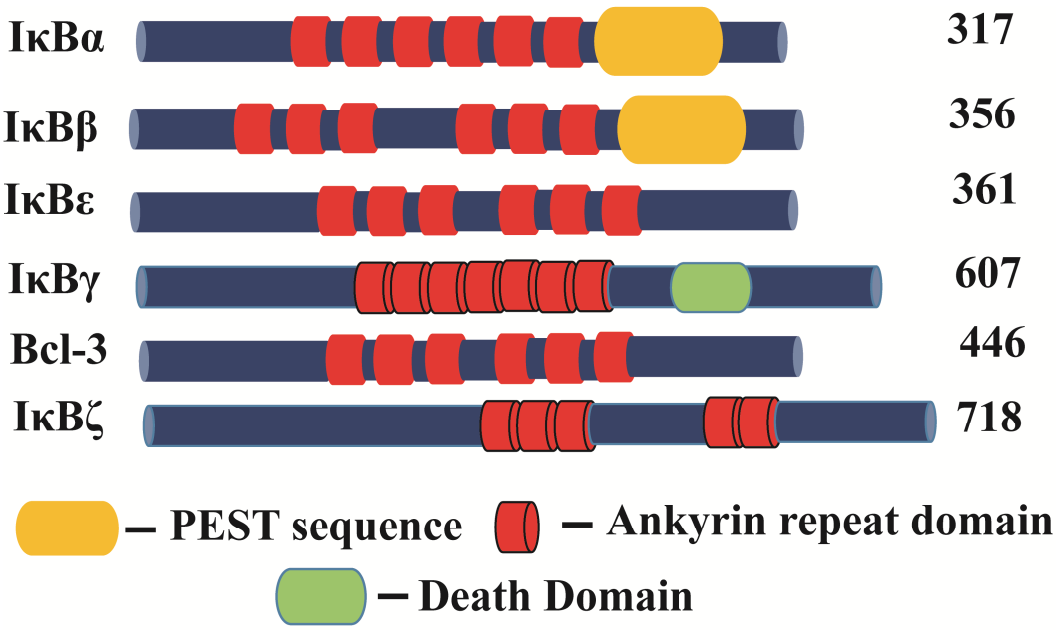

Figure 2. Different subunits of IκB proteins and their domain organization. The numbers indicate the length of each subunit in terms of amino acids.

NFκB gets induced by a verity of external stimuli which ranges from bacterial and virus infection to various cytokines (e.g. - IL-1, IL-2, TNF-α etc.) and drugs (e.g. - Donorubicin, Tamoxifen, Cisplatin etc.) (Aggarwal *et al*, 2006; Lawrence, 2009; Baldwin, 2001). The NFκB activation is generally associated with the IκB kinase (IKK) mediated phosphorylation of IκB proteins (Chen *et al*, 1995; Chen *et al*, 1995; Karin and Ben-Neriah, 2000). Upon activation, IKKβ phosphorylates serine residue of IκBα at 32 and 36 position followed by ubiquitination by E3 ubiquitine ligase (Traenckner *et al*, 1995; Scherer *et al*, 1995). Then the free p50/p65 heterodimer enters the nucleus and induces the pro-inflammatory and pro-survival genes (Figure 3).

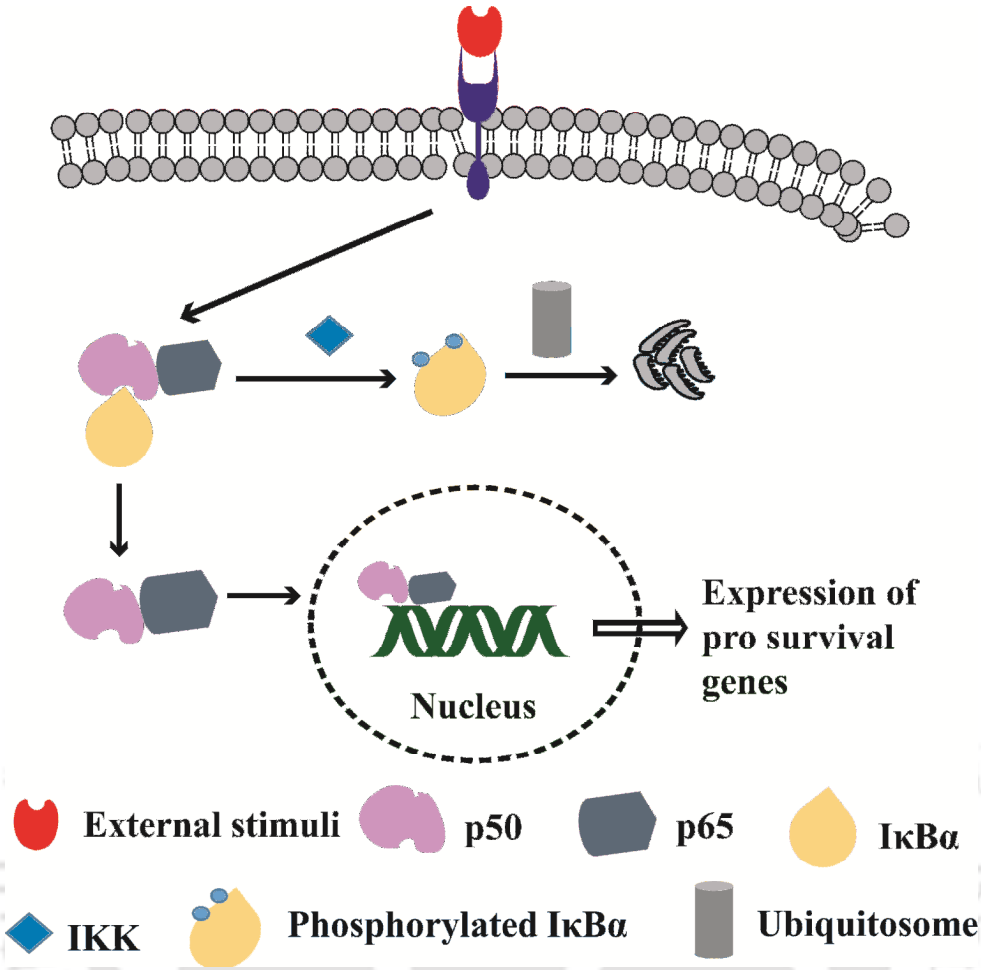

Figure 3. Activation of NFκB and regulation of pro survival genes.

Many genes are target of NFκB transcription factor. With the intense research, the list is growing almost every day. Interestingly, many of such genes have been found to be related to different kind of diseases (Baldwin, 2001; Yamamoto and Gaynor, 2001; Kumar *et al*, 2004; Dolcet *et al*, 2005). Thus, it has been evident that higher expression of NFκB plays an important role in diseases and their drug resistivity (Kumar *et al*, 2004; Lin *et al*, 2004; Mitsiades *et al*, 2002; Bentires-Alj *et al*, 2003). The constitutive expression of NFκB (in cancer) causes persistent inflammation which ultimately leads to the formation of tumor micro environment and helps to aggravate cancer (Hideshima *et al*, 2001). On the other hand, TNF-α induced activation of NFκB plays a critical role in chronic inflammation in rheumatoid arthritis (RA) (Foxwell *et al*, 1998; Tak and Firestein, 2001; Simmonds and Foxwell, 2008). The administration of antibodies against TNF-α or truncated TNF-αR

shows improvement in condition of RA patient. The following table mentions the list of few disease related genes regulated by NFκB (Baldwin, 2001).

Table 1-

Disease	**Gene**
Cancer	Cyclin D1, c-Myc, Bcl-xL, c-IAP2, MMP-9
Arthritis	MMP-9
Colorectal cancer	Cox-2
Asthma	Interleukin-8
Atherosclerosis	MCP-1

Other than the diseases mentioned in table 1, there are numerous other diseases where NFκB plays a pivotal role and induces many genes. Thus, NFκB holds promises as therapeutic target. Several approaches have been considered-

1.1. *Functional repression of NFκB by super repressor IκBα*- In stimulated cells, IκBα gets phosphorylated at serine 32 and serine 36 position, and subjected to 26S proteasome mediated ubiquitosome mediated degradation. Mutations at these two serine residues do not phosphorylated by IKK, thus become ubiquitination resistance. Several reports suggested that this super repressor form of IκBα (SR IκBα) sensitizes the cells towards apoptosis (Muenchen *et al*, 2000; Gilmore *et al*, 2002; Magné *et al*, 2006). Generally, Jurkat cells are found to be resistant to apoptosis while treated with TNF-α as it induces NFκB pathway (Wang *et al*, 1996; Van Antwerp, 1996). But the presence of super repressor (SR) IκBα (mutated at serine 32 and 36 position), inhibits NFκB pathway, and cells undergo apoptosis. SR IκBα expressing fibrosarcoma cells are found to be susceptible towards ionizing radiation and daunorubicin (chemotherapeutic drug), which normally induces NFκB pathway, thus making the cells resistant toward it (Wang *et al*, 1996). So, SR IκBα may play an important role in regulation of constitutive expression of NFκB in aberrant cells.

1.2 *NSAID mediated inhibition of NFκB*- Anti-inflammatory drugs aspirin and sodium salicylate inhibit NFκB and thus reduce the degradation of IκB (Pierce *et al*, 1996; Yin *et al*, 1998). Therefore, NFκB resides in cytoplasm. Recent study showed that those drugs prevent the ATP binding to IKKβ, thus phosphorylation of IκBα is significantly decreased, so does its proteasome mediated degradation.

1.3 *Blocking NFκB pathway by immunosuppressive agents*- Immunosuppressive agents like glucocorticoid and cyclosporine A (CsA) (Meyer *et al*, 1997) are found to inhibit NFκB activity. Generally, CsA is used to avoid the problem of transplant rejection in organ transplanted patients. In lymphoid cells, CsA binds with calcineurin, thus inhibiting the activity of NFκB. But in nonlymphoid cells, CsA inhibits NFκB via induction of C/EBP family of protein, especially through C/EBPβ and C/EBP homologous protein (CHOP) (Marienfeld *et al*, 1997). Thus the conventional immunosuppressive agents may be used as anti-inflammatory agents as well.

1.4 *Natural compounds mediated inhibition of NFκB*- Several plant derived natural compounds like flavonoids (Nam, 2006) and curcumin (Singh and Aggarwal, 1995) are found to have anti-inflammatory and anti-cancer activities. Several reports suggest that these activities are mostly due to their ability to inhibit NFκB pathway.

1.5 *Inhibition of 26S proteasome function*- Inhibition of 26S proteasome is done varieties of protein aldehydes which inhibit the protease activity of the proteasome (e.g. - bortezomib) (Adams *et al*, 1999; Milo *et al*, 2011). Another class of non-peptide inhibitor is lactacystin which is isolated from *Sterptomyces* genus of bacteria. These proteasome inhibitors are commonly used in laboratory to study the effect of inhibition of NFκB activity on other cellular events e.g. - inflammation, apoptosis, proliferation etc. Few of these inhibitors have been studied upon human e.g. – bortezomib, salinosporamide A, carfilzomib etc. (Bilotti, 2013) for the treatment of refractory multiple myeloma.

One major concern of inhibiting NFκB system is its role in different cellular activities. There are several reports which suggest the role of NFκB in regulation of cell death, osteoclast formation. Also, NFκB is responsible in immune response as many cytokines and chemokines related genes are regulated by NFκB. Thus inhibition of NFκB may cause detrimental effects also, e.g. – as proteasome function is necessary for many important regulatory mechanisms, thus inhibition of 26S proteasome may cause severe side effects.

The balance of NFκB: IκBα inside the cell is crucial in maintaining normal cellular function. It has been found that microinjection of GST tagged IκBα into the cells at a very high concentration (as high as 1 μg/μL) causes cell death (Wu *et al*, 1996; Bellas *et al*, 1997). Thus, Instead of inhibiting NFκB with its degradation resistant super repressor form, the usage of native form of IκBα may be an attractive option as over expression of IκBα was found to block G1 phase in HeLa cells (Kaltschmidt *et al*, 1999). Also, it is found to initiate apoptosis in Reed-Sternberg cells (Emmerich *et al*, 1999). Thus, native IκBα or recombinant form of IκBα was found to play an active role in chemo-sensitization of cancer cells.

2. Cancer therapy- A vareity of techniques has been employed to treat cancer cells. Majorly, this treatment regime is subdivided into surgery, radio- and chemo-sensitization of cancer cells. Chemotherapeutic drugs play a major role in fighting with cancer. These chemotherapeutic drugs can be subdivided into several groups-

2.1 *Alkylating agent*- This is the first chemotherapeutic agent used to treat cancer (e.g. – Aminopterin). They kill cancer cells by damaging DNA strand (Hurley, 2002; Helleday *et al*, 2008). They also have the same effect on normal cells. Many types of cancer e.g. – lymphoma, leukemia, multiple myeloma etc. are treated with alkylating agents (Dolan *et al*, 1991). As they are not cancer cell specific, they have major side effects (Reimer *et al*, 1977). Nitrogen mustards, nitroso-urea etc. are potent DNA damaging alkylating agents.

2.2 *Antimetabolite*- this type of drugs interfere with nucleic acid polymerization. They act as cell cycle specific manner by disrupting the G1 phase (Li *et al*, 2004). They are used to treat verities of cancer including ovarian cancer, breast cancer, leukemia etc. 5-Fluorouracil, hydroxyurea, methotrexate etc. are the examples of antimetabolites (Grem, 2000; Colleoni *et al*, 2010).

2.3 *Antitumor antibiotics*- Daunorubicin, doxorubicin etc. are the examples of anthraxcyclin kind of antitumor antibiotics (Scott and Williams, 2002). They inhibit topoisomerase II activity, thus blocking the process of replication (Galm *et al*, 2005).

2.4 *Mitotic inhibitors*- as the name suggests, this kind of drugs majorly affects the cells in M phase. They affect the cells across the phases of cell cycle. Vinca alkaloids (Vinblastine, vincristine etc.), taxols etc. inhibit the replication machinery of cells (Creasey and Markiw, 1964; Owellen *et al*, 1972).

Although the mode of actions of these types of drugs are different, but they have one thing in common. All the drugs have major and broad spectrum side effects including heart failure, liver damage, skin problems etc.

Among these drugs, 5-fluorouracil (5-FU), an antimetabolite drug is used to treat breast and ovarian cancers and solid tumors (Longley *et al*, 2000). It is anabolized in live cells into 5- fluorodeoxyuridine monophosphate (5-FdUMP) and 5-fluorouracil tri phosphate (5-FUTP). 5-FdUMP inhibits the catalytic activity of thymidylate synthase, thus disrupting DNA replication. 5-UTP is incorporated into RNA, thus impairing its function (Parker and Cheng, 1990; Longley *et al*, 2000). The problem of toxicity and undesired side effects are also present in 5-FU (Wigmore *et al*, 2010). But, another drug, 5-fluorocytosine (5-FC) is nontoxic to mammalian cells. It is converted to 5-FU by a bacterial enzyme cytosine deaminase (CD). Another bacterial enzyme, uracil phophoribosyl transferase (UPRT) further converts 5-FU into 5-FUMP (Kanai *et al*, 1998; Kawamura *et al*, 2000), which finally gets converted into 5-FUTP and inhibits RNA functions. Thus, the concept of gene dependent enzyme prodrug therapy (GDEPT), commonly known as 'suicide gene therapy' has come into therapeutic approaches.

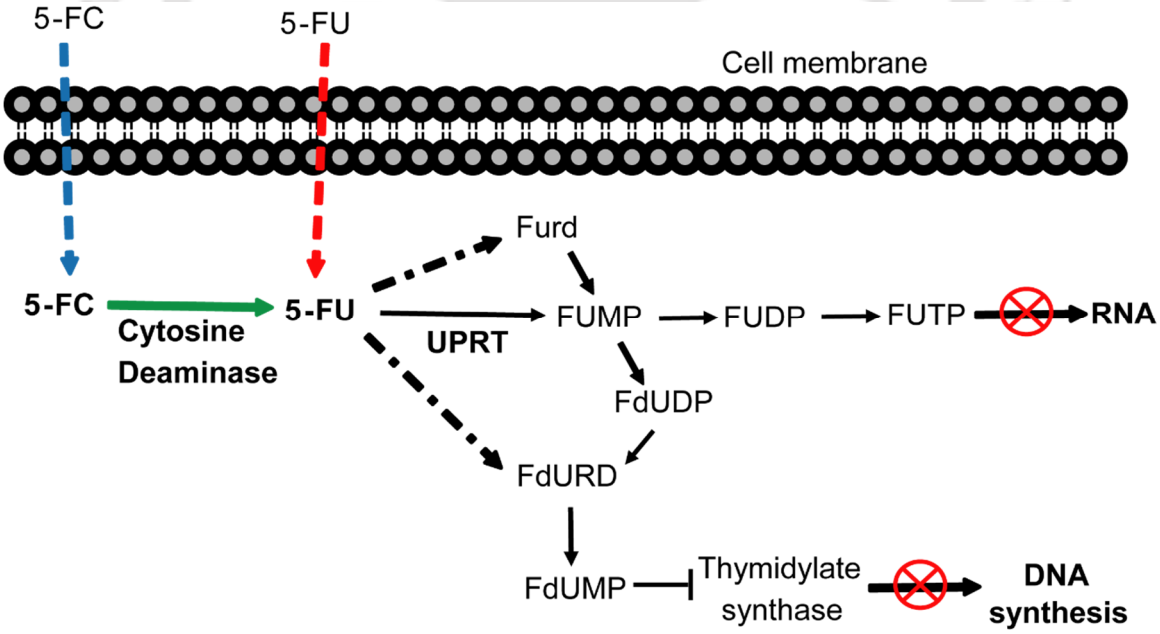

Figure 4. Schematic of 'suicide gene therapy' and mode of action of 5-FU inside the cells. Abbreviations are mentioned in text.

However, because of limitations of efficient gene therapy methods, this approach has become restricted to laboratories. Another way of reducing the toxicity of chemotherapeutic agents is lowering their effective concentration. Thus, combination therapy comes into the scene, where, not only a lower dosage of drugs are used, but also, cancer cells can be encountered with multiple approaches. Combination therapy may be of different varieties, in combination of chemotherapeutic drugs, radiosensitization followed by chemotherapy, conventional chemotherapeutic drugs (e.g. – 5-FU) with other bioactive molecules (e.g. – curcumin) (Koo *et al*, 2004), nanoparticles (e.g. – silver NPs) (Gopinath *et al*, 2008), monoclonal antibodies (e.g. - cetuximab) (Folprecht *et al*, 2010) or cytokines (e.g. – Interferon-γ, interleukin-2, interferon-α) (Atzpodien *et al*, 1994; Ota *et al*, 2005).

Proteins or peptides are being used as biotherapeutics agent for different types of diseases (e.g. – rheumatoid arthritis, diabetes, atherosclerosis, cancer etc.) (Schrama *et al*, 2006; Bertz *et al*, 2012) for last three decades. Proteins have many advantages over their synthetic small molecule counterparts. The substrate specificity, catalysis of biochemical reactions, usage as a scaffold etc. can be best obtained from protein molecules (Vermonden *et al*, 2012). Thus, as a therapeutic agent, the efficacy of protein has been proven in many instances, but delivery of protein in their active form is a big challenge for the researchers and pharmaceutical industries. Different approaches have been tested for functional delivery of protein. One among them is using hydrogel nanoparticles to deliver proteins inside the cells.

3. Hydrogels for protein delivery- Hydrogels are polymeric meshwork of hydrophilic polymers, showing a gel like feature. Hydrogels contain large amount of water (>50%), but themselves become insoluble in water, so they are commonly known as hydrogels (Hamidi *et al*, 2008). Delivery of protein in native form is crucial for its function. The large amount of water in hydrogel provides an ideal platform for protein to maintain its native form (Bertz *et al*, 2012; Vermonden *et al*, 2012). Also, mild synthesis process and soft meshwork provides ideal platform for immobilized protein to contain their 3-D structure. Different types of hydrogels have been developed and applied in biomedical and pharmaceutical research ranging from drug delivery (Vinogradov *et al*, 2002) to tissue engineering (Nguyen and West, 2002; Patel *et al*, 2005) and preparation of contact lenses

(Hyon *et al*, 1994). A variety of hydrogels has been used to deliver the following pharmaceutically important proteins- erythropoietin (Kobayashi *et al*, 2008), CD-40L (Yoo *et al*, 2008), interleukins (Nakase *et al*, 2002), interferons (Kamei *et al*, 2009), GMCSF (Seo *et al*, 2009), TGF-β1 (Jaklenec *et al*, 2008), VEGF (Seliktar *et al*, 2004) etc. Different types of polymers are used for the formation of hydrogel (polyethylene glycol, polyvinyl pyrrolidone, polyvinyl alcohol, poly L-Lactide etc.) and they are often made biodegradable as per the requirement. In order to prevent their dissolution into the water, the constituent polymers are required to be cross-linked physically or chemically.

3.1 *Physical cross linking*- Physical cross linking of hydrogels is achieved by using different non covalent interactions such as hydrogen bonding, ionic interaction, hydrophobic interaction etc. There are various physical cross linking methods used for the formation of hydrogels (Bertz *et al*, 2012; Vermonden *et al*, 2012). Choice of the polymers play a crucial role in synthesis of hydrogels. Different types of physical crosslinking methods are employed for the synthesis of hydrogels such as a) stereocomplexation (co-crystallization of enantiomers) (Ikada *et al*, 1987; Van Tomme *et al*, 2008), b) formation of inclusion complexes (oligosaccharide functionalized large and complementary small molecules interact to form hydrogel by *in situ* gelling method) (Van de Manakker *et al*, 2008).

3.2 *Chemical cross linking*- Formation of covalent bonds between the polymeric subunits by chemical reaction is the key to chemical cross linking method. Generally chemically cross linked hydrogels show higher mechanical strength. Besides the conventional chemical coupling (e.g. – photopolymerisation, Michael addition etc.) reactions, there are other techniques for obtaining chemically cross linked hydrogels e.g. – click chemistry (azo-alkaline cyclo-addition) (Malkoch *et al*, 2006; Van Dijk *et al*, 2009), native chemical ligation (thioester linked coupling) (Hu *et al*, 2009) etc. for *in situ* gelling method.

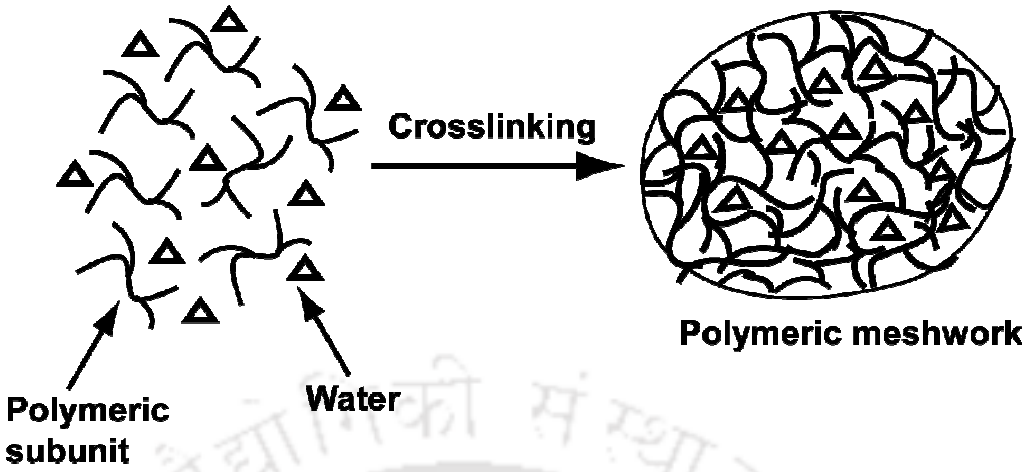

Figure 5. Synthesis of hydrogel by crosslinking method.

There are different types of polymers which are used for the synthesis of hydrogels. Broadly they are subdivided into two types-A) natural polymers, B) synthetic polymers.

3.A *Natural polymers*- Many natural polymeric materials have been used for hydrogel synthesis. Natural polymers have certain advantages in biomedical application over the synthetic polymers e.g. – biocompatibility, biodegradabality etc. Thus, special attention is given to natural polymers especially when the hydrogels have to be delivered inside the body.

3.A.1 Protein based polymers- Collagen, gelatin, fibrin etc. are the protein molecules used to synthesize the hydrogels for delivery of growth factor and wound healing. As these proteins are found in connective tissues, they have higher tensile strength and are favored for hydrogel formation. But their crosslinking is obtained by glutaraldehyde or carbodiimide (De Paoli Lacerda *et al*, 2005) which are toxic to the cells, thus limiting their application.

3.A.2 Polysaccharide based hydrogels- For protein delivery purpose, chitosan, alginate, hyaluronic acid and dextran are the choice of materials which come under the category of polysaccharide based hydrogels (Ohya *et al*, 1993; George and Abraham, 2006; Coviello *et al*, 2007). As they are hydrophilic, they are suitable for hydrogel capable of protein delivery. Low immunogenicity, low cost and simple gelation process with divalent cation (e.g. – Ca^{+2}) makes alginate an attractive agent for hydrogels. Alginate hydrogels can be prepared in an injectable form and can be used for delivery of insulin and many growth

factors (Lee *et al*, 2000; Coviello *et al*, 2006). Chitosan is another natural polysaccharide, which is only soluble at low pH. Many derivatives of chitosan are used to synthesize hydrogels. Chitosan hydrogels are prepared by physical and chemical crosslinking method even by photo-crosslinking by UV irradiation (Zhou *et al*, 2011). Different proteins of therapeutic importance including insulin, bFGF etc. have been successfully tested for sustained *in vivo* protein release in mouse model.

3.B *Synthetic polymers*- Synthetic polymers are chemically synthesized polymers used for different industrial purpose. These polymers are synthesized by organic reactions with higher durability and physical strength. Some of these polymers are used for hydrogel synthesis e.g. – polyvinyl alcohol (PVA), polyvinyl pyrrolidone (PVP), poly-(N isopropyl acrylamide) (PNIPAAm) etc (Langer and Peppas, 2003; Vermonden *et al*, 2012). The advantage of synthetic polymers over the natural polymer is that a variety of functional groups may be attached or modified, as a result of which the degree of polymerization can be altered. Some of these polymers (e.g. – PVP, PVA etc.) are approved by the FDA, and safe for biological application. Two polymers of our interest will be discussed in details here-

3.B.1 Polyvinyl pyrrolidone- It is one of the most widely used synthetic polymer for biological application. It is a derivative of acetylene, obtained by reacting acetylene with pyrrolidone followed by radical polymerization (Hamidi *et al*, 2008). The properties of PVP like water solubility, physiological compatibility, pH stability, colorless appearance etc. have made it a very important excipient for pharmaceutical industry and biomedical application (D'Souza *et al*, 2004). Besides using it as plasma volume expander and binder for pharmaceutical tablets, it has a large application in synthesizing hydrogels. Specially, PVP based hydrogels are synthesized by crosslinking with other polymers e.g. – chitosan, poly acrylic acid, alginate etc (Razzak *et al*, 1999; El-Hag Ali *et al*, 2003).

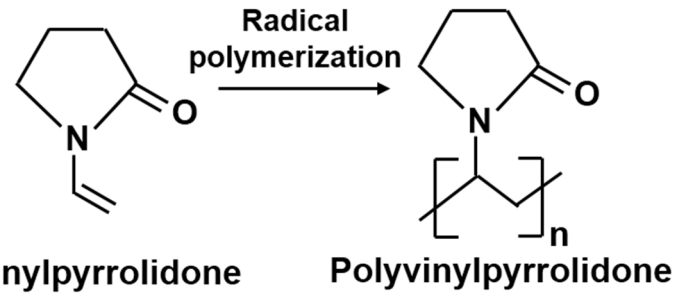

3.B.2 Polyvinyl alcohol- Another constituent used for hydrogel synthesis is polyvinyl alcohol. It is obtained from alcoholysis, hydrolysis or aminolysis of polyvinyl acetate. PVA has a number of biomedical applications including soft contact lenses, implants etc (Hassan and Peppas, 2000). Also, it can form hydrogels by either chemical crosslinking or physical crosslinking method. Chemical crosslinking is obtained by glutaraldehyde (Mansur *et al*, 2008) or epichlorohydrin (Sreedhar *et al*, 2006). Physical crosslinking is achieved by repeated freeze thaw method (Hassan and Peppas, 2000), which is ideal for protein delivery as this method avoids the usage of crosslinkers which are toxic and inhibit protein function. Also, this method confers mechanical strength and form hydrogels at several hundred nanometer range (Ricciardi *et al*, 2004). Controlled delivery of BSA has been achieved from this type of hydrogels (Li *et al*, 1998). Also, citric acid or succinic acid can be grafted with PVA by irradiation. The two layer hydrogel of polyurethane membrane and PVA/PVP/glycerin/chitosan was prepared for wound healing.

The role of the naturally synthesized phytochemicals to fight cancer is a major topic in the field of anticancer therapeutics. There are several plant polyphenolic compounds such as alkaloids, flavonoids etc. which have shown significant efficacy against some form of cancer. The advantages of choosing plant agents are their antitumor properties with minimal side effects and ready availability in ingestive form. Many of the phytochemicals have defined modes of action. Majorly, bioactive molecules play their anticancer role by 4 different means: a) methyltransferase inhibitor (Moiseeva *et al*, 2007; Paluszczak *et al*, 2010), b) histone deacetylase inhibitor (Rajendran *et al*, 2011), c) DNA damaging drugs (Surh *et al*, 2001; Thomasset *et al*, 2007), d) mitotic inhibitors (Owellen *et al*, 1972; Delmas *et al*, 2011). From the discussion in the earlier part of this section, the important role of NFκB in carcinogenesis is evident and it plays an important role in regulating some

of those above mechanisms in cancer cells. One plant derived bioactive molecule that acts as an inhibitor of NFκB is curcumin (Singh and Aggarwal, 1995).

4. Curcumin- Turmeric is obtained from rhizome *Curcuma longa* which is predominantly found in India and some other South Asian countries. Curcumin (diferuloylmethane) is a major constituent of turmeric and confers saffron color to it (Aggarwal *et al*, 2007). Curcumin is found in two tautomeric form- keto and enol in the environment (Figure 6).

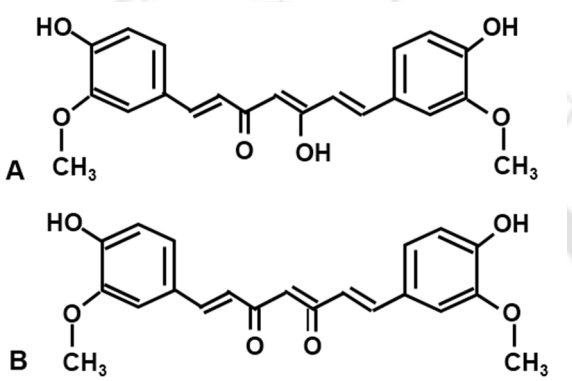

Figure 6. Structure of diferuloylmathane (curcumin). (A) Enol form, (B) Keto form.

It shows anti-inflammatory, anticancer, antibacterial, antifungal, anti-thrombotic and antiviral activities (Srimal and Dhawan, 1973; Srivastava *et al*, 1985; Mahady *et al*, 2002; Duvoix *et al*, 2005; Akhtar *et al*, 2012). In traditional medicine it has been used for ages to treat diabetes, allergies, arthritis and other chronic illness (Aggarwal *et al*, 2007; Aggarwal and Sung, 2009). As a potent anticancer agent, curcumin is found to regulate various transcription factors, growth factors and cytokines required for the proliferation of cancerous growth (Duvoix *et al*, 2005; Singh and Khar 2006). It also acts as a cell cycle blocker and induces apoptosis (Chen and Huang, 1998; Lee *et al*, 2009). Curcumin shows its chemopreventive activity against blood, lung, pancreas, intestinal tract etc. Thus, in short curcumin exhibits a wide spectrum of anticancer activities, which can play a crucial role to prevent or cure some forms of cancers alongside other chronic illness like diabetes or Alzheimer's disease (Hamaguchi *et al*, 2010). Curcumin has shown to be effective against malignant glioblastoma U87MG cells and induces apoptosis (Karmakar *et al*, 2007). Most prominent effect of curcumin on some detrimental illness are shown in figure 7.

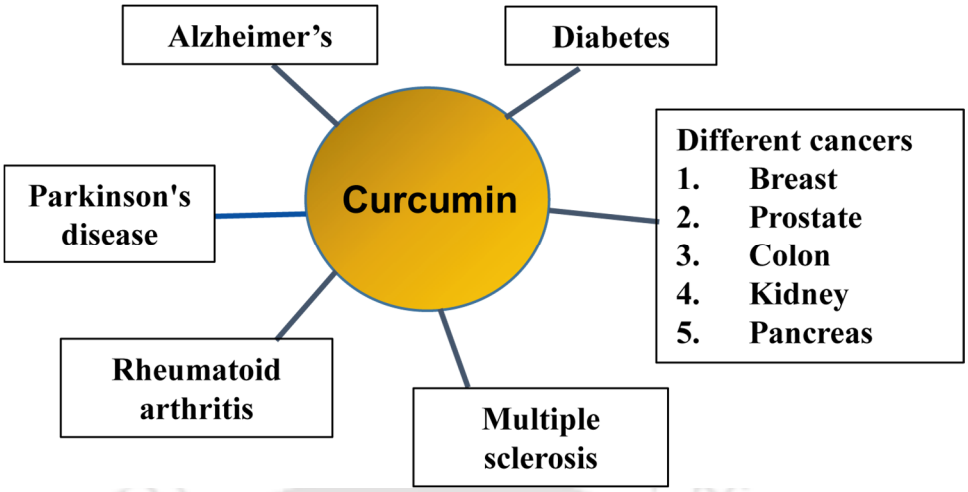

Figure 7. Some of the prominent illness where curcumin plays a major inhibitory role.

Curcumin plays a crucial role in regulating many signaling molecules ranging from transcription factors to cellular receptors (Fig. 8) (Kunnumakkara *et al, 2008;* Shishodia, 2013; Shehzad and Lee, 2013). This demonstrates the versatile role of curcumin against host of diseases.

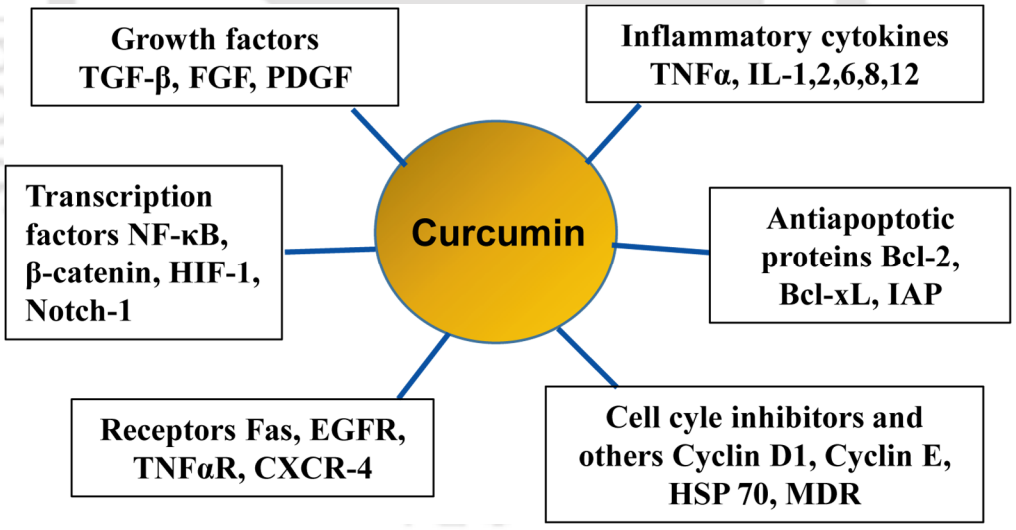

Figure 8. Signaling molecules regulated by curcumin.

The role of curcumin upon inhibition of proinflammatory transcription factor NFκB is well studied. It has been found that curcumin inhibits constitutive NFκB activation by blocking G1/S phase of cell cycle (Bharti *et al*, 2003; Choudhuri *et al*, 2005; Srivastava *et al*, 2007). Thus it inhibits cell cycle, which in turn induces apoptosis. The inhibition of

NFκB in turn increases the half-life of IκBα and modulates the inhibition of cell proliferation (Shishodia *et al*, 2003; Shishodia *et al*, 2005).

The poor solubility and very low bioavailability have hindered the application of curcumin as a therapeutic molecule (Anand *et al*, 2007). Many approaches have been undertaken to circumvent this inherent problem. One such approach is nanoparticle mediated delivery. A number of papers has shown the higher residence time of 'nanocurcumin' *in vitro* (Bisht *et al*, 2007) and *in vivo* (Kim *et al*, 2011). As a result, higher efficacy was obtained. Different nanocarriers were synthesized to deliver curcumin such as liposomes (Li *et al*, 2005; Wang *et al*, 2008) and polymers (Bansal *et al*, 2011). Polymeric nanoparticle encapsulated curcumin is of special interest, and thus a plethora of polymers have been tested e.g. – NIPAM, PEG, PLGA, chitosan etc (Bisht *et al*, 2007; Gupta *et al*, 2009; Yallapu *et al*, 2010; Duan *et al*, 2010; Anitha *et al*, 2011). Also, curcumin encapsulated protein nanoparticle was synthesized and tested against HIV (Gandapu *et al*, 2011). Thus, curcumin is found to be more effective in nanoparticle formulation.

Salient features:

From the literature review, the findings are as follows:

- IκBα is an important regulator of cell death and survival
- Functional delivery of therapeutic proteins plays an important role in bio-therapeutic regime
- Combination therapy with suitable therapeutic small molecules may augment the therapeutic efficacy

Thus, based on those key findings, the following strategies were devised to achieve the goal.

1. Cloning, expression and purification of IκBα as recombinant protein
2. Synthesis of hydrogel nanocarrier for encapsulation of recombinant IκBα
3. Functional delivery of recombinant recombinant IκBα to cancer cells
4. Synthesis of water soluble curcumin nanoparticles to load recombinant IκBα
5. Delivery of recombinant IκBα loaded curcumin NPs to cancer cells
6. Investigation of drug sensitivities of IκBα overexpressing cancer cells
7. Combination therapy using curcumin NPs, 5-fluorouracil along with IκBα to sensitize drug resistant cancer cells

3

MATERIALS & METHODS

MATERIALS & METHODS 3

The detailed methods and the materials used for this work have been described in this section. The details of materials used have been documented below-

Materials-

Different types of materials were used to carry out the thesis work including chemicals, buffers, DNA primers, plasmids, bacterial strains, purification kits, antibodies, plasticwares etc. The used materials and their companies are documented in the following manner-

1) **Chemicals and Reagents**-

Luria Bertani (LB) Broth, Bacteriological agar powder, ampicillin sodium salt, 3-(4, 5-dimethylthiazol-2-yl)-2, 5-diphenyltetrazolium bromide (MTT), curcumin, Bovine serum albumin (BSA) (**Himedia, India**)

Sodium chloride, potassium chloride, di sodium hydrogen phosphate, potassium di hydrogen phosphate, ammonium acetate, ethylene di-amine tetra acetic acid disodium salt, boric acid, chloroform, formaldehyde, ammonium persulphate (APS), tetramethylethylenediamine (TEMED), acrylamide, bis-acrylamide, bromophenol blue, sodium lauryl sulphate, glucose (**SRL, India**)

Absolute ethanol, acetic acid, sodium acetate, sodium carbonate, sodium thiosulphate, glycine, glutaraldehyde, methanol, hydrochloric acid, glycerol, β-mercaptoethanol, postassium acetate (**Merck, India**)

Agarose electrophoresis grade, trizma base (Tris), Triton X-100, Tween 20, reduced glutathione, glutathione-agarose beads, magnesium chloride hexahydrate, Polyethylene glycol 8000, Dimethylsulphoxide, Tris saturated phenol, Tri reagent, RIPA buffer, Diethylpyrocarbonate (DEPC), Trypsin-EDTA, Dulbecco's modified Eagle's media (DMEM), sodium bicarbonate, 2,3-bis-(2-methoxy-4-nitro-5-sulfophenyl)-2H-tetrazolium-5-carboxanilide (XTT), polyvinyl pyrrolidone (PVP), polyvinyl alcohol (PVA), G418, Ponceau S, Bradford reagent, Penicillin-Sterptomycin solution (**Sigma**)

5-bromo-4-chloro-3-indolyl-β-D-galactopyranoside (X-gal), Isopropyl-1-thio-β-D galactopyranoside (IPTG), Trisure (**Bioline, UK**)

Ribonuclease A, dithiothreitol (DTT), 3, 3'-diaminobenzidine tetrahydrochloride (DAB) (**Amresco, USA**)

Fetal Bovine Serum (**PAA, Austria**)

Power SYBR green PCR mastermix (**Applied Biosystems, USA**)

2) **Kits-** QIAquick gel elution kit (**Qiagen, USA**)

Genelute plasmid miniprep kit, Genelute mammalian total RNA miniprep kit, trypsin profile IGD kit, chemiluminiscence peroxidase substrate kit (**Sigma, USA**)

Revert aid H minus reverse transcription kit (**Fermentas, Germany**)

Quick Ligase kit (**New England Biolabs, USA**)

FITC-Annexin V apoptosis detection kit-1, Apo-BrDU TUNEL assay (**BD Pharmingen**)

3) **Enzymes, Markers and PCR components-** *Eco* RI, *Bam* HI, *Xho* I *Spe* I, *Xba* I, *Not* I, Hyperladder DNA marker (200 bp to 10 kb), Protein marker, Broad range (2-212 kDa), Color plus prestained protein marker (7-170 kDa) (**New England Biolabs, USA**)

Red Taq, dNTPs, $MgCl_2$ (**Bioline, UK**)

Table -1. List of primers-

Sl No.	Primer name	Sequence
1.	For cloning IκBα full length	Fwd: 5′ **ATGTTCCAGGCGGCCGAGCGCCC** 3′ Rev: 5′ **TCATAACGTCAGACGCTGGCCTCCAAAC** 3′
2.	pGEX4T2-IκBα	Fwd: 5′ **CGTGGATCCATGTTCCAGGCGGCCGAG** 3′ Rev: 5′ **CGACCCGGGTCATAACGTCAGACGCTG** 3′
3.	Semi quantitative PCR β Actin	Fwd: 5' **CTGTCTGGCGGCACCACCAT** 3' Rev: 5' **GCAACTAAGTCATAGTCCGC** 3'
4.	P53	Fwd: 5' **TGGCCCCTCCTCAGCATCTTAT** 3' Rev: 5' **GTTGGGCAGTGCTCGCTTAGTG** 3'
5.	Caspase 3	Fwd: 5' **TTTGTTTGTGTGCTTCTGAGCC** 3' Rev: 5' **ATTCTGTTGCCACCTTTCGG** 3'
6.	Bax	Fwd: 5' **AAGCTGAGCGAGTGTCTCAAGCGC** 3' Rev: 5' **TCCCGCCACAAAGATGGTCACG** 3'
7.	c-Myc	Fwd: 5' **CCAGGACTGTATGTGGAGCG** 3' Rev: 5' **CTTGAGGACCAGTGGGCTGT** 3'

8.	Bcl-xL	Fwd: 5' **ATGGCAGCAGTAAAGCAAGCGC** 3' Rev: 5' **TTCTCCTGGTGGCAATGGCG** 3'
9.	Cyclin D1	Fwd: 5' **CGCCCCACCCCTCCAG** 3' Rev: 5' **CGCCCAGACCCTCAGACT** 3'
10.	Cyclin E	Fwd: 5' **CCACACCTGACAAAGAAGATGATGAC** 3' Rev: 5' **GAGCCTCTGGATGGTGCAATAAT** 3'
11.	P50	Fwd: 5' **AAACCTTTCCTCTACTATCCTGA** 3' Rev: 5' **GCACTCTCTTCTTTTGTTCCTGT** 3'
12.	P65	Fwd: 5' **ATAGAAGAGCAGCGTGGGGACT** 3' Rev: 5' **GGATGACGTAAAGGGATAGGGC** 3'
13.	For Real time PCR β Actin	Same as semi quantitative PCR
14.	IκBα	Fwd: 5' **TGCACTTGGCCATCATCCAT** 3' Rev: 5' **CGTGTGGCCATTGTAGTTGG** 3'
15.	Cyclin D1	Same as semi quantitative PCR
16.	Cyclin D2	Fwd: 5' **AAAGTTGGCTCCAAAGGGTCCTT** 3' Rev: 5' **GAAACTGGCTGAACCTGTAAAAAT** 3'
17.	P27	Fwd: 5' **CTGCAACCGACGATTCTTCTACT** 3' Rev: 5' **GGGCGTCTGCTCCACCAGA** 3'
18.	P21	Fwd: 5' **GGACAGCAGAGGAAGACCATGT** 3' Rev: 5' **TGGAGTGGTAGAAATCTGTCATGC** 3'

4) **Western blotting membrane**- Polyvinyl di fluoride (PVDF) membrane (0.2 µm) (**Millipore, USA**)

4) **Antibodies**- *Primary antibodies*- Human anti-mouse IκBα, anti-mouse β actin, PE conjugated rabbit anti Caspase-3 antibody (**BD Pharmingen, USA**), Rabbit anti β-tubulin (**Cell Signalling Technologies, USA**).

Secondary antibodies- Goat anti-mouse HRP conjugated IgG (**Sigma**), anti-rabbit HRP conjugated IgG (**Cell Signalling Technologies, USA**)

5) **Plasmids**- pGEM T easy (Amp^r), pCINeo (Amp^r in bacteria, Neo^r in mammalian cells) (**Promega, USA**)

pGEX4T2 (Amp^r) (**GE Healthcare, Sweden**)

6) **Bacterial strains**- DH5α (fhuA2, lacΔU169, phoA, glnV44, Φ80', lacZΔM15, gyrA96, recA1, relA1, endA1, thi-1, hsdR17), BL21 (dcm, ompT, hsdS (rB^-mB^-), gal) (MTCC, India)

7) **Mammalian cells**- HeLa (Cervical carcinoma), U87MG (glioblastoma), HT29 (colorectal adenocarcenoma), HEK (embryonic kidney) (**NCCS, India**)

8) **Plastic wares**- various types of plastic wares were used in this current work. They can be broadly subdivided as follows-

8.1 Microcentrifuge tubes- 0.5 mL, 1.5 mL and 2 mL (**Tarsons, India**)

0.2 mL PCR tube (**Grenier BioOne, USA**)

8.2 Microtips- 0.2-2 µL, 2-200 µL, 200-1000 µL (**Tarsons, India**)

8.3 Petridish for bacterial culture (**Tarsons, India**)

8.4 Mammalian cell culture plates- 35 mm, 60 mm and 100 mm diameter plates (**BD Falcon, USA**)

9) **Buffers and their constituents**-

Table 2.

Buffers	Composition
4X protein loading dye (for 10 mL)	2.0 ml 1M Tris-HCl (pH 6.8), 0.8 g SDS, 4.0 ml 100% glycerol, 0.4 ml 14.7 M β-mercaptoethanol, 8 mg bromophenol blue in water
6X DNA loading dye	0.25 (%)(w/v) bromophenol blue, 0.25% (w/v) xylene cyanol FF, 30% (v/v) glycerol in H_2O
Acetate buffer	1 M ammonium acetate and 0.077% (v/v) glacial acetic acid in sterile distilled water, pH 4.2
Alkaline lysis solution I	50 mM glucose, 25 mM Tris-Cl (pH-8.0), EDTA (10 mM)
Alkaline lysis solution II	0.2 N NaOH, (freshly diluted from 10 N stock), 1% (w/v) SDS
Alkaline lysis solution III	5 M potassium acetate (60 mL), glacial acetic acid (11.5 mL), water (28.5 mL)

Blocking buffer	5% (w/v) BSA in TBST
Cleaning buffer 1(pH-8.5)	0.1 M boric acid, 0.5 M NaCl, adjust the pH 8.5 with sodium hydroxide
Cleaning buffer 1(pH-4.5)	0.1 M sodium acetate, 0.5 M NaCl, adjust the pH 4.5 with acetic acid
Lysis buffer for protein purification	10 mM PBS (pH-7.4), 1 mM EDTA, 1 mM Dithiothreitol, 1% Triton X-100 and 2.5 µM Phenylmethylsulfonylfluoride
Phosphate buffered saline	137 mM NaCl, 2.68 mM KCl, 7.98 mM Na_2HPO_4, 1.4 mM KH_2PO_4, pH-7.4
Polyacrylamide solution (30%)	29.2% (w/w) acrylamide, 0.8% (w/w) N,N'-methylenebisacrylamide
Tris Buffered Saline Tween-20	Tris-HCl (50 mM), NaCl (150 mM), Tween-20 (0.1% v/v) pH-7.5
Tris-acetate EDTA (TAE) 50X (100 mL)	24.2 g Tris base, 5.71 mL of glacial acetic acid, 10 mL of 0.5 M EDTA (pH-8.0)
Tris-EDTA	10 mM Tris-HCl (pH-8.0), 1 mM Na_2EDTA
TSS buffer for transformation	10% (w/v) PEG 8000, 0.6% (w/v) $MgCl_2.6H_2O$, 5% (v/v) DMSO in LB

Methods-

Different methods were used to carry out the whole work ranging from cloning to expression and purification of protein, synthesis of nancarriers and mammalian cell culture. The methods are described in this section.

3.1 Isolation of RNA from HT29 cells

RNA was isolated from cultured HT29 cells. HT29 cells were seeded in 35 mm culture dish. After the cells reached ~90% confluency, the media was removed and cells were washed with PBS to remove the residual media. Then, 0.5 mL TriSure was added to the plate, pipetted thoroughly to lyse the cells on the plate and collected in a microcentrifuge tube. Then, 100 µL chloroform was added to the tube, shaked vigourously with cap closed to mix thoroughly and kept at room temperature for 10-15 min. Then the mixture was centrifuged at 12000xg for 15 min at 4°C to separate the aquous and organic phase. The top aquous phase was collected in another fresh tube without disturbing the adjacent phase. With the aquous phase, 250 µL of isopropyl alcohol was added to precipitate the RNA. The alcohol and aquous phase was mixed throughly by shaking and kept for 10 min at room temperature. Then the RNA was precipitated by centrifuging at 12000xg for 10 min at 4°C. The supernatant was carefully removed without disturbing the transparent pellet. Further, to wash off the residual salt, one time 75% ehtanol (in DEPC water) wash was given at 7500xg for 5 min at 4°C. Then, the supernatant was decanted carefully, and the pellet was air dried to remove residual alcohol. Then the pellet was dissolved in DEPC trated water. The amount of RNA was measured by Nanovue™ instrument (GE Healthcare). It should be mentioned here that all the microtubes and microtips were DEPC treated and autoclaved.

3.2 Cloning of IκBα in pGEMT Easy vector

After the isolation and quantification of total RNA from HT29 cells, the cDNA of IκBα was prepared by using RevertAid H-minus Reverse Transcriptase kit with random hexamer by following. Subsequently, cDNA was amplified by polymerase chain reaction (PCR) using the forward primer 5′ ATGTTCCAGGCGGCCGAGCGCCC 3′ and the reverse primer 5′ TCATAACGTCAGACGCTGGCCTCCAAAC 3′. The PCR amplification condition was fixed for denaturation at 94°C for 40 s, annealing at 57°C for 40 s and extension at 72°C for 1 min to amplify 954 base long IκBα. The amplified cDNA

of IκBα was cloned into pGEMT Easy vector by following manufacturer's protocol. Then the ligation product was transformed into *E.coli* DH5α competent cells, and the positive transformed colonies were selected on LB-agar plate by IPTG/X-gal compounds based blue-white colony screening technique. The white colonies were streaked on another LB-agar plate with identical IPTG/X-gal concentration. The plasmid was isolated from each colonies by alkaline lysis based method, checked on 1% agarose gel for plasmid 'band shifting' which is nothing but retardation of positive clones (with IκBα) as compared to the 3 kb pGEM T Easy plasmid. The retarded plasmids were digested with *Eco* RI to release the gene of interest.

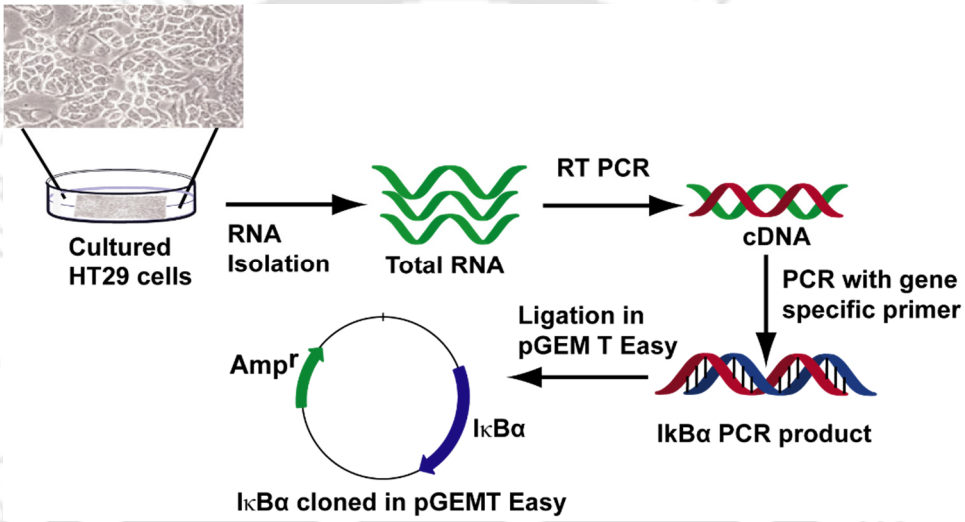

Scheme 1- Cloning of IκBα in pGEMT Easy vector

3.3 Cloning into pGEX4T2

IκBα cloned in pGEMT Easy vector was further re-cloned in bacterial expression vector pGEX4T2 with the following primer pairs:

Forward 5′-CGTGGATCCATGTTCCAGGCGGCCGAG-3′ and reverse 5′-CGACCCGGGTCATAACGTCAGACGCTG-3′ (with *Bam* HI and *Xho* I overhangs respectively). The PCR product and the vector were digested with *Bam*HI and *Xho*I to generate linear fragments with 5' *Bam* HI and 3' *Xho* I overhang. Then the digested vector and insert were ligated by NEB quickligase kit with slight modification of manufacturer's protocol by incubating the ligation mix in 25°C for 15 min before transforming in DH5α cells. Next, the transformed cells were selected on ampicillin added LB-agar plate. The colonies were picked by sterile toothpick, streaked on another ampicillin added LB-agar

plate. The plasmids were isolated from the colonies and digested with *Bam* HI and *Xho* I enzymes and checked on agarose gel for positive clones.

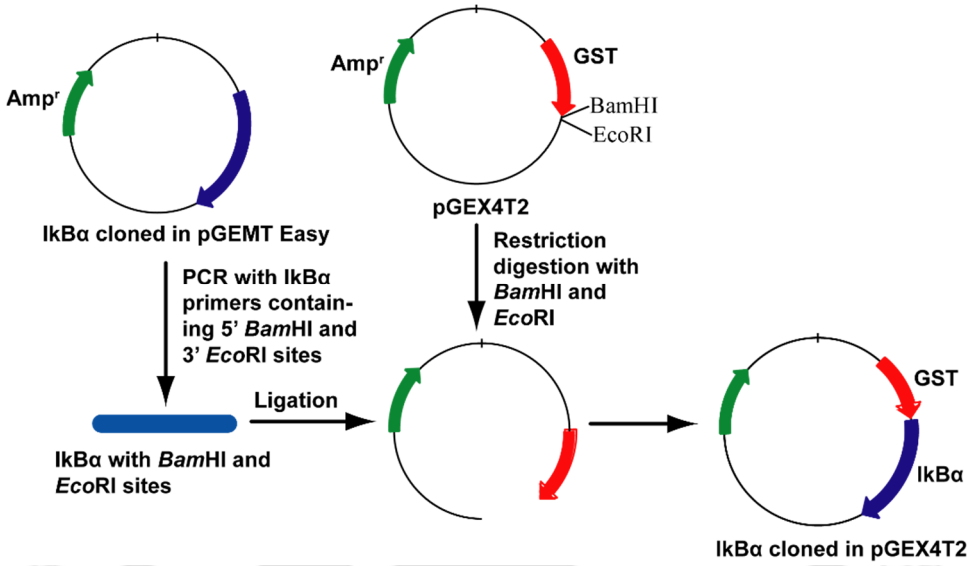

Scheme 2- Cloning of IκBα into pGEX4T2 vector.

3.4 Cloning into pCINeo vector

The IκBα was transferred from pGEM T Easy to pCINeo by digestion with restriction enzymes followed by ligation. IκBα cloned pGEM T Easy vector was digested with *Eco* RI (cutting site 5' GAATTC 3') and *Spe* I (cutting site 5' ACTAGT 3'). Similarly, pCINeo was digested with *Eco* RI and *Xba* I (cutting site 5' TCTAGA 3'). As, *Spe* I and *Xba* I has compatible cohesive ends, they share a common ligation site. Thus, after digestion, digested product IκBα and digested linear fragment of pCINeo were gel eluted from agarose gel using gel elution kit (Sigma, USA). The purified digested product was ligated by NEB quick ligation kit following manufacturer's protocol. The ligation product was transformed into *E.coli* DH5α strain, and the colonies were screened by ampicillin. Further, the purified plasmids from the colonies seen on the plate were isolated and digested with *Eco* RI and *Not* I, which release digestion product of expected size. To further confirm the clone, the full length IκBα was PCR amplified using purified plasmid as a template.

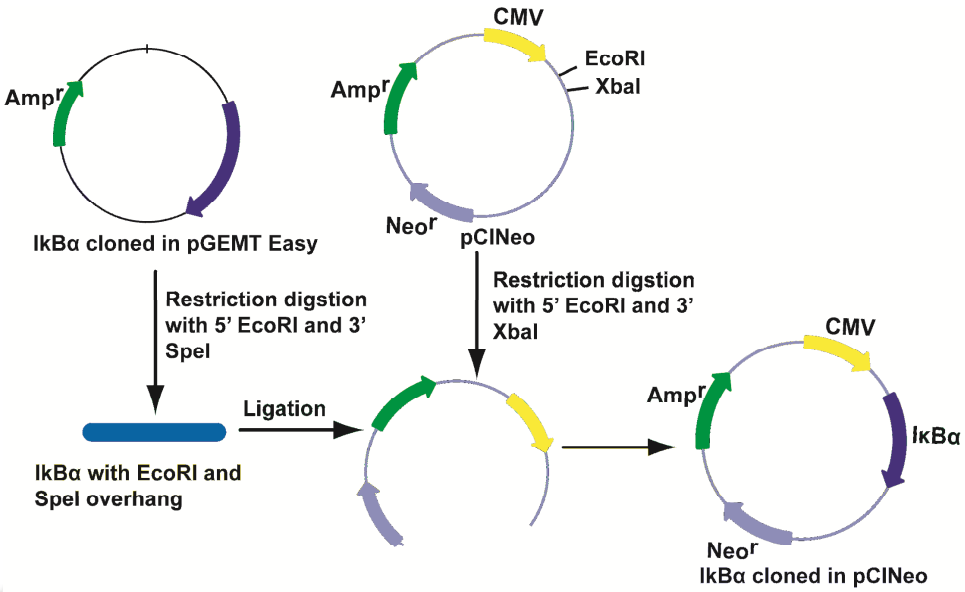

Scheme 3- Cloning of IκBα into pCINeo vector.

3.5 Expression and purification of recombinant GST tagged IκBα

The pGEX4T2 vector containing IκBα was transformed into *Escherichia coli* strain BL21 (DE3) and the transformed cells were grown in Luria-Bertany (LB) broth medium at 37°C at 180 rpm up to OD_{590} at 0.6. Thereafter, 500 µM isopropyl-1-thio-β-D galactopyranoside (IPTG) was added and the cells were further grown at 28°C for 6 h for protein expression. The bacterial cells were centrifuged at 5000 rpm for 10 min at 4°C and the pellet was stored at -20°C. The cell pellet was lysed with lysis buffer for protein purification, followed by high pressure cell disruption at 4°C. The supernatant was collected after centrifugation at 15000xg for 30 min at 4°C. Finally, the recombinant GST tagged IκBα was purified by either glutathione-agarose bead loaded PD-10 column or GSTrap FF column (5 mL) with slight modifications of the manufacturer's protocols.

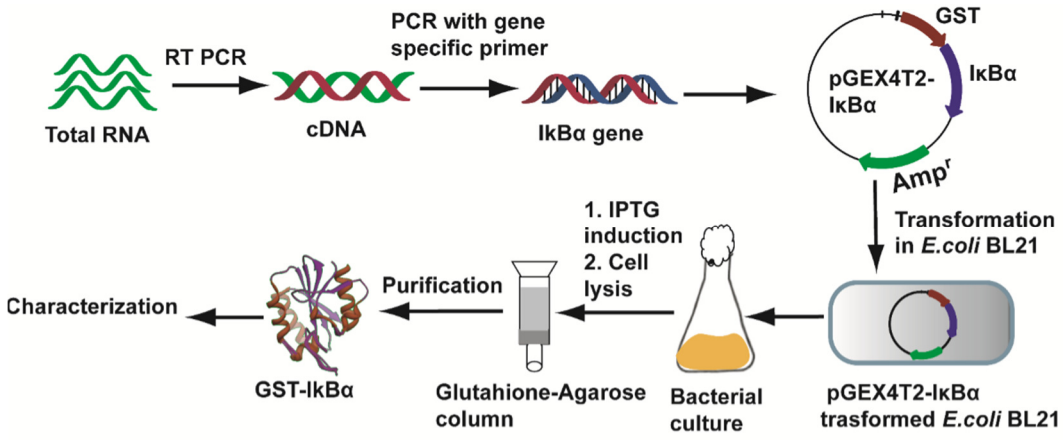

Scheme 4- Purification of GST-IκBα from *E. coli* BL21 cells.

3.6 Western blotting experiment

The purified recombinant GST tagged IκBα protein was confirmed by Western blot analysis. The purified protein was electroblotted to PVDF membrane (pre incubated with methanol) at constant 25 V for 3 h in cooling condition. The transfer efficiency was checked by Ponceaue staining and blocked with blocking buffer for 1 h in room temperature. Then the membrane was incubated overnight at 4°C with human anti-mouse IκBα antibody in blocking buffer (1:2000 dilution). Subsequently, the membrane was washed 5 times with TBST and incubated with horseradish peroxidase (HRP) conjugated goat anti-mouse polyclonal IgG secondary antibody in blocking buffer (1:5000 dilution) for 2 h at room temperature. Next the membrane was washed 5 times with TBST, and probed by chemiluminiscence peroxidase substrate kit.

3.7 Characterization of purified recombinant GST tagged IκBα

The purified protein was further characterized by MALDI-TOF (4800 plus, Applied Biosystems). For that, the protein was digested with trypsin within the gel using trypsin digestion kit, and the resultant fragments were mixed with α-cyano-4-hydroxycinnamic acid, which served as matrix for MALDI analysis. The secondary structure of recombinant IκBα was confirmed by using circular dichroism spectroscopy (CD, Jasco) at 20°C. The measurements were done in cell with path length of 10 mm with 50 nm/min scan speed in 100 mM Tris-Cl buffer solution.

3.8 Synthesis of protein loaded PVP-PVA hydrogel nanocarrier

The hydrogel NCs were synthesized by physical cross linking of PVA-PVP (70:30 w/w) by repeated freeze thaw method. For that, 1.4 mL of PVA (5 mg/mL) and 0.6 mL of PVP (5 mg/mL) were taken in a 50 mL falcon tube containing 5 mL of paraffin oil for generation of oil-aqueous layers. To synthesize the protein loaded hydrogel NCs, 400 µg of protein (GST-IκBα) was mixed with above constituents in the tube. Then, this mixture was sonicated by probe sonicator (Hielscher) for 2 min with 30 s pulse in ice by keeping the probe fixed at the interface of the oil-aqueous layers. Subsequent to sonication, the mixture was immediately incubated at –20°C for 12 h and the frozen mixture was melted at room temperature; this freeze-thaw step was repeated for another two times for complete cross linking of polymers. After complete removal of upper oil layer by washing with hexane, the hydrogel NCs and aqueous supernatant (to know unbound protein) were collected by centrifugation at 8000 rpm for 5 min in 4°C. Finally, pellet of the protein encapsulated and blank hydrogel NCs were again dispersed in sterile phosphate buffered saline (PBS) before adding to the cells.

To find out the protein loading efficiency of the NCs, the amount of free (P^f) protein present in the supernatant was determined by measuring the absorbance at 280 nm by UV-Vis spectroscopy (Perkin-Elmer Lambda 45, Fremont, CA) and subtracted from the amount of protein (P^i) initially used for encapsulation.

$$\mathbf{LE}\ (\%) = \frac{P^i - P^f}{P^i} \times 100 \qquad (1)$$

3.9 Study of protein release profile of hydrogel nanocarriers

To study the protein release from hydrogel NCs as a function of pH, the protein loaded hydrogel NCs were incubated up to 48 h in PBS (pH 7.4) and acetate buffer (pH 4.2) respectively, at 37°C. After specific time intervals (1, 3, 6, 12, 24 and 48 h), the supernatants were collected by centrifugation and the amount of protein present was measured by probing UV-Vis absorbance at 280 nm.

3.10 Synthesis of protein loaded curcumin nanoparticles

The solid curcumin was dissolved in acetone at 4 mg/mL. The curcumin solution was added drop-wise to 1 mg/mL poly vinyl pyrrolidone (PVP, molecular weight 10000)

solution (in water) at 75°C to 80°C under constant stirring up to a final concentration of curcumin 100 µg/mL of curcumin. After addition of curcumin, stirring was continued for 2-3 min, the solution was sonicated in probe sonicator (Hielscher, Germany) with 1 min pulse for 5 min in room temperature. Then, the solution was centrifuged for 5000xg for 5 min at 4°C to pellet down the larger particles. The supernatant was further centrifuged at 12000xg for 10 min to collect the curcumin nanoparticles (NPs). The pellet was dissolved in Milli-Q water, and further probe sonicated to disperse the curcumin NPs. For its application upon cells, the process was carried out in aseptic condition. After synthesis of curcumin NPs, 0.001% (w/v) poly-L-lysine (PLL, Sigma, USA) was added to the curcumin NPs solution to apply positive charge to the NPs, then the recombinant GST tagged IκBα was added at required concentration to the PLL coated curcumin NPs.

3.11 Transmission electron microscopy (TEM)

The hydrogel NCs and synthesized protein loaded curcumin NPs were analyzed using a high resolution transmission electron microscope (TEM; JEM 2100; Jeol, Peabody, MA, USA) operating at a maximum accelerating voltage of 200 KeV. For that, 7 µL of synthesized NCs were drop-coated onto a carbon coated copper TEM grid, air dried and analyzed under TEM.

3.12 Field emission scanning electron microscopy (FESEM)

GST-IκBα encapsulated hydrogel NCs were characterized by FESEM (Zeiss, Germany) at a magnification of x25000. Similarly curcumin NPs were also analyzed by the same machine at a magnification of x20000. Both samples were analyzed as dried sample with gold coating.

3.13 FTIR Spectroscopy

The FTIR spectra of PVA/PVP hydrogel and GST-IκBα encapsulated PVA/PVP hydrogel were measured using Perkin Elmer- FTIR spectrometer, in the range 4000–400 cm^{-1}, after mixing with KBr.

3.14 Dynamic Light scattering study for hydrogel NCs and curcumin NPs

Hydrodynamic diameter of the NCs was determined by dynamic light scattering analysis using a Malvern Zetasizer Nano ZS. Measurements were recorded while keeping the

samples in PBS buffer. The hydrodynamic diameter of curcumin NPs, curcumin NPs attached with PLL and curcumin NPs attached with PLL and GST- IκBα was measured by dynamic light scattering in the same instrument. The zeta potential was also recorded for the samples in the same instrument.

3.15 Cell Culture and recombinant IκBα encapsulated hydrogel treatment

HeLa (human cervical carcinoma) and U87MG cell lines were obtained from National Center for Cell Sciences (NCCS), India and were propagated in Dulbecco's Modified Eagle's Medium (DMEM) supplemented with L-glutamine (4 mM), penicillin (50 units/mL), streptomycin (50 mg/mL) (Sigma), and 10% (v/v) fetal bovine serum (PAA Laboratories, Austria) in 5% CO_2 humidified incubator at 37 ^{0}C. Then, 1×10^4 cells were seeded into each well of a 96-well plate and the same physiological conditions as well as media were maintained for 12 h prior to adding different amounts of protein loaded hydrogel NCs to study the cell viability.

3.16 Cell viability assay

To quantify the cell viability, 1×10^4 HeLa cells/well were seeded in 96-well microtiter plate and maintained in the same medium and condition. After overnight incubation, the cells were treated with different concentrations of the recombinant IκBα encapsulated hydrogel NCs for another 24 h and then XTT assay was performed (Scudiero *et al*, 1988). Respiring mitochondria in viable cells convert tetrazolium compound, XTT [2, 3-bis-(2-methoxy-4-nitro-5-sulfophenyl)-2H-tetrazolium-5-carboxanilide] (Sigma-Aldrich) to water soluble orange color formazan product in presence of phenazinemethosulfate (PMS). The quantity of formazan product as measured by the absorbance at 450 nm (A450) is directly proportional to the number of live cells in culture. A690 means the absorbance of the culture media recorded at 690 nm as background absorbance. The percentage (%) of cell viability was calculated as

$$\% \textbf{ of cell viability} = \frac{\textbf{(A450 – A690) sample}}{\textbf{(A450 – A690) control}} \textbf{x100} \qquad \textbf{(2)}$$

3.17 Acridine Orange/Ethidium Bromide (AO/EB) double Staining

After the treatment with protein encapsulated hydrogel and blank hydrogels for 12 h and 24 h, the cells were treated with a mixture of ethidium bromide (20 µg/mL) and acridine orange (20 µg/mL) for 5min in dark. Then, the media was removed and supplemented with 10 mM PBS; and the cells were observed under the fluorescent microscope (Nikon ECLIPSE, TS100, Japan).

3.18 Delivery of hydrogel encapsulated recombinant IκBα into the cell

To confirm the delivery of hydrogel encapsulated GST tagged IκBα into the cells, we performed immunoblotting of the cell lysates of IκBα-hydrogel treated HeLa cells against the untreated HeLa cells (control), cells treated with PVA/PVP hydrogel only and the cells treated with GST tagged IκBα. HeLa cells were grown in 60 mm cell culture plate (BD Falcon) and treated with the IκBα encapsulated hydrogel, blank hydrogel and purified GST tagged IκBα for 24 h. The media was removed, the cells were thoroughly washed with 10 mM PBS (pH-7.4) and lysed with RIPA buffer (Sigma), supplemented with cocktail of protease inhibitor (1:1000 dilution, Sigma). Lysed cells were detached from the cell culture plate with scraper. Then the cell debris was pelleted by centrifugation at 12000xg for 10 min at 4^{o}C, and the supernatant containing intracellular proteins was collected. The protein present in the supernatant was determined by Lowry's method of protein determination. Then equal amount of protein boiled with protein loading dye was loaded in 12% SDS-PAGE and ran for 2 h. The total protein was electroblotted to PVDF membrane (pre incubated with methanol) at 25 V for 3 h (Hoeffer Miniblot™). The transferred protein was blocked with blocking buffer and incubated over night at 4°C with primary antibody IκBα (dilution 1:1000) with mild shaking. Then the membrane was washed thoroughly with TBST for 5 times. Then the membrane was incubated with HRP conjugated goat anti mouse secondary antibody (dilution 1:5000) for 1 h in room temperature. Again the membrane was washed in TBST for 5 times and the membrane was developed by DAB and hydrogen peroxide.

3.19 Cell Cycle Analysis

Cell cycle analysis was performed by measuring the DNA content of control and treated cells in a flow cytometer. Around 1×10^5 of HeLa cells were grown in 60 mm tissue culture dishes (BD Falcon) followed by protein encapsulated hydrogel and blank hydrogel treatment for 24

h. The cells were collected by trypsinization, washed with PBS, fixed by slowly adding 1 mL of cold 70% ethanol, and finally stored at -20°C. The fixed cells were centrifuged, washed in ice-cold PBS and incubated with PI (40 µg/mL) and RNase A (100 µg/mL) at 37°C for 30 min in the dark. After incubation, the samples were analyzed in FACS Calibur (BD Biosciences, NJ). PI fluorescence data were recorded with the CellQuest pro in FL2 channel for 10,000 cells in each sample and subsequently analyzed by WinMDI software.

3.20 APO-BrdU Assay

Apoptotic cells were detected by TUNEL labeling using the APO-BrdU TUNEL Assay Kit (BD Pharmigen, NJ) as per the manufacturer's protocol. Briefly, the treated cells were centrifuged for 10 min at 4°C at 650 ×*g*, and washed in cold PBS. Cells were then fixed and permeabilized with 70% ethanol for 30 min on ice, and incubated with 50 µL DNA-labeling solution containing TdT enzyme and Br-dUTP at 37°C for 60 min. After labeling, the cells were washed and stained with fluorescein-labeled anti-BrdU antibody for 30 min. Subsequently, they were treated with propidium iodide and RNAse A, before being analyzed by FACS.

3.21 UV-Visible and Fluorescence spectroscopic analysis of curcumin NPs

UV-Visible spectroscopic recording was done in LS45 spectrophotometer (Perkin-Elmar, USA) and Fluorescence spectroscopy in Fluorolog 3 (Horiba, Japan). The curcumin NPs was dissolved in water in both cases.

3.22 Addition of protein curcumin NPs on HeLa and U87MG cells

Cervical carcinoma (HeLa) and glioblastoma cell line (U87MG) were cultured in DMEM supplemented with 10% (v/v) fetal bovine serum and 50 mg/mL streptomycin and 50 units/mL penicillin in humidified condition with 5% CO_2. HeLa cells were seeded at 10^4 cells per well in 96 well plate and U87MG cells were seeded with 2000 cells per well. For FACS and gene expression studies, the cells were cultured in 6-well and 60 mm plates (BD Biosciences, USA). The different concentrations of protein loaded curcumin NPs were added to the cells after overnight growth of the cells.

3.23 Cell viability assay

Cell viability assay was carried out in 96 well plates. After 24 h of the addition of IκBα loaded curcumin NPs, 500 µg/mL 3-(4, 5-dimethylthiazol-2-yl)-2, 5-diphenyltetrazolium bromide (MTT) dissolved in DMEM was added to each well. After 3 h, the media was carefully discarded, and the purple color tetrazolium salt formed due to cellular respiration, was dissolved in 100 µL DMSO (SRL, India). The colorimetric measurement was performed in multi-well plate reader (Tecan Infinite M200 PRO, Switzerland) by recording the absorbance at 570 nm, and 650 nm for background subtraction. Thus, the cell viability was measured by following equation

$$\% \text{ of cell viability} = \frac{(A570 - A650)\text{sample}}{(A570 - A650)\text{control}} \times 100 \qquad (3)$$

A_{570} represents Absorbance at 570 nm and A_{650} represents Absorbance at 650 nm.

3.24 Cell cycle analysis for protein loaded curcumin NPs treated cells

The effects of IκBα loaded and BSA loaded curcumin NPs on the cell cycle of HeLa and U87MG were investigated by propidium iodide (PI) (Sigma Aldrich, USA) based flow cytometric analysis. After 24 h of treatment (at IC50 dose), the cells were fixed by chilled ethanol (70%). The fixed cells were pelleted at 450xg at 4°C for 6 min and washed thrice with cold PBS. The fixed cells were incubated in dark for 30 min with 50 µg/mL PI and 100 µg/mL RNaseA (Amresco, USA) and 0.1% (v/v) Triton X-100 (Sigma, USA) in PBS. Then, the 15000 cells for each sample were analyzed in FACS Calibur (BD Biosciences, USA) in FL-2 channel, and the data was subsequently analyzed by ModFit™.

The effect of 5-FU was upon the cell cycle of U87MG and U87-IκBα cells was checked in a slightly different manner. First the cells were synchronized for 48 h with serum free media, which was then replaced with media containing serum along with 5-FU. The rest of the procedure is same as above.

3.25 FITC Annexin V- Propium iodide (PI) assay for Detection of apoptosis

To determine the cell death, cells were double stained with FITC conjugated recombinant Annexin V and PI (FITC Annexin V Apoptosis Detection Kit II, BD Biosciences, USA) and analyzed by flow cytometry. Loss of integrity of plasma membrane is the first stage of

apoptosis, where phosphotidylserine (PS) flips from inner to outer part of the membrane. Calcium dependent phospholipid binding protein Annexin V has a very high affinity to PS. By exploiting this event, cells undergoing apoptosis can be quantitatively detected following manufacturer's protocol. In brief, both U87MG and HeLa cells grown in 60 mm plates were treated with IκBα loaded curcumin NPs for 16 h. Then the floating as well as attached cell population were collected, washed with PBS, counted by Neubauer hemocytometer and then suspended in the binding. The cells were incubated with Annexin V antibody and PI and analyzed using FACS.

3.26 Reactive oxygen species determination

The reactive oxygen species generated by curcumin inside the cells was determined by 2', 7'-dichlorfluorescein-diacetate (DCFH-DA). DCFH-DA readily enters into the cells and cleaved by the cellular esterase into DCFH, hence it does not come out from the cell. DCFH gets oxidized inside the cells to generate highly fluorescent end product. After treatment with IκBα loaded curcumin NPs and BS loaded curcumin NPs for 2 h, the cells were washed with PBS (10 mM) twice, then 10 µM DCFH-DA was added to the cells along with 1 mL DMEM and incubated for 30 min in dark in CO_2 incubator. The media was removed and the cells were washed with PBS and harvested by trypsin. The cells were pelleted, washed with PBS and immediately analyzed by FACS Calibur. The fluorescence was recorded in FL1 channel with 15000 cell counts.

3.27 Semi-quantitative reverse transcription PCR

The cDNA of IκBα loaded curcumin nanoparticles treated and untreated U87MG cells were synthesized in following condition- after adding the RNA (total 1 µg), random hexamer primer and nuclease free water, the mixture was incubated at 65°C for 5 min in PCR machine. Then, the tubes are chilled on ice and reaction buffer, RNase inhibitor, dNTPs and reverse transcriptase was added to each tube as per company protocol and mixed and centrifuged. Then in PCR machine, it was kept for 5 min at 25°C followed by 60 min at 42°C. The reaction was terminated by heating at 70°C for 5 min. The semi quantitative reverse transcriptase PCR was performed to study the relative expression of p53, bax, caspase-3, bcl-xL, c-myc, cox-2, cyclin E, cyclin D1 with β- actin as housekeeping gene in Palmcycler machine with following PCR condition- initial denaturation at 95°C for 3 min, followed by a 3 stage PCR cycle with

denaturation at 95°C for 30 s, annealing at 55°C for 30 s and amplification at 72°C for 35 s for 30 cycles. Then final extension was given at 72°C for 5 min. The PCR samples were analyzed at 1.2% agarose gel stained with ethidium bromide.

3.28 Establishment of IκBα overexpressing U87-IκBα cell line

The IκBα cloned pCINeo plasmid was purified by GenElute™ plasmid extraction kit following by manufacturer's protocol. The purified plasmid was transfected into U87MG cells by lipofectamine mediated transfection method. Here, as per the manufacturer's protocol, U87MG cells were seeded in equal number in 12 well pate, and after the cells reached 90% confluency, they were treated with lipofectamine conjugated pCINeo-IκBα plasmid. Initially, 5 µL lipofectamine and 5µg of purified plasmid was incubated in serum free media separately for 10 min, then the diluted DNA and lipofectamine was mixed together and incubated for maximum of 30 min, and added onto the cells. After 12 h, the media was replaced by normal media with 600 µg/mL G418 for selection of clonal population. The selection process was carried out until there is no cell death, with replenishing fresh media with drugs after every 3 days. Then, the RNA was isolated and the over expression of IκBα was checked to confirm the establishment of IκBα over expressing U87-IκBα cell line.

3.29 Real time PCR

Real time PCR was performed for different cell cycle related genes using c-DNA of treated and untreated U87MG cells. For that purpose, the cells were seeded in 60 mm plate in equal number.After they reached 80% confluency, the cells were serum synchronized for 48 h. The serum free media was replaced with serum media. Within 2 h, the BSA loaded curcumin NPs were added upon the cells and incubated for 18 h. Then, the RNA was isolated and c-DNA was synthesised from 1 µg equivalent RNA. The final concentrations of primers were used as follows- β-actin (100 nM) and cyclin D1, D2, p21 and p27 (200 nM each). The primers, template (c-DNA) and 2X SYBR green master mix and required amount of water were mixed up to a final volume of 20 µL. The real time PCR was performed for each sample in triplicate in optical 8 tube strip (0.2 mL) (MicroAmp™, Applied Biosystems, Singapore). Real time PCR was carried out in ABI 7500 Prism real time PCR machine (Applied Biosystems, USA) with standard 2 step PCR protocol. The fold change was calculated from

threshold cycle (C_t) by the following formula (Pfaffl, 2001) -

Fold change= $E^{\Delta\Delta C}{}_t$ where, E= PCR amplification efficiency and $\Delta\Delta C_t = \Delta C_{t,\ target} - \Delta C_{t,\ reference}$

Now, $\Delta C_{t,\ target}$= (C_t of gene of interest-C_t of housekeeping gene) $_{target}$

And $\Delta C_{t,\ control}$= ((C_t of gene of interest-C_t of housekeeping gene) $_{refernece}$

3.30 Cell proliferation assay

The cell proliferation assay was carried out by carboxyfluorescein diacetate succinimidyl ester (CFDA-SE) dye based flow cytometry analysis. The rate of cell division can be estimated by this experiment as the CFDA-SE concentration gets exactly half with each cell division and the after entry into the cells, the ester bonds gets cleaved by esterase, thus, only live cells show the fluorescence. Here, the cells were counted and equal number of IκBα over expressing as well as ordinary U87MG cells were stained with 5 µM CFDA-SE dye for 10 min, then the reaction was stopped with 1% BSA in PBS (10 mM) and the cells were washed three times with PBS by centrifugation at 300xg for 6 min at 4°C. Then the cells were equally subdivided into 4 parts, of which, 3 parts were seeded in 35 mm plate (BD falcon) for 24 h, 48 h and 72 h time point. Another part was immediately analysed by FACS.

3.31 Caspase-3 assay for detection of apoptosis

Caspases (Cistenyl Aspartate specific proteases) are the specific family of protein, which plays important role in apoptosis. Caspases play different roles in various stages of apoptosis. Caspase-3 is commonly regarded as effector caspase. Thus, caspase-3 level is an important indicator of apoptosis. U87MG and U87-IκBα cells were plated in equal number (10^5 cells per plate) in 100 mm plate. Then the cells were left to become confluent upto 70% of plate surface area, and the cells were treated with BSA loaded curcumin NPs. After 14 h of treatment, the media removed carefully, washed with cold PBS (10 mM, pH-7.4) and harvested with trypsin. The detached or semi attached cells were taken out with DMEM with FBS (also trypsin was neutralized), centrifuged at 450xg for 6 min in 4°C. The cells were counted in hemocytometer and washed with cold PBS twice. Then, cells were fixed with 0.1% formaldehyde in PBS in 37°C for 10 min. After the fixing solution was removed, the cells were washed carefully with PBS to avoid losing the cells and permeabilized with 0.5% tween-20 in PBS for 10 min in room temperature with mild shaking. After 10 min, the cells were collected by centrifugation and washed with PBS for two times. As per the initial count,

20 µL of antibody/10^6 cells (as per manufacturer's instruction) were added to the samples and incubated for 30 min in room temperature in dark. Then the samples were immediately analysed by FACS with 15000 cells per experiment. The data was analysed by histogram analysis in BD Cellquest Pro™ software.

4

RESULTS & DISCUSSIONS

RESULTS & DISCUSSIONS 4

This setion is subdivided into three parts-

PART-1. Cloning, expression, purification of recombinant IκBα. Synthesis of PVA/PVP hydrogel by oil based green synthesis method and encapsulation of recombinant GST tagged IκBα followed by functional delivery to the cancer cells. Further the combination effect of the protein and 5-FU was tested on glioblastoma cells.

PART-2. Polymeric curcumin nanoparticles were synthesized by PVP stabilization and the purified recombinant IκBα was loaded onto it via PLL. Then the combination module was tested against cancer cells for higher therapeutic efficacy.

PART-3. In order to check the effect of IκBα on the cancer cells, the IκBα gene was cloned in mammalian expression vector and transfected in U87MG cells. U87-IκBα stable cell line was established by G418 selection. 5-FU and BSA loaded curcumin NPs was administered to the U87-IκBα cells and U87MG cells to check the effect of IκBα on the sensitization of these cells.

Thus as a whole, this section documented the effect of IκBα on the cancer cells by adding from outside in a recombinant form and overexpressing in its native form inside the cancer cells when challenged with conventional anticancer drug 5-FU.

PART 1- *Functional delivery of hydrogel nanocarriers encapsulated recombinant IκBα to the cancer cells*

The work is presented in scheme 1-

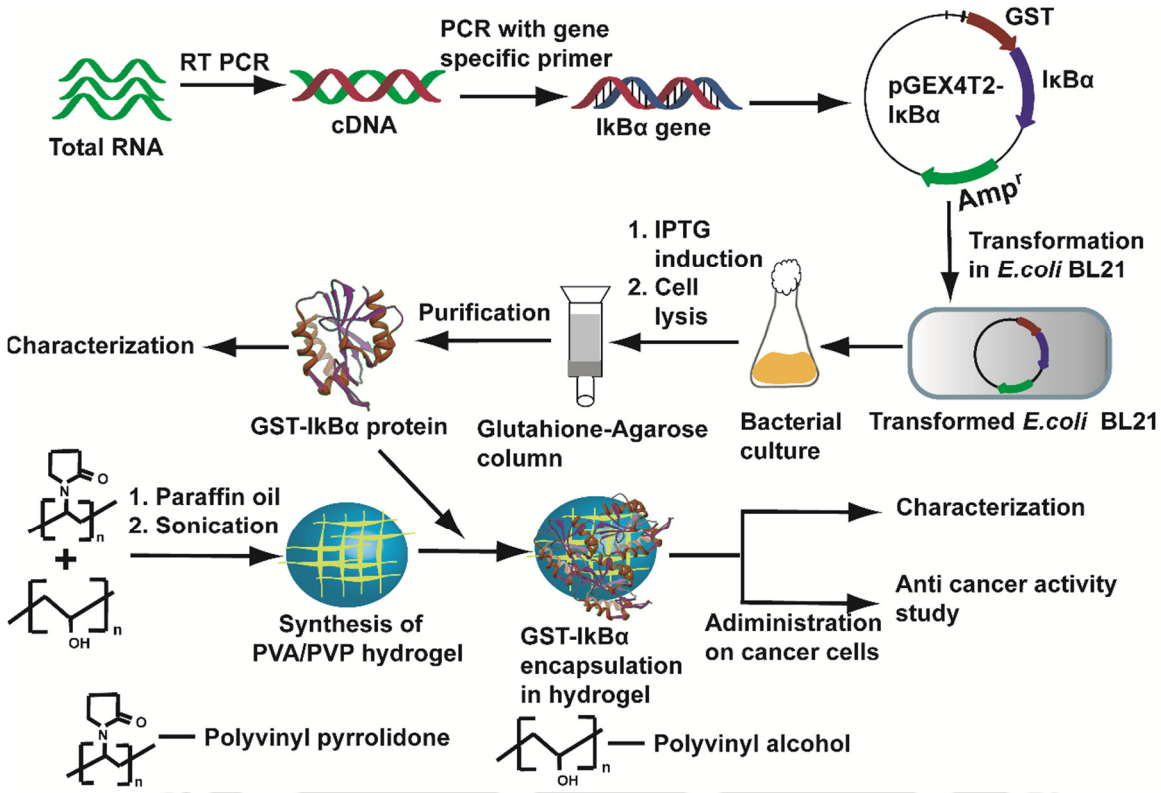

Scheme 1.1 Work plan of part 1.

1.1 Cloning of IκBα in pGEM T Easy vector

RNA was isolated from HT29 cells by RNA isolation method mentioned in the previous section. From the RNA, c-DNA was synthesised with random hexamer primers. The full length IκBα (954 bp) was PCR amplified by gene specific primers. The PCR amplicon was checked against DNA marker in 1% agarose gel, and the single band was observed in desired position (954 bp). The PCR amplfied full length IκBα was cloned into pGEM T Easy vector by using T4 DNA ligase. Then, the clone was confirmed by digestion with *Eco*RI restriction enzyme and the digested fragment was found in the same position of IκBα PCR amplicon against the DNA marker. Also, the cloning was reconfirmed by PCR based screening with gene specific primer (Figure 1). Further, the IκBα gene cloned in pGEMT Easy vector was sequenced by Sanger method and the sequncing result was compared with original IκBα sequnce to confirm that no mutations had occured during the process.

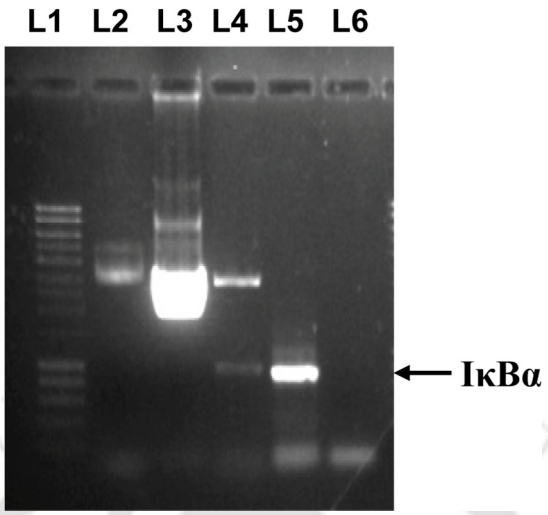

Figure 1.1 Cloning of IκBα in pGEM T Easy vector. L1: Marker, L2: control pGEM T, L3: IκBα-pGEMT, L4: IκBα-pGEMT digested with *Eco*RI, L5: PCR product of IκBα (954 bp), L6: no template control for PCR**.**

1.2 Cloning, expression and purification of IκBα in pGEX4T2 vector

Further, IκBα gene was subcloned in bacterial pGEX4T2 vector to generate the recombinant pGEX4T2-IκBα plasmid, as mentioned in the Materials and Methods section. The release of 954 bp IκBα fragment was observed by agarose gel electrophoresis after double digestion of the recombinant plasmid with *Bam*HI and *Xho*I restriction enzymes (Figure 2A). The pGEX4T2-IκBα clone was transformed in *Escherichia coli* BL21 (DE3) cells. The GST-IκBα recombinant protein was expressed upon IPTG induction and then purified to homogeneity using glutathione-agarose affinity column. The purified recombinant protein of molecular weight ~63 kDa was observed against protein marker in 12% SDS-PAGE (Figure 2B), which was further confirmed by immunoblotting with anti-IκBα antibody (Figure 2C).

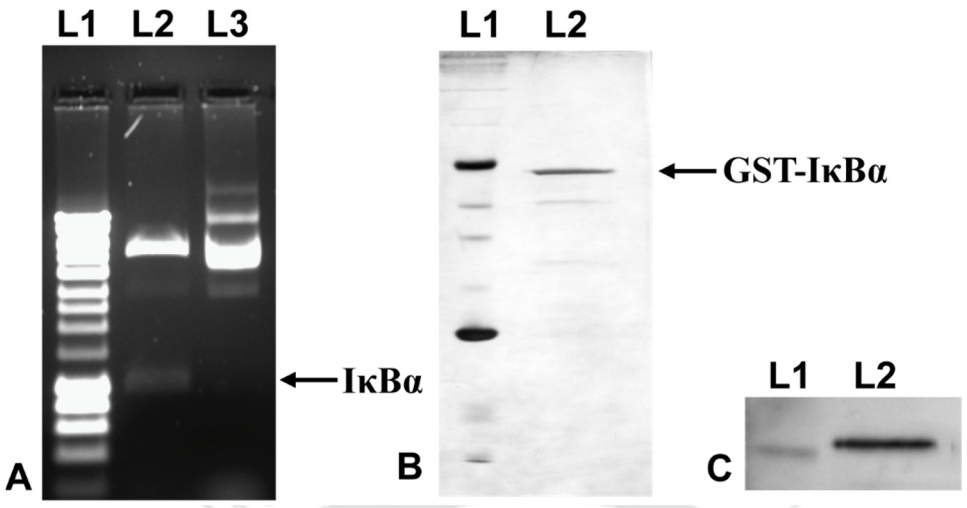

Figure 1.2 Cloning, expression and purification of IκBα in pGEX4T2 vector. (A) Lane 1-DNA marker (NEB Hyperladder), Lane 2- release of IκBα fragment upon double digestion with BamHI and EcoRI of recombinant IκBα-pGEX4T2 plasmid, Lane 3-undigested IκBα-pGEX4T2. (B) SDS-PAGE profile of purified recombinant GST- IκBα where Lane1- protein marker (NEB Broad range), Lane 2-purified GST- IκBα matches with expected 63 kDa size. (C) Western blot profile of confirmation of GST- IκBα where Lane 1-58 kDa band of protein marker (NEB color plus), Lane 2- GST- IκBα immunoblotted against mouse anti -human IκBα antibody.

1.3 Characterization by MALDI-TOF analysis

The purified protein was characterized by trypsin digestion profiling detected by MALDI-TOF analysis. The purified protein was eluted from 12% SDS-PAGE and trypsin digested following manufacturer's protocol (In gel trypsin digestion kit). Then, the trypsin digested peptide fragments were desalted by C_{18} column based ziptip™ method. The desalted peptides were mixed with 4-α cyano hydroxy cinnamic acid (CHCA) and subjected to MALDI-TOF analysis. The purpose of this experiment was to match the trypsin digestion pattern of the purified protein with available database. The representative mass spectra (MS) is shown below (Figure 3). The database search was done after MS-MS analysis by ProteinPilot™ software. The corresponding fragments were analyzed by searching against MASCOT database for human protein. The result matched with Nuclear Factor kappa B inhibitor alpha with a significant MOWSE score, which identified the purified protein as IκBα. When the same data was analyzed against prokaryotes, it gave the match with Glutathione S Tranferase

isolated from *Schistosoma japonicum*, which corroborated the previous data (Figure 1.2 B) with a proof that the protein had proper in frame translation and no mutation had happened during the process.

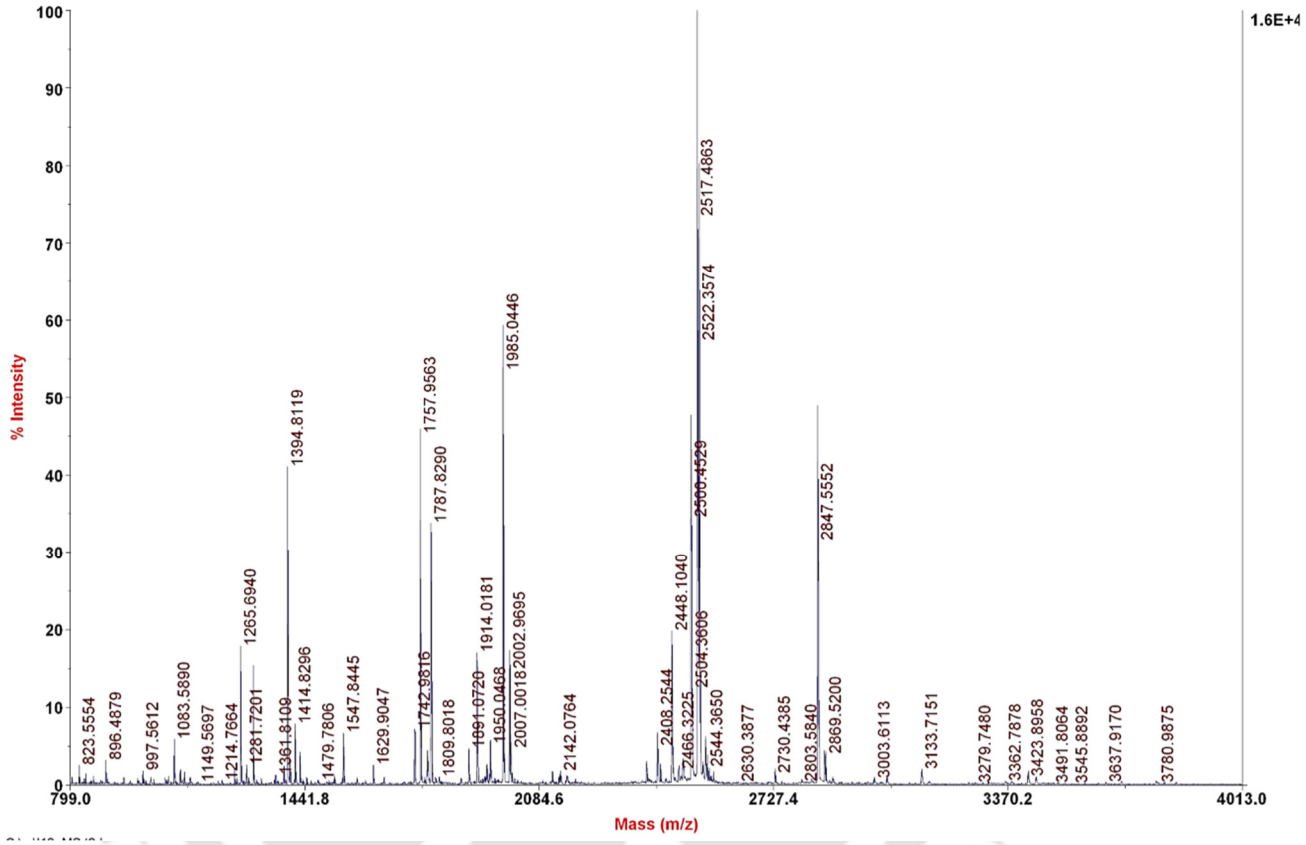

Figure 1.3 MALDI-TOF analysis. Mass spectra for trypsin digested GST-IκBα.

1.4 Secondary structure analysis by circular dichroism

The secondary structure of recombinant IκBα was analyzed by circular dichroism (Figure 1.4) which revealed the alpha helical signature of the protein with double minima at 222 nm and 208 nm and maximum at 193 nm (Greenfield and Fasman, 1969; Holzwarth and Doty, 1965; Croy *et al*, 2004; Greenfield, 2006) at 20ºC, which corresponds to the previous report of IκBα to support the structural integrity of purified recombinant IκBα.

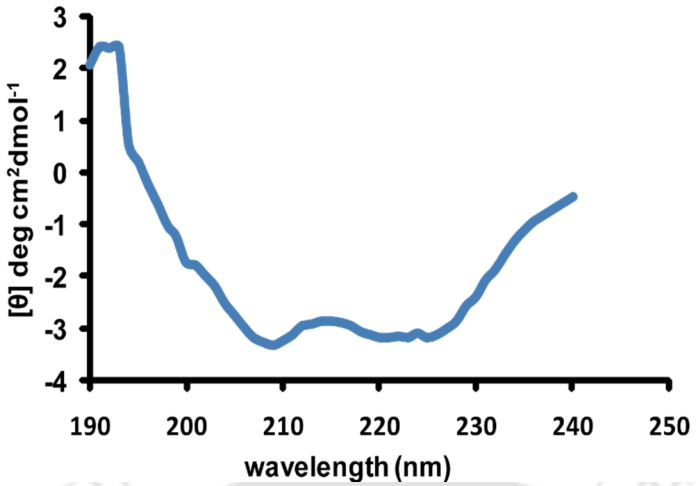

Figure 1.4 Circular dichroism. The CD spectra represents the secondary structure of purified GST-IκBα which shows predominance of alpha helix.

1.5 Characterization of recombinant IκBα encapsulated PVA/PVP hydrogel

The PVA/PVP hydrogel was synthesized by oil based phase separation followed by repeated freeze thaw method. The recombinant IκBα was encapsulated during the synthesis. After synthesis, the hydrogel was characterized by following methods-

1.5.1 TEM analysis

The synthesis of the NCs was confirmed by TEM analysis, which showed that majority of the NCs were spherical in shape and monodisperse in nature (Figure 1.5 A). The average particle size was found to be 320 ± 26 nm (Figure 1.5 C).

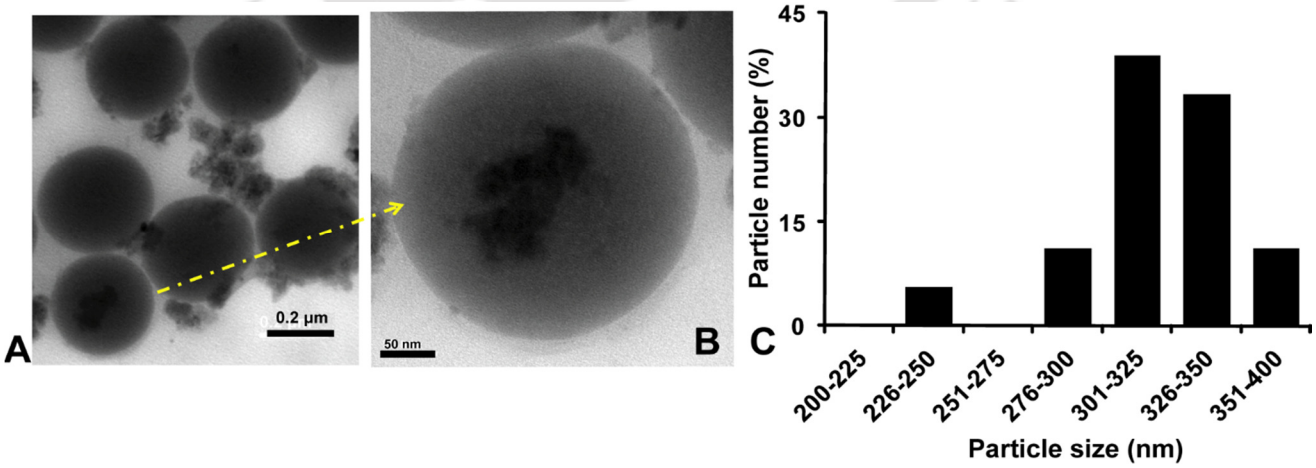

Figure 1.5 TEM image. (A) Protein (GST-IkBa) loaded hydrogel NCs and (B) Magnified

image of NC indicated by arrowhead. (C) Particle size distribution calculated based on TEM image, average particle size was found to be 320±26 nm.

1.5.2 FESEM analysis

The FESEM analysis reconfirms the spherical nanoparticle formation at a magnification of X25000 (Figure 1.6).

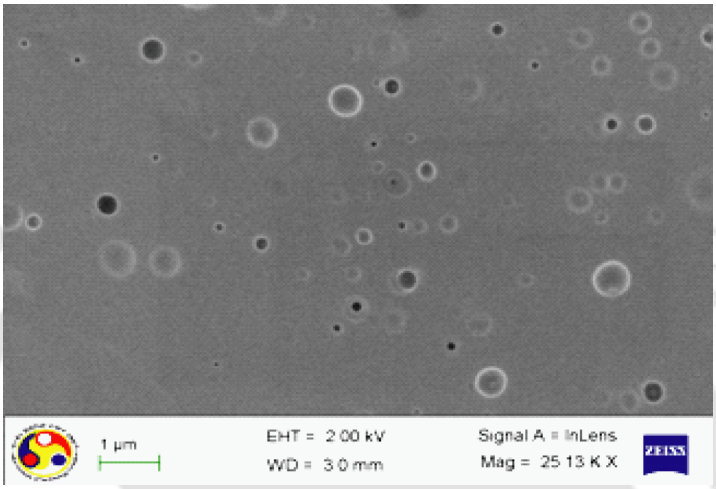

Figure 1.6 Field emission scanning electron micrograph of hydrogel nanocarriers.

1.5.3 Dynamic light scattering and zeta potential

The dynamic light scattering study revealed the mean hydrodynamic diameter of the protein loaded hydrogel NCs to be 421 nm (Figure 1.7 B), which is suitable for cellular uptake (Cleland *et al*, 1997). The blank hydrogel showed Z average diameter at 420 nm (Figure 1.7 A) with a smaller subset of particles below 300 nm. This is probably due to using the as synthesized particles for hydrodynamic diameter analysis, whereas for protein loaded hydrogel NCs, the solution used to be centrifuged before analysis. The zeta potential of the protein loaded NCs in PBS was found to be +0.65 mV.

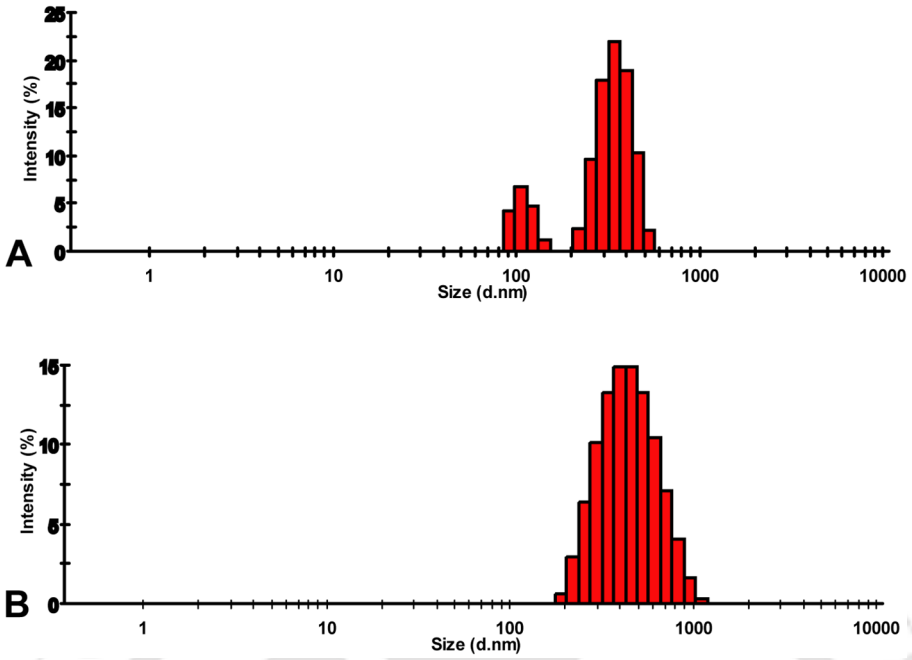

Figure 1.7 Dynamic light scattering. (A) Blank hydrogel Nanocarrier (average diameter 420 nm) and (B) protein loaded hydrogel nanocarrier (average diameter 421.18 nm).

1.5.4 FT-IR analysis

To probe the interaction between hydrogel and protein we have carried out the FTIR analysis. It showed that all the peaks remain unaltered in case of protein loaded hydrogel NCs as compared to the hydrogel NCs alone. However, one extra peak was observed at 1650 cm-1 for C=O stretch for amide band I and another peak was found at 1549 cm-1, which corresponds to the stretching vibrations of C-N and bending vibrations of N-H of amide band II (Kong and Yu, 2007) confirming the presence of the protein with hydrogel NCs (Figure 1.8).

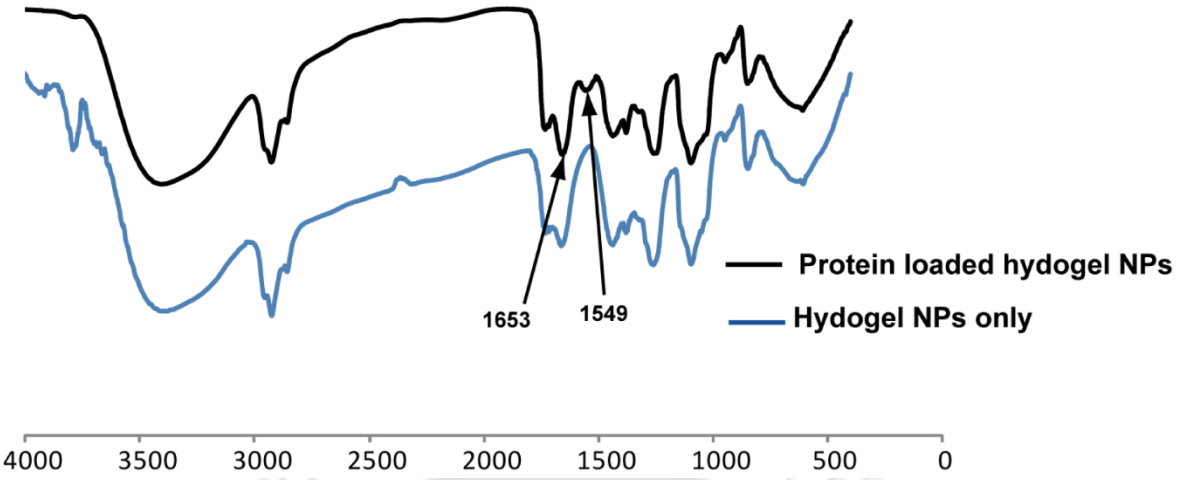

Figure 1.8 FT-IR analysis of only hydrogel NPs and protein loaded hydrogel NPs.

1.6 pH dependent protein release

Before adding the protein loaded hydrogel NCs to the cancer cells, protein release was studied *in vitro*, which revealed that about 80% protein was released within 3 h at pH 4.2 ± 0.2, whereas 65% of release was obtained around 24 h at pH 7.2 ± 0.2 at 37°C (Figure 1.9). It implies that the protein release was significantly low in physiological condition or cell culture media. Therefore, these conditions might allow sustained release of GST-IκBα once internalized inside the cells (Rejman *et al*, 2004). The recombinant protein (GST-IκBα) might have interacted with the PVA/PVP hydrogel via non-covalent interactions (H-bonding, hydrophobic etc.) (Oh *et al*, 1980; Rawat *et al*, 2010). That would exist predominantly in neutral form at lower pH, as the pI of the protein is ~4.9 (theoretical value obtained from ExPASy). As a consequence, the interactions involved might have been affected, which had led to the higher release of protein at lower pH as compared to physiological pH. It is to be mentioned here that about 69% protein was encapsulated in the PVA/PVP NCs calculated based on the loading efficiency mentioned in equation 1 in Materials and Methods section.

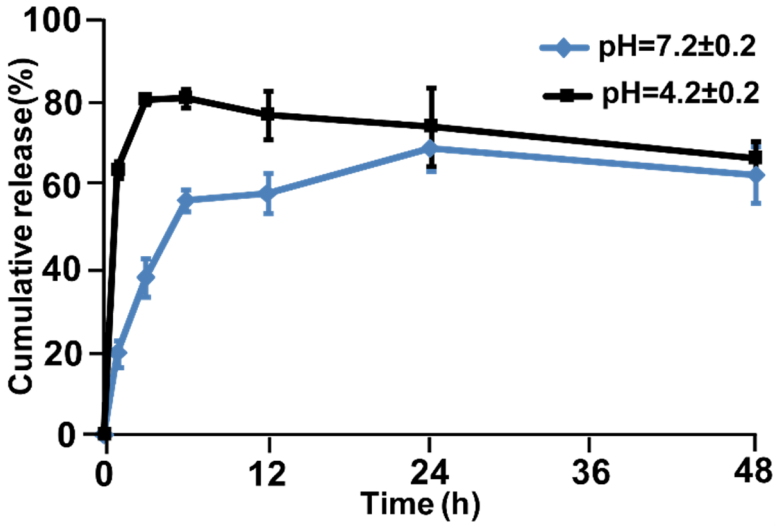

Figure 1.9 pH tunable protein release. *In vitro* protein release study at pH 4.2 ± 0.2 and pH 7.2 ± 0.2 at 37° C. All data were represented as mean ± SD of three individual experiments.

1.7 Hydrogel NC mediated delivery

Before adding the protein loaded hydrogel NCs onto the cancer cells, the interactions of hydrogel NCs with the cells was probed. For that, FITC-dextran was encapsulated into the hydrogel NCs and was administered to the HeLa as well as U87MG cells. Epi fluorescence microscopy image (Figure 1.10 A and Figure 1.10 C) of hydrogel NC treated cells (for 3 h) showed green fluorescence of FITC-dextran (excitation band pass filter at 480/30 nm).

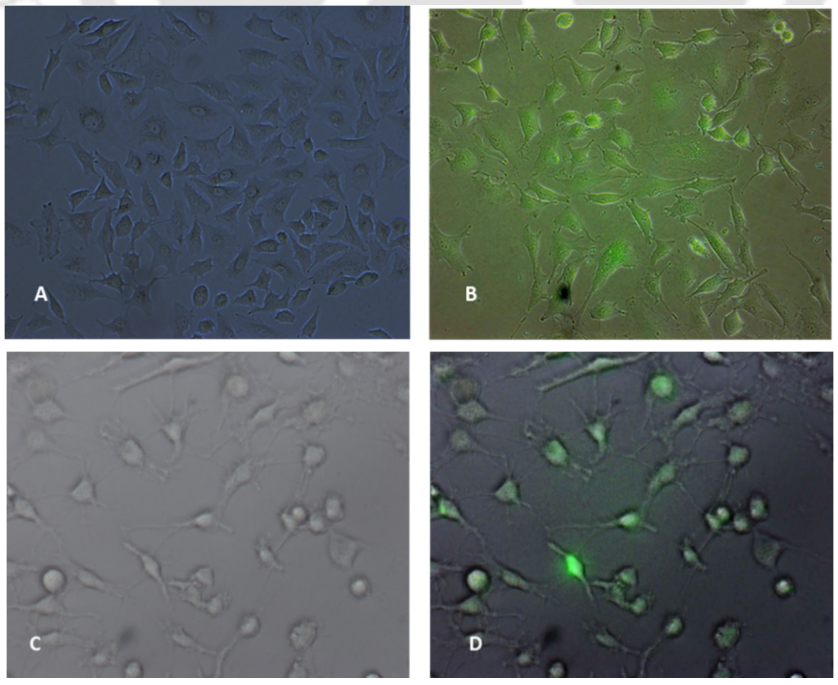

Figure 1.10 Microscopic observation of hydrogel NCs delivery. (A) Bright field image of HeLa cells, (B) Merged image of bright field image and blue light (480/30 nm) of HeLa cells. (C) Bright field image of U87MG cells, (B) Merged image of bright field image and blue light (480/30 nm) of U87MG cells.

In addition, flow cytometry (FACS) was carried out for FITC-dextran loaded NCs treated and untreated (control) cells, where visible shifting of fluorescence intensity was observed in the FL1 channel (which corresponds to green emission) for both HeLa and U87MG (Figure 1.11 B and Figure 1.11 D) with 5.28 % and 5.35 % uptake were observed for HeLa and U87MG respectively (Figure 1.11), which unambiguously established the interactions between NCs and cells.

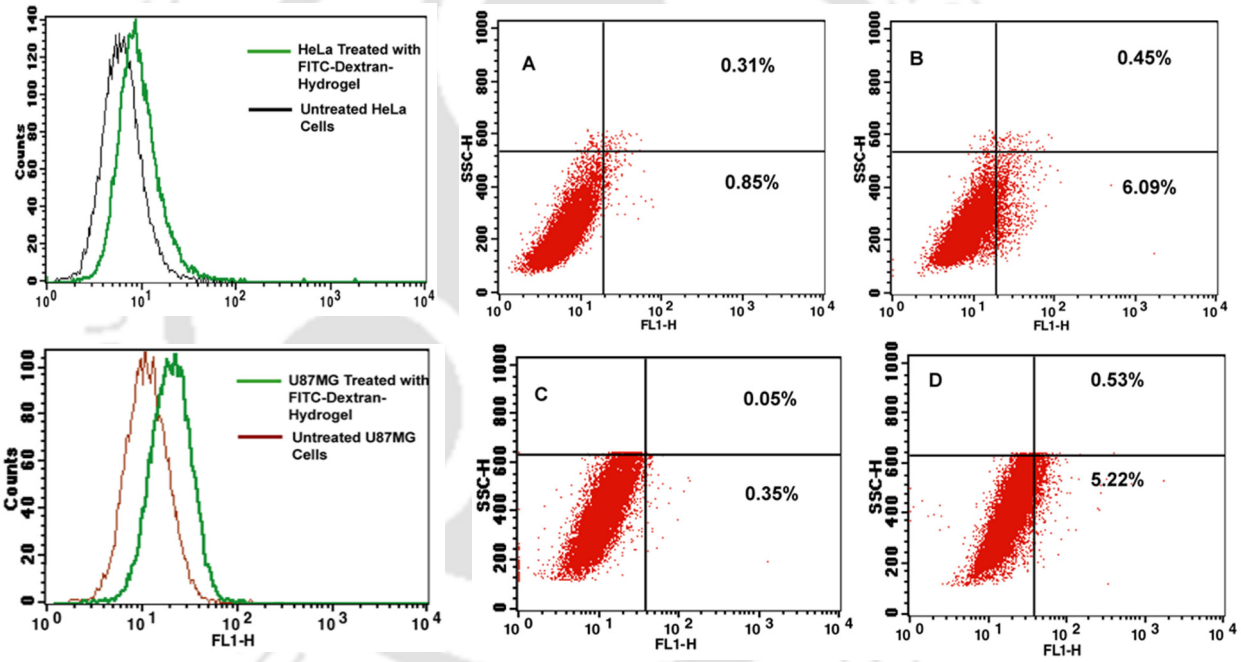

Figure 1.11 Flow cytometry based analysis of hydrogel NCs mediated FITC-Dextran delivery. Upper panel represents the flow cytometry based uptake analysis of HeLa cells with a visible shift of FITC-dextran encapsulated hydrogel treated cells in histogram plot and quantitative analysis of uptake by dotplot analysis of (A) untreated HeLa cells, (B) HeLa cells treated with FITC-dextran encapsulated hydrogels. Lower panel represents the flow cytometry based uptake analysis of U87MG cells with a visible shift of FITC-dextran encapsulated hydrogel treated cells in histogram plot and quantitative analysis of uptake by dotplot analysis of (C) untreated U87MG cells, (B) U87MG cells treated with FITC-dextran encapsulated hydrogels.

The cellular uptake (~5%) at 3 h was possibly due to time dependent quenching of FITC-Dextran fluorescence in cellular environment, as higher uptake (~12%) was observed at initial 1 h (Figure1.12 A). When the treated HeLa cells were analyzed by flowcytometry after 6 h, much lower fluorescence was observed at Fl-1H channel (1.12 B).

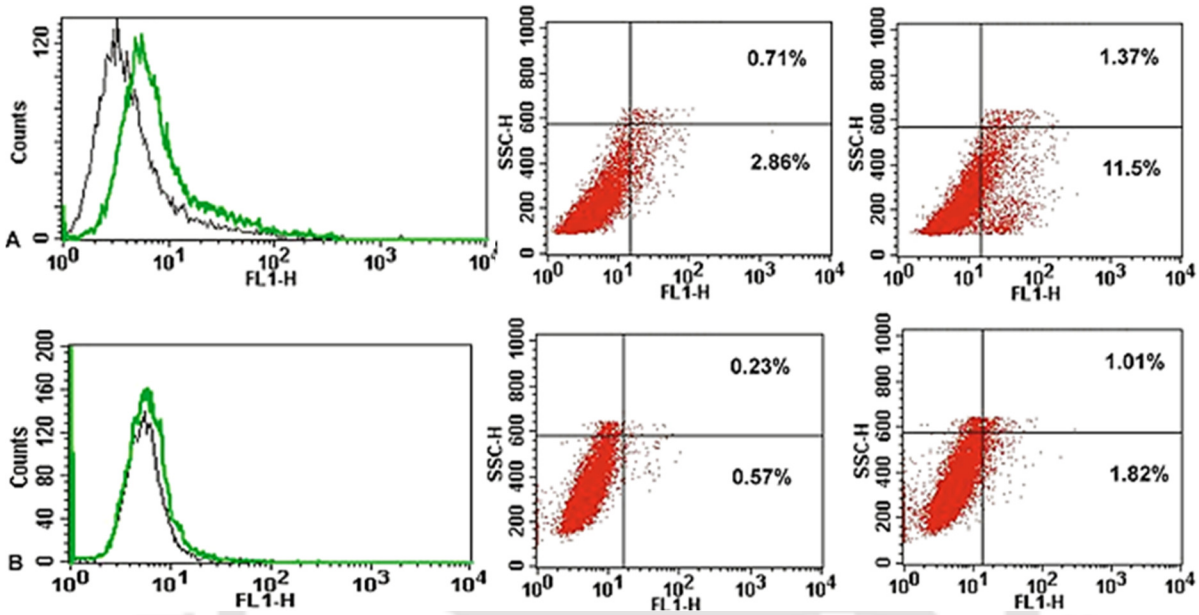

Figure 1.12 Uptake of FITC-Dextran encapsulated hydrogel by HeLa cells (A) in 1 h and (B) 6 h.

1.8 Detection of recombinant protein delivered via nanocarriers

Western blot analysis using mouse anti-human IκBα was performed to ensure hydrogel mediated delivery of GST- IκBα inside the cells (Figure 1.13). For that, the Hela cells were treated with 22.8 µg/mL of GST-IκBα loaded hydrogel NCs containing 300 ng/mL of GST-IκBα (2IC50). Similarly, the cells were treated with blank hydrogels and purified GST- IκBα protein for 12 h. The 63 kDa band corresponding to GST-IκBα in lane 6 of treated cell lysate confirmed that the protein was delivered into the HeLa cells. The 37 kDa band in lanes 3-6 was due to endogenous IκBα. β tubulin (55 kDa) was used as loading control (Figure 1.13 B).

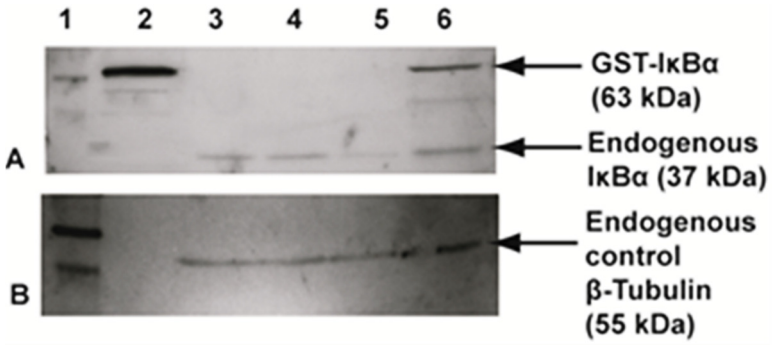

Figure 1.13 Western blot showing hydrogel mediated GST-IκBα delivery to HeLa cells, where (A) Lane 1-protein marker, Lane 2-purified GST-IκBα (positive control), Lane 3-untreated cells, Lane 4-cells treated with only hydrogel, Lane 5-cells treated with purified GST-IκBα (only protein), Lane 6-cells treated with GST-IκBα encapsulated hydrogel (B) β tubulin loading control in same order of sequence

1.9 Effect of GST- IκBα on cell growth

To find out the effects of recombinant IκBα encapsulated hydrogel NCs, the HeLa cells were treated with different concentrations of protein loaded for 24 h. The same weight ratio of blank hydrogel NCs was used to find out the effects of hydrogel NCs only. XTT assay showed that cell viability was significantly decreased with the increasing concentrations of protein (Figure 1.14), as compared to their respective controls (blank hydrogel NCs treated cells) (Figure 1.15). The IC_{50} (the dosage at which cell viability reduces to 50%) concentration of GST- IκBα loaded NCs was found to be 150 ng/ml of protein. The IC_{50} value of GST- IκBα loaded NCs was found to be 11.4 µg/mL, containing 150 ng/ml of GST-IκBα protein.

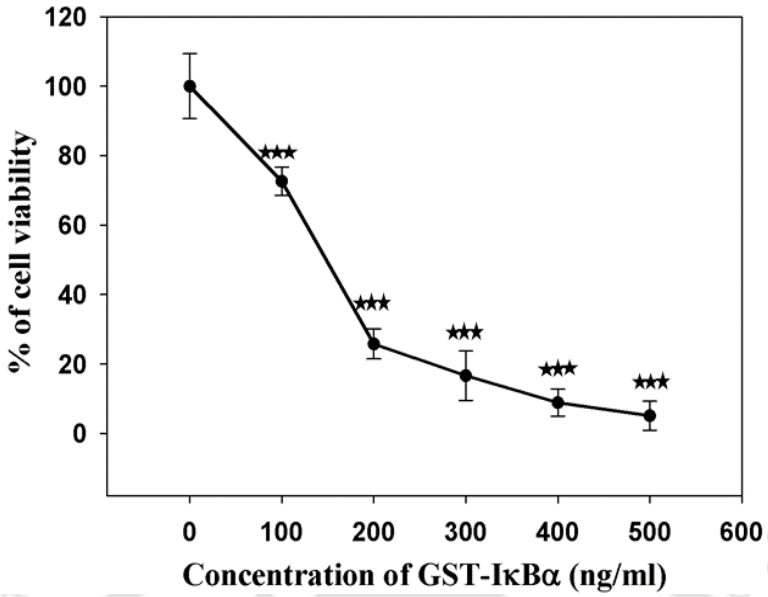

Figure 1.14 Cell viability assay of HeLa cells treated with different concentrations of hydrogel encapsulated GST-IκBα. All data are represented as mean ± SD of three individual experiments. Statistical significance between non treated control and treated samples were denoted by *** ($p<0.001$).

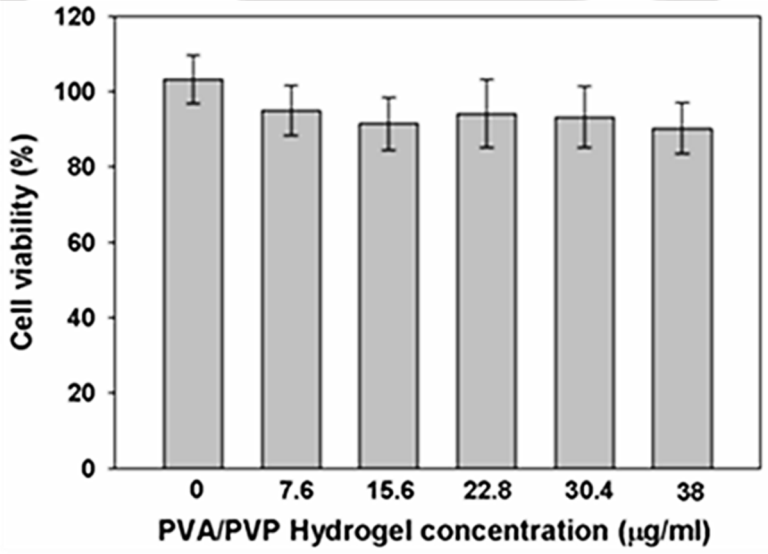

Figure 1.15 Cell viability assay of HeLa cells treated with different concentrations of blank hydrogel NCs. All data are represented as mean ± SD of three individual experiments.

Also, cytotoxicity assay performed under similar conditions on human embryonic kidney (HEK 293) exhibited cell growth inhibition (Figure 1.16) as the hydrogel was not functionalized with any cancer cell targeting molecule (e.g.-folic acid), which also indicated

that this module may exert anti cell proliferative effect on a range of cell lines.

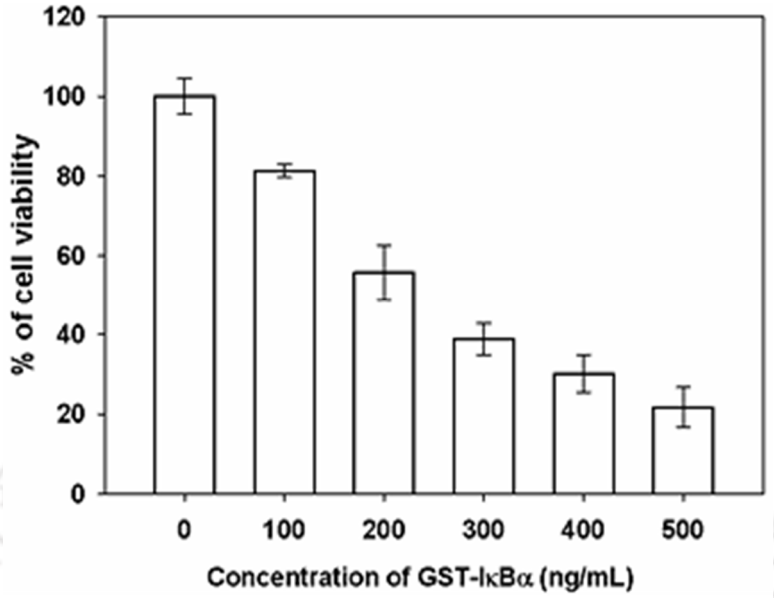

Figure 1.16 Cell viability assay of normal cell line (HEK cells) treated with different concentrations of hydrogel NCs encapsulated GST-IκBα. All data are represented as mean ± SD of three individual experiments.

1.10 Effect of GST IκBα on cell cycle

To investigate possible role of GST- IκBα hydrogel nanocarriers on the cell cycle, propidium iodide based cell cycle analysis (measurements of amount of DNA in various stages of cell division cycle such as G0/G1, S and G2/M) was performed for treated cells against control untreated cells and blank hydrogel NCs by FACS. For that, HeLa cells were treated with IC_{50} dose of protein loaded NCs for 24 h. From the FACS analysis (Figure 1.17), a significant sub-G_0 (5.6%) apoptotic population was observed in treated cells as compared to the control cells. It should be mentioned here that, treatment with only hydrogel NCs resulted in increased numbers of cells for both S and G_2/M populations, but there was no significant increase in sub G_0 population observed. This result indicated that GST-IκBα, delivered via hydrogel NCs played role in the apoptotic death of HeLa cells.

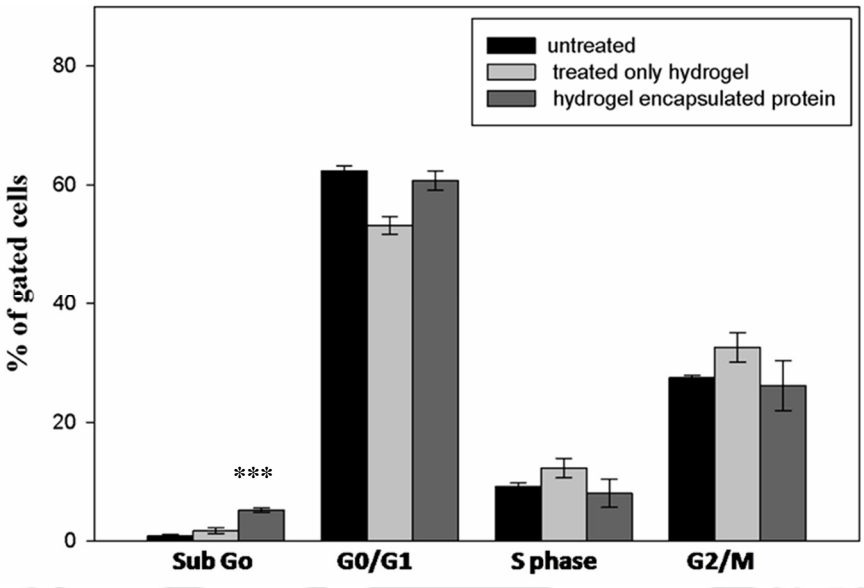

Figure 1.17 Effect of hydrogel encapsulated GST-IκBα on cell cycle in HeLa cells evaluated by calculating the percentage of cells in each phase from flow cytometry data. The values are represented as mean ± SD of three individual experiments. Statistical significance between untreated control and treated samples were denoted by *** ($p<0.001$).

1.11 GST-IκBα induces apoptosis

Further, to confirm the above observation, IC_{50} dose of protein loaded hydrogel NCs was added into the HeLa cells for 12 h (first and second panel from top) and 24 h (third and fourth panel) and the AO/EB dual staining was performed. Fluorescence microscopy of merged images revealed that live cells showed green fluorescence and dead cells showed red fluorescence due to differential uptake of AO and EB, respectively. The number of red cells (EtBr positive cells) increased with time in case of hydrogel NCs treated cells as compared to the respective control cells (without NCs treated cells) (in the third and fourth panel where HeLa cells are treated for 24 h). Careful observation revealed that protein treated cells with red fluorescence depicted nuclear condensation and fragmentation, which were typical signatures of apoptosis, as compared to the normal cells which mostly stained with green.

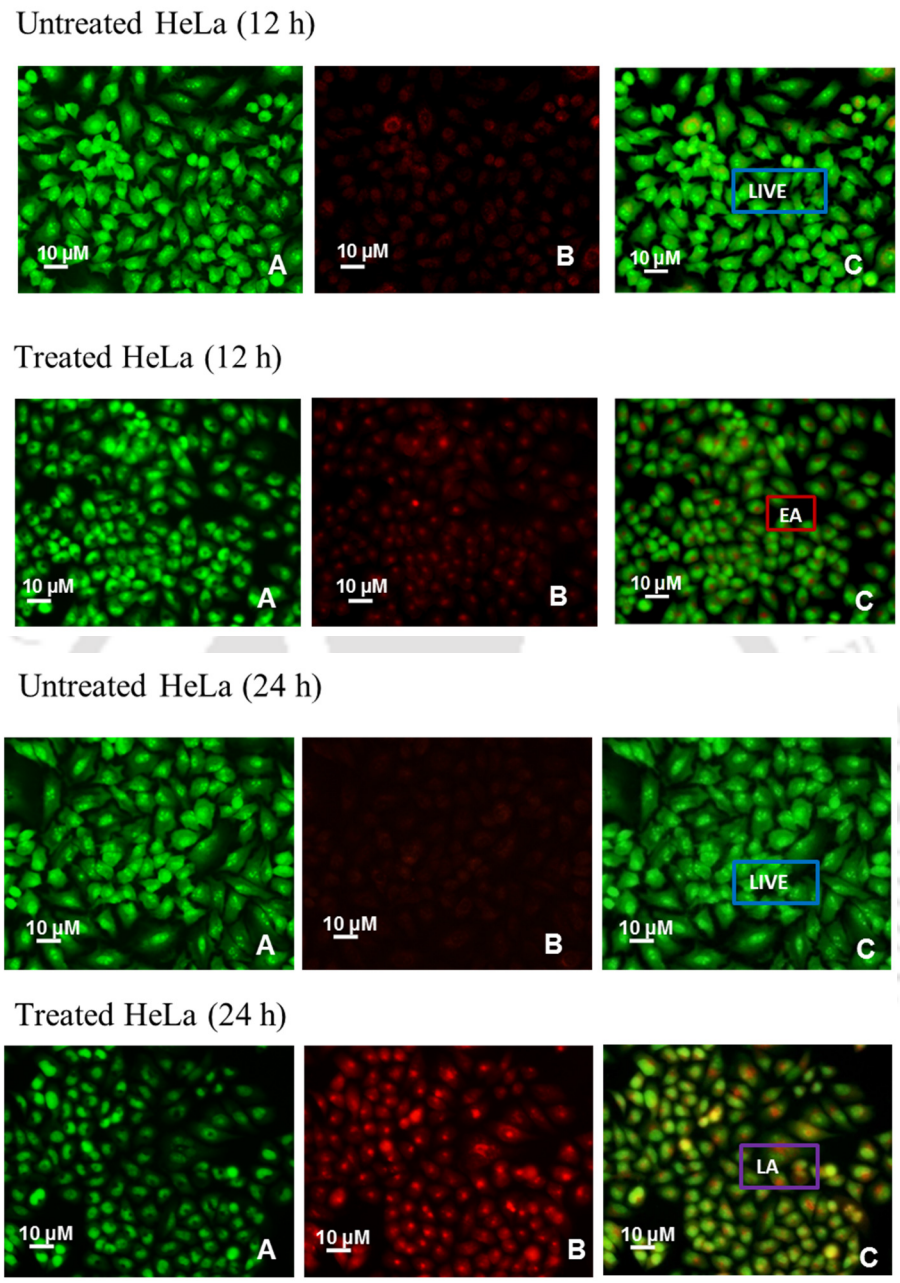

Figure 1.18 For all panels, (A) Acridine orange stained HeLa cells, (B) Ethidium bromide stained HeLa cells and (C) Merged image of (A) and (B). EA indicates early apoptotic cells, LA indicates late apoptotic cells.

The scanning electron microscopy image of the treated cell (for 24 h) (Figure 1.19 B) also showed the membrane blebbing of the HeLa cells, a typical signature of apoptosis, whereas the control cells (Figure 1.19 A) were had a comparatively smooth surface.

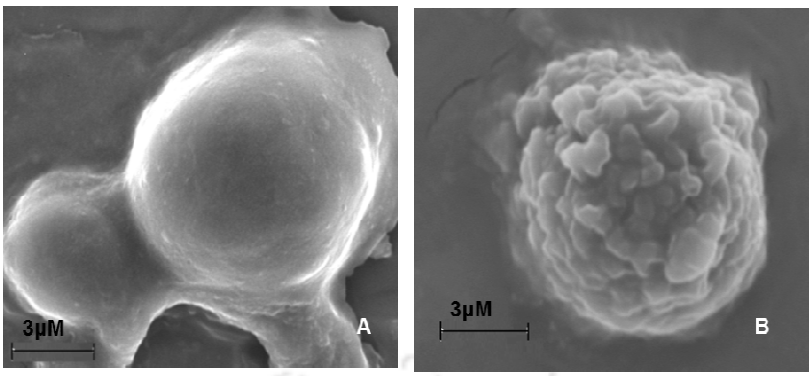

Figure 1.19 Scanning electron micrograph of (A) untreated HeLa cells, (B) treated HeLa cells showing membrane blebbing.

1.12 TUNEL Assay

To further confirm the characteristics of apoptotic cells, HeLa cells treated with 150 ng/mL IκBα-hydrogel for 24 h, were analyzed by APO-BrDU TUNEL assay as per the manufacturer's protocol. The assay displayed significant increase in bromodeoxyuridine incorporation to the 3' OH end of the broken DNA strand, which is a characteristic feature of late apoptosis. FACS analysis showed about 10% TUNEL positive apoptotic population of the treated cells (Figure 1.20).

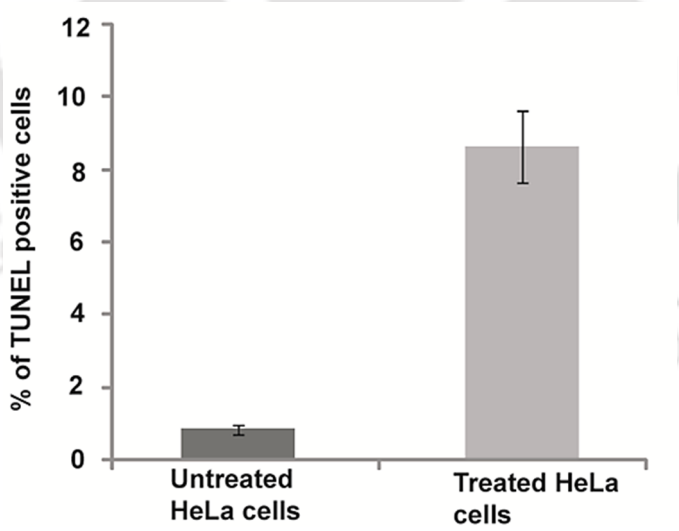

Figure 1.20 Effect of hydrogel encapsulated GST-IκBα on HeLa cells evaluated by APO-BrDU TUNEL assay by calculating the percentage of cells in live and apoptotic population from flow cytometry data. The values are represented as mean ± SD of three individual experiments.

1.13 Effect of GST-IκBα in conjugation with 5-FU

Finally, we have chosen 5- fluorouracil (FU) resistant U87MG cells (glioblastoma) to measure any possible effect of GST-IκBα loaded hydrogel NPs in combination with 5-FU. As U87MG cells are drug resistant, only 5-FU (Figure 1.21 B) and only GST-IκBα protein encapsulated NCs (Figure 1.21 A) did not show significant anti-cell proliferative effects even at their highest concentration. However, combination of 5-FU and GST-IκBα loaded NCs (containing 300 ng/mL of protein) showed significant cell growth inhibition. The IC_{50} value of 5-FU was found to be 100 µM. Interestingly our results indicated that the 'combination therapy' with 5-FU and GST-IκBα protein encapsulated NCs could possibly augment sensitization of drug resistant U87MG cells compared to the individual components.

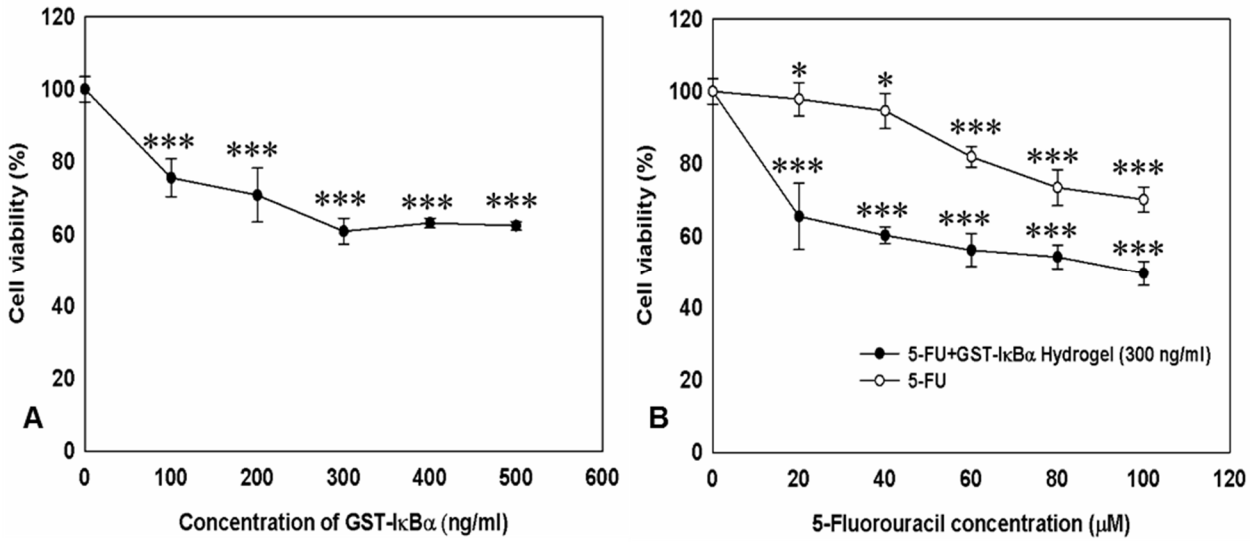

Figure 1.21 (A) Effect of hydrogel encapsulated GST-IκBα on U87MG cells, (B) Hydrogel encapsulated GST-IκBα mediated sensitization of U87MG upon treatment with 5-FU. All data are represented as mean ± SD of three individual experiments. Statistical significance between untreated control and treated samples were denoted by *** ($p<0.001$) and *($p<0.05$)

Conclusions of part 1

In brief, IκBα was cloned and expressed as recombinant GST tagged IκBα protein. The functional delivery was performed by using conventional nontoxic hydrogel NCs composed of PVA/PVP. The cell growth inhibition was observed and Western blot experiment confirmed delivery of recombinant IκBα into the cells. Moreover, FACS based cell cycle analysis and TUNEL assay confirmed apoptotic cell death. The obtained results indicate that after internalization via hydrogel NCs, the GST-IκBα was released inside the cells, which

induced apoptosis (**Scheme 1.2**). The excess amount of IκBα inside cells may have block translocation of NFκB and thereby, alter the expression of downstream genes causing cell death. The use of recombinant IκBα is a quite novel approach in protein therapeutics of cancer. The experiment on drug resistant U87MG cells showed that the recombinant IκBα administration could ameliorate the action of 5-FU, which may further be explored to augment chemotherapeutic efficacy of anticancer drugs in drug resistant cancer cells. Thus, the recombinant IκBα may have important implications as a therapeutic agent in cancer treatment, based on inhibition of the overexpressed NFκB protein - primarily responsible for conferring drug resistance to cancer cells.

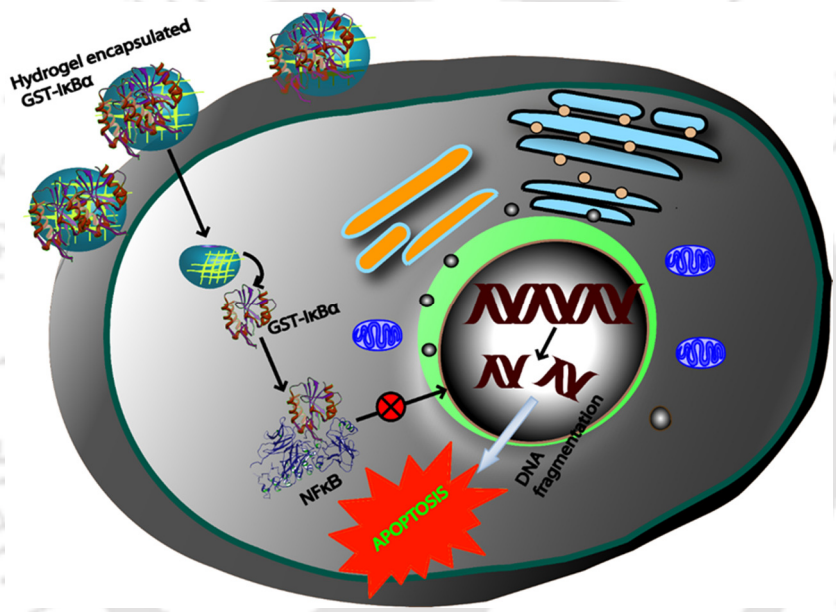

Scheme 1.2 Mode of action of GST tagged IκBα encapsulated hydrogel upon cancer cells.

From the above result, it was clear that IκBα has different effects on two different types of cancer cells. The drug resistant U87MG cells were found to be sensitized by combination effect of 5-FU and IκBα. This result leads to the work of second part of this thesis work.

PART 2- *Effect of IκBα loaded curcumin nanoparticles on cancer cells*

The work plan is presented by the following scheme-

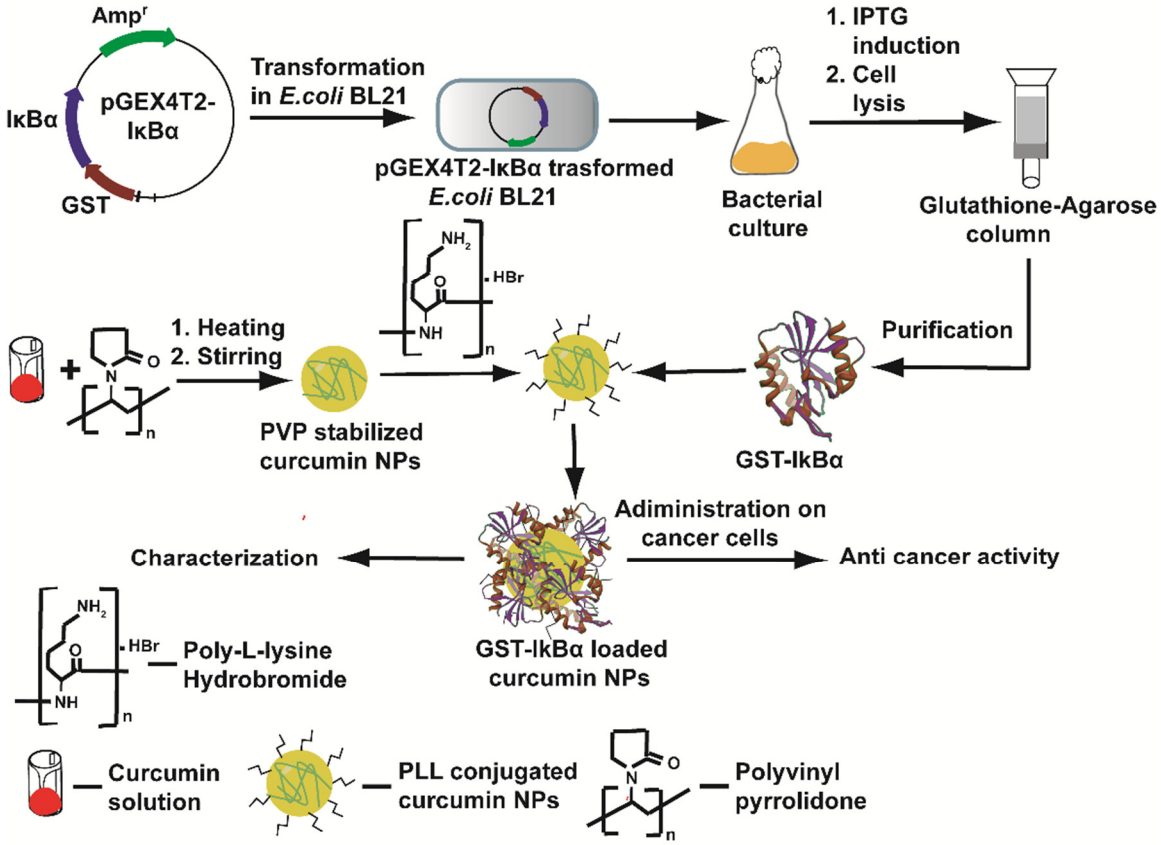

Scheme 2.1 Work plan for part 2

In continuation of the work of first part, another bioactive agent was chosen for combination therapy in a single module. For that purpose, curcumin was selected, and nanoparticle was synthesized as mentioned in previous section and recombinant IκBα was loaded onto it. Then the combined module was tested against HeLa and U87MG cells for heightened effects.

2.1 Generation of GST tagged IκBα loaded curcumin nanoparticles

Initially, the recombinant GST tagged IκBα was purified by glutathione-agarose affinity chromatography to homogeneity, which appeared as a 63 kDa single band protein in 12% SDS-PAGE (Figure 1A). Then, we developed an aqueous 'green synthesis' method for making curcumin NPs by solvent evaporation induced chemical precipitation using PVP and PLL. The UV-vis absorbance maximum of the curcumin NPs observed at 430 nm remained almost unchanged when conjugated with PLL and recombinant IκBα protein (Figure 2.1).

However, the absorbance spectrum of curcumin solution alone appeared at 420 nm as a shoulder.

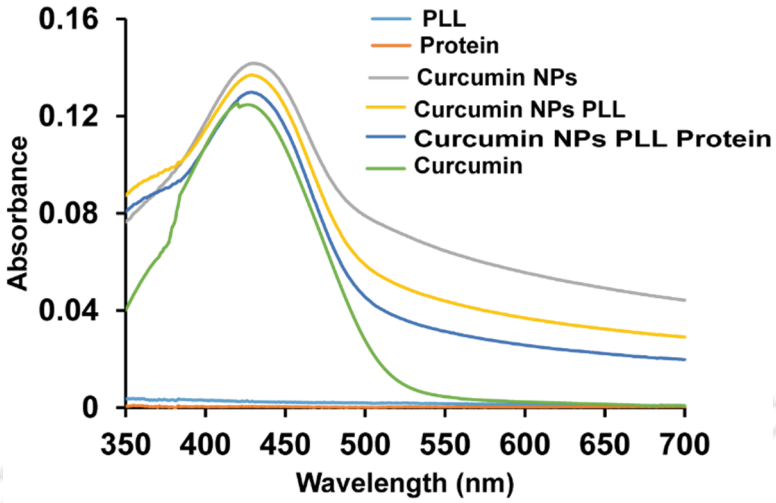

Figure 2.1 UV-Vis spectroscopy of IκBα loaded curcumin NPs and its various controls.

In fluorescence spectroscopy, curcumin NPs showed emission at 550 nm when excited by blue light (430 nm) (Figure 2.2). It should be mentioned here that curcumin has intrinsic green emission upon blue light excitation although its emission maxima varies based on the solvent polarity. The emission maximum (λmax) of free curcumin in aqueous solution was found to be at 555 nm with characteristic broad spectrum in polar solvent as reported (Chignell *et al*, 1994). With addition of PLL on the curcumin NPs, the emission maxima (λemission at 550 nm) marginally blue shifted accompanied by decreased in fluorescence intensity. The emission peak further shifted to 541 nm after addition of recombinant IκBα.

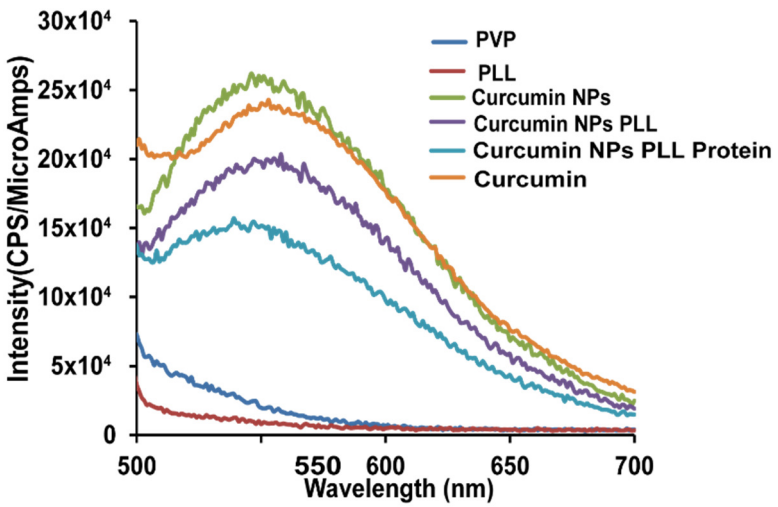

Figure 2.2 Fluorescence spectroscopy of IκBα loaded curcumin NPs and its various controls.

2.2 Characterization of protein loaded curcumin NPs

The PVP and PLL acted as stabilizing agents for curcumin NPs, where PLL additionally provided overall positive charge to the NPs at physiological pH. The recombinant IκBα is negatively charged (isoelectric point = 4.2), offering the plausibility of electrostatic interactions with the positively charged NPs. The interaction was supported by the sequential analysis of zeta potential of the curcumin NPs, the same NPs conjugated with PLL and the recombinant IκBα. It revealed that the zeta potential value was -9.3 mV for curcumin NPs, whereas PLL conjugated curcumin NPs had zeta potential of +23.7 mV, which further decreased to +18.2 mV when loaded with the recombinant protein. The hydrodynamic diameter of the curcumin NPs was found to be 160.3 nm (Figure 2.3 A), whereas the PLL coated curcumin NPs was 195.7 nm (Figure 2.3 B), which further increased to 203.1 nm (Figure 2.3 C) for protein immobilized NPs.

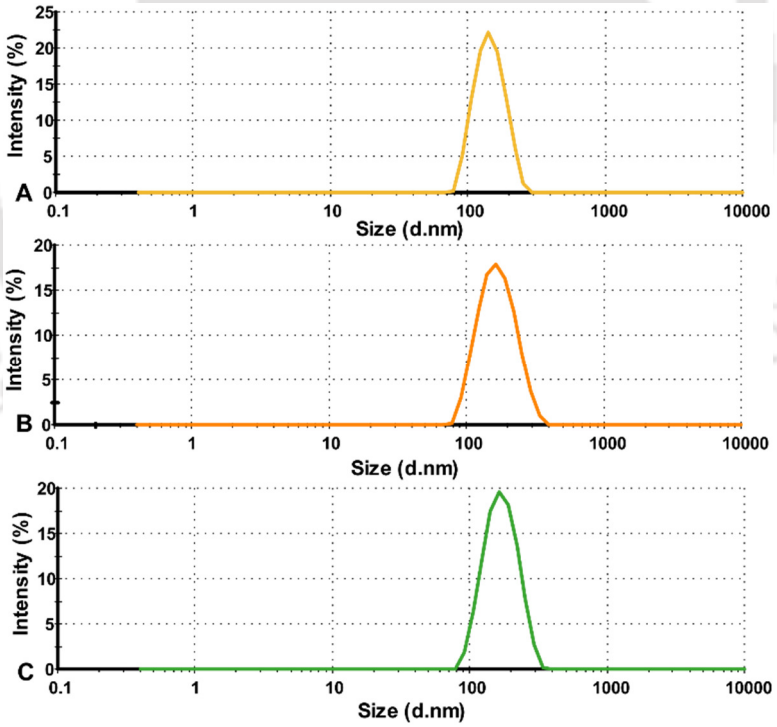

Figure 2.3 Hydrodynamic diameter analysis. (A) Curcumin NPs was 160.3 nm, (B) Curcumin NPs with PLL was 195.7 nm and (C) Curcumin NPs with PLL and recombinant IκBα was 203.1 nm respectively.

The recombinant IκBα loaded curcumin NPs were also characterized by TEM analysis (Figure 2.4 A and B), and the particle size distribution was calculated from different images (Figure 2.4 C). The average particle size obtained by TEM analysis was found to be 102 ±10 nm.

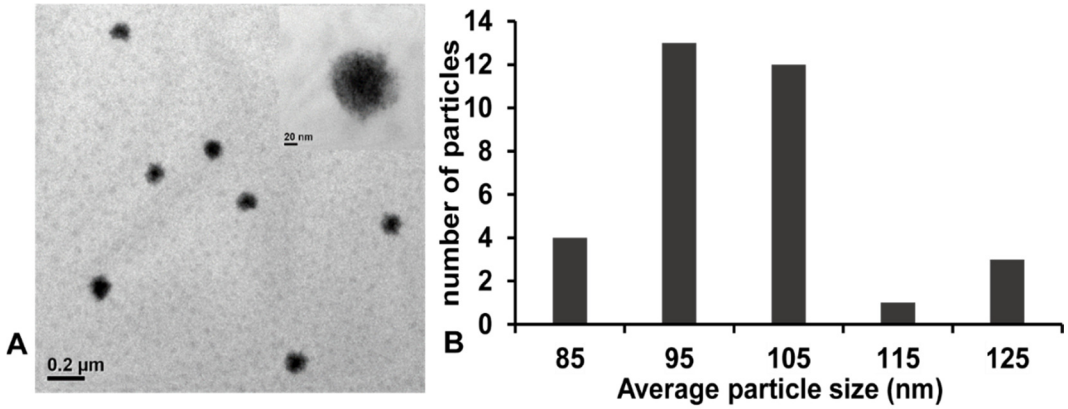

Figure 2.4 (A) TEM image of IκBα loaded curcumin NPs, NPs shown at higher magnification in the inset. (B) The particle size distribution calculated based on the TEM image with class interval of 5 nm. Average particle size was found to be 102±10 nm.

The nanoparticle formation and shape was further reconfirmed by field emission scanning electron microscopy (FESEM) (Figure 2.5).

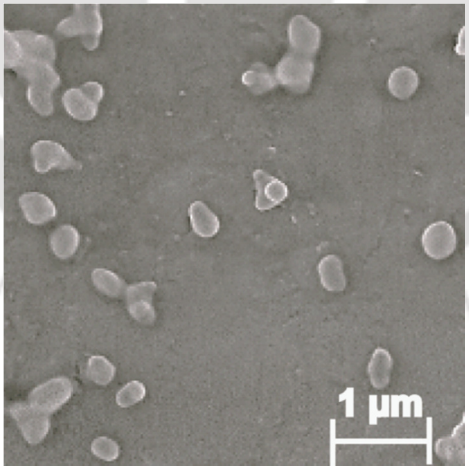

Figure 2.5 Field emission scanning electron micrograph of protein loaded curcumin NPs.

2.3 Interaction of IκBα loaded curcumin NPs with cancer cells

The interaction of the NPs with the cell surface was established by microscopy study. For that, U87MG and HeLa cells were incubated with 6 µg/mL of recombinant IκBα loaded

curcumin NPs (each µg of curcumin NPs contains 31 ng of GST-IκBα) for 2 h, and washed thoroughly to remove residual NPs. Then, the treated cells were stained with nuclear staining dye DAPI and observed under the epi-fluorescence microscopy. Fluorescence microscopy images showed green fluorescence emission at the surface of the treated cells when excited with UV light due to interaction of curcumin NPs with the cells. The nuclei showed blue emission due to characteristic emission of DAPI when excited with UV light (Figure 2.6 B and D).The merged images showed both blue and green emission in case of NPs treated cells (Figure 2.6 B and D), whereas the control (untreated) cells showed only blue emission due to the uptake of DAPI only (Figure 2.6 A and C).

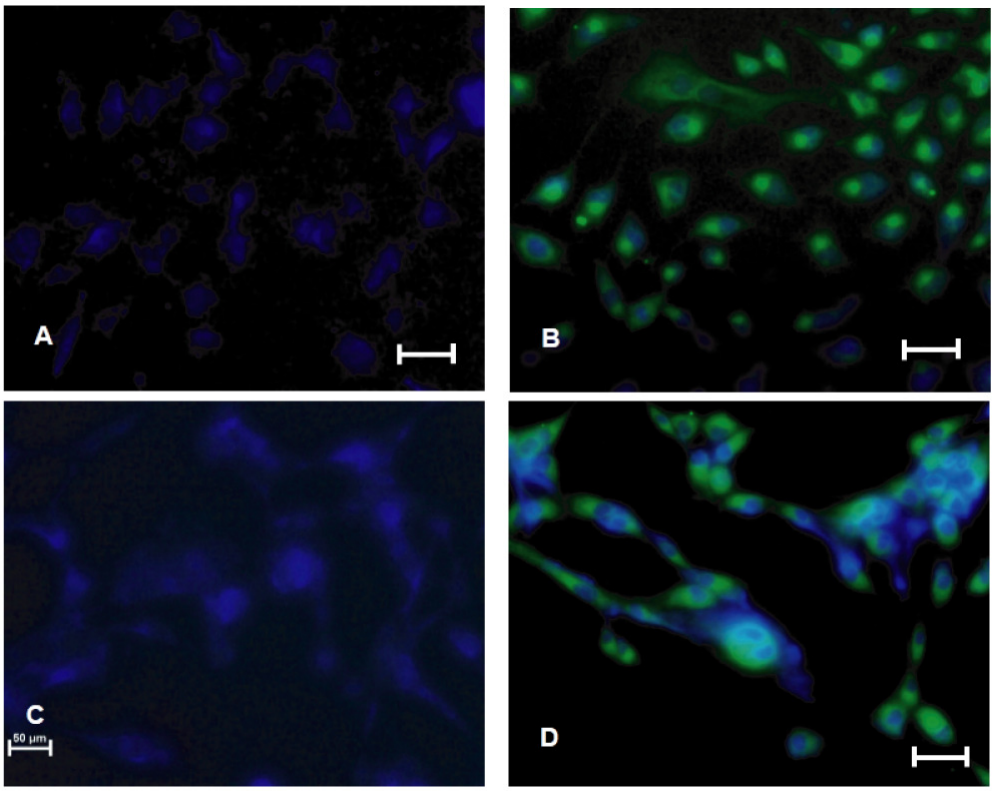

Figure 2.6 Merged fluorescence microscopr image of (A) untreated and (B) treated HeLa and (C) untreated and (D) treated U87MG.

2.4 Induction of cell death

We have studied the effects of the recombinant IκBα loaded curcumin NPs and the BSA loaded curcumin NPs on HeLa and U87MG cells, where BSA was used as a nontoxic protein control (Asharani et al, 2008). The cells were treated with various amounts of protein

immobilized NPs followed for 24 h and MTT assay was performed. Our results revealed that both recombinant IκBα and BSA loaded NPs had cytotoxic effect on the cells (U87MG and HeLa), but the recombinant IκBα loaded curcumin NPs had higher cytotoxicity than BSA loaded curcumin NPs. The Figure 2.7 A and B indicated that the cytotoxicity shown by BSA-curcumin NPs was actually from curcumin itself, as BSA is nontoxic. However, BSA loaded curcumin NPs showed different degrees of cytotoxicity on HeLa and U87MG cells, which was more on HeLa as compared to U87MG cells. But the recombinant IκBα loaded curcumin showed similar IC_{50} (the concentration at which 50% of the cells die) value (138 ng/mL GST-IκBα in 4.43 µg/mL of curcumin NPs) for both the cell types. Thus, MTT based cytotoxicity assay revealed that the recombinant IκBα loaded curcumin NPs were much more effective in reducing cell viability than BSA loaded curcumin NPs controls.

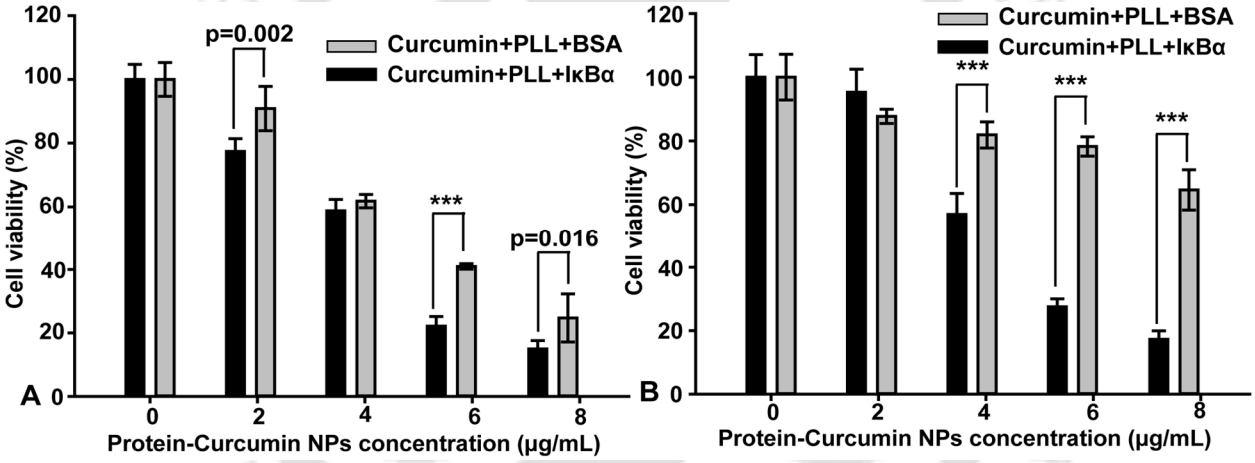

Figure 2.7 Cytotoxic effect of protein-curcumin NPs. (A) HeLa cells. (B) U87MG cells. All data are represented as Mean ± S.D. and statistical analysis was done by two way ANOVA in Sigma Plot software. Statistical significance between treated samples with significant p value (<0.05) are mentioned and p<0.001 are denoted by ***.

Interestingly, the Hela and U87MG cells treated with only curcumin NPs, which were negatively charged (-9.3 mV), showed much less cytotoxicity which indicated the nontoxic nature of free curcumin NPs (Figure 2.8 A and B).

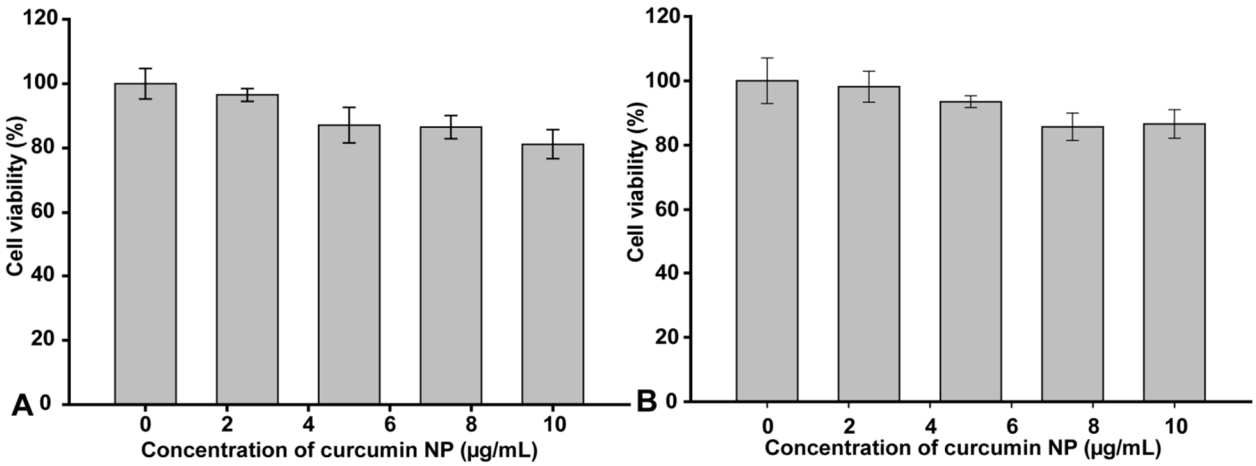

Figure 2.8 Non cytotoxicity of only curcumin NPs. (A) HeLa cells, (B) U87MG cells.

2.5 Effect of protein-curcumin NPs on cell cycle

Further, the effect of recombinant IκBα loaded curcumin NPs on the cell cycle was studied by flowcytometry. The cells were treated with 4.57 µg/mL of recombinant IκBα loaded curcumin NPs (IC50) for 12 h. FACS based cell cycle analysis demonstrated prominent apoptotic population for HeLa cells (calculated by ModFit™) treated with the recombinant IκBα loaded curcumin NPs (11±1.11%), as compared to the BSA loaded curcumin NPs (5.3±1%) controls (Fig. 2.9 A). In U87MG cells, this effect was even more prominent, as the apoptotic population was found to be 21.53±2.77% in the recombinant IκBα loaded curcumin NPs compared to 8.31±1.7% in the BSA loaded curcumin NP treated cells (Fig. 2.9 B). Hence, the results indicated that recombinant IκBα loaded curcumin NPs had more cell inhibitory effects.

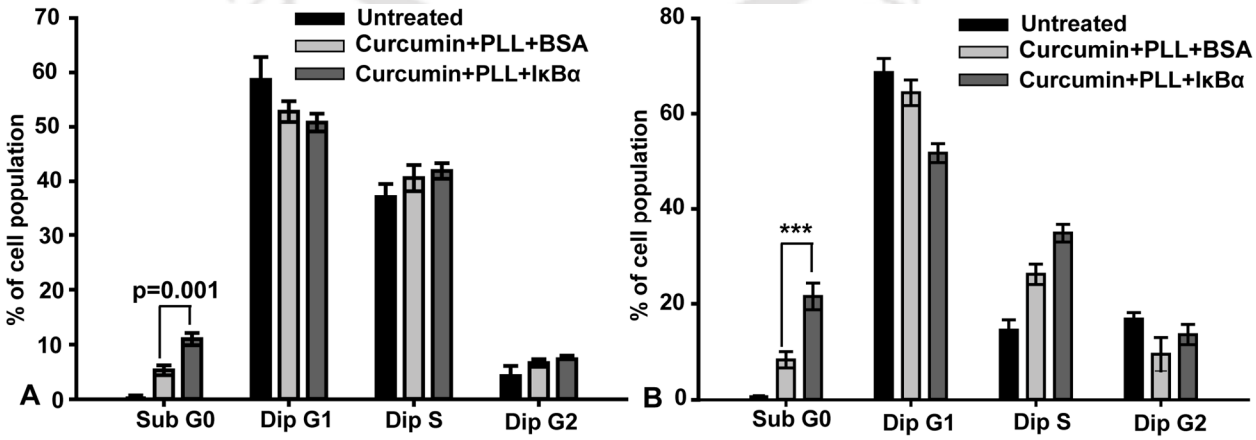

Figure 2.9 Effect of protein-curcumin NPs on cell cycle. (A) HeLa cells. (B) U87MG cells. All data are represented as Mean ± S.D. and statistical analysis was done by two way ANOVA in Sigma Plot software. Statistical significance between treated samples with significant p value (<0.05) are mentioned and p<0.001 are denoted by ***.

2.6 Induction of ROS

Reactive oxygen species induce apoptosis in many types of cells (Simon *et al*, 2000). Curcumin has also been reported to mediate apoptosis through generating ROS (Thayaullathil *et al*, 2008; Khan *et al*, 2012). Here, we used flowcytometry to measure induction of ROS generation of HeLa (Figure 2.10 A) and U87MG (Figure 2.10 B) cells after treating with the recombinant IκBα loaded curcumin NPs as well as the BSA loaded curcumin NPs using DCFDA staining method. The DCFDA, a non-fluorescent dye, can be oxidized to DCF by the intracellular ROS showing green emission at 529 nm corresponding to FL1-H channel during FACS analysis. The amount of fluorescence directly correlates to the amount of ROS generated inside the cells. Upon treating the cells with 4.57 µg/mL of IκBα loaded curcumin NPs and similar amount of BSA loaded curcumin NPs for 1 h, we found that there was a prominent shift in the FL1-H channel due to ROS activation in IκBα loaded curcumin NP treated cells as compared to the BSA controls. The FACS results demonstrated that the amount of ROS production was almost same in both protein loaded curcumin NPs, which indicated that curcumin was responsible for the cellular ROS generation in protein loaded curcumin NPs module. The generation of ROS could induce apoptosis in cancer cells. The free IκBα did not produce any ROS.

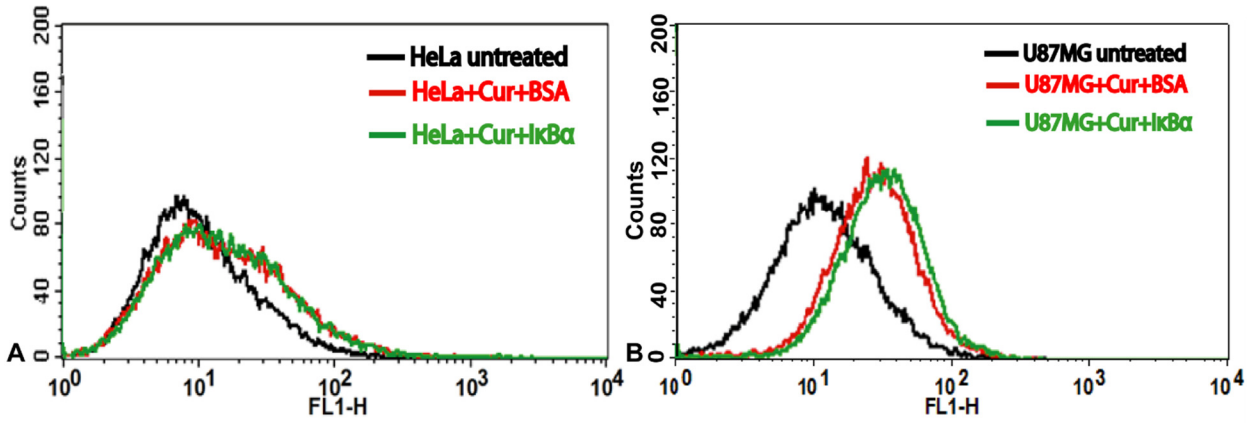

Fig 2.10 Induction of reactive oxygen species. (A) HeLa cells. (B) U87MG cells.

2.7 IκBα loaded curcumin NPs induce apoptosis

After monitoring the cytotoxic and ROS inducing effects of the recombinant IκBα loaded curcumin NPs, the mode of cell death was further confirmed by measuring FITC conjugated Annexin V antibody mediated flowcytometry for apoptosis. The flow cytometry results showed a significant apoptotic population in treated HeLa cells with lower right quadrant 3.21% of Annexin V positive cells and upper right quadrant 17.5% Annexin V and PI double positive cells (Fig 2.11) after 14 h of treatment with IκBα loaded curcumin NPs (4.57 µg/mL).

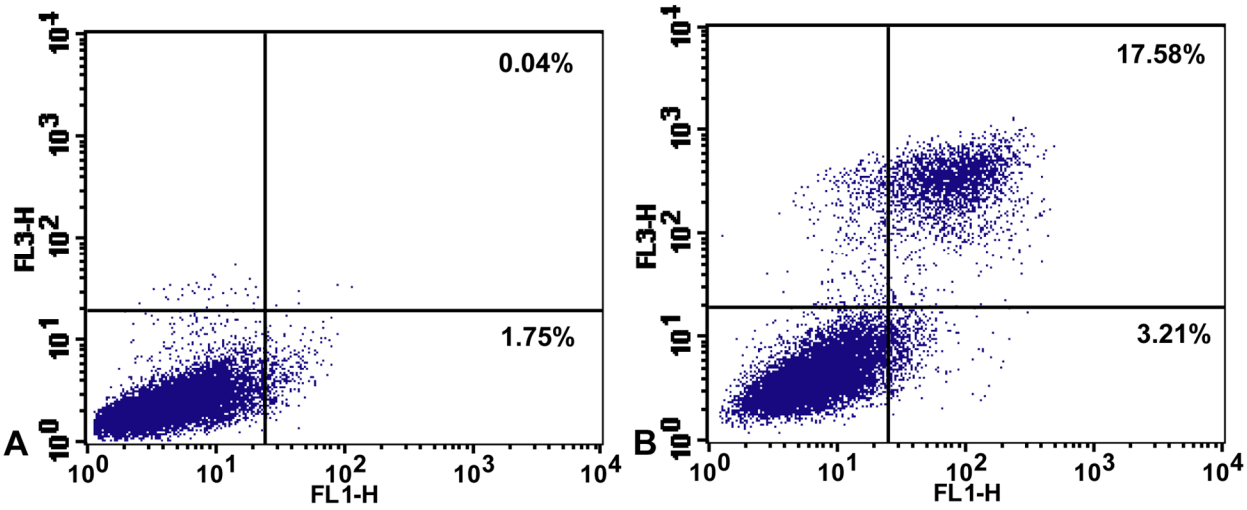

Figure 2.11 Detection of apoptosis by FITC-Annexin V and PI double staining for HeLa cells. (A) Untreated cells, (B) Treated cells.

For U87MG cells, treated population comprised of almost similar percentage of Annexin V positive cells and Annexin V and PI double positive cells (Fig 2.12) after 14 h of treatment with IκBα loaded curcumin NPs (4.57 µg/mL). However, much difference in the overall apoptotic response in between HeLa and U87MG cells (Fig 2.12 A and B) was not observed after treatment of IκBα loaded curcumin NPs (4.57 µg/mL) for 14 h. The results confirmed the induction of apoptosis upon treatment with recombinant IκBα loaded curcumin NPs.

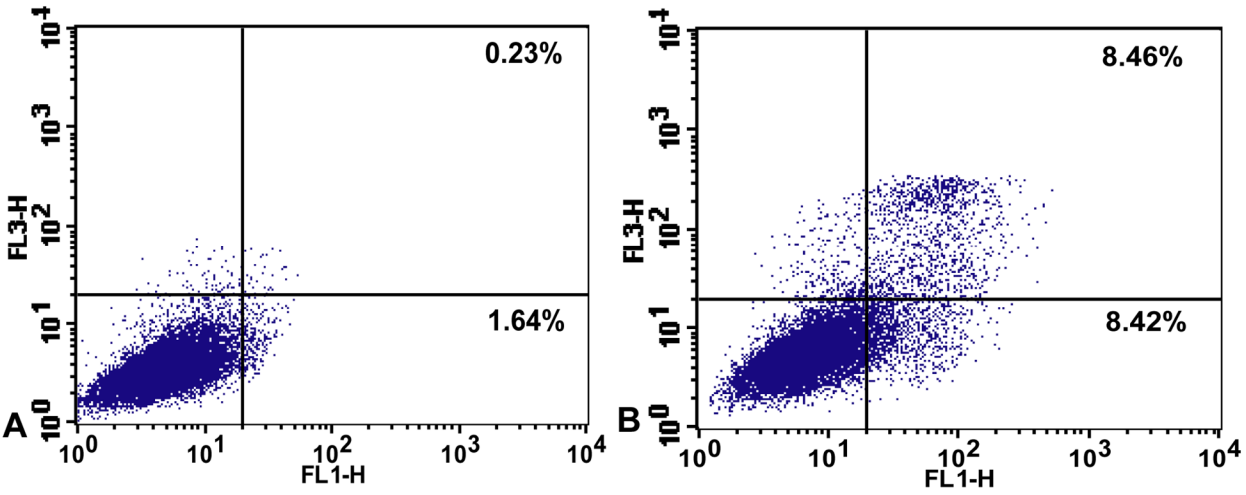

Figure 2.12 Detection of apoptosis by FITC-Annexin V and PI double staining for U87MG cells. (A) Untreated cells, (B) Treated cells.

2.8 Gene expression analysis to decipher molecular events

The relative expression of important apoptosis regulatory genes was studied by semi-quantitative reverse transcriptase PCR in U87MG cells treated with the recombinant IκBα loaded curcumin NPs and untreated U87MG control cells. Since IκBα and curcumin are known individually to down regulate the expression of NFκB (Hayden and Ghosh, 2004; Aggarwal and Singh, 1995), we have examined the combined effects of recombinant IκBα and the curcumin NPs on the expression levels of some important NFκB target genes such as, cyclin D1, cyclin E, cox-2 and bcl-xL. We observed that the expressions of those genes were significantly down regulated (Figure 2.13). Cyclin D1 and E are known to control cell growth and survival (Baldin *et al*, 1993; Kern *et al*, 2006) and hence, down regulation of their expressions would certainly cause cell arrest in treated samples. Further, the cox-2 inhibition is known to induce apoptosis (Kern *et al*, 2006). Hence, down regulation of cox-2 (Figure 2.13) indicated apoptotic mediated cell death. This result was supported by down regulation in expression of anti-apoptotic bcl-xL gene, a negative regulator of effector caspase-3 (Finucane *et al*, 1999) and a known downstream target of NFκB (Figure 6A). Simultaneously, up-regulation of caspase-3, a known executioner of programmed cell death confirmed apoptosis in treated cells (Figure 2.13). Further, a notable upregulation of c-myc, a known regulator of p53 (Hoffman and Liebermann, 2008), was observed (Figure 2.13). This

in turn induced p53, which possibly upregulated another pro-apoptotic bax gene (Cregan *et al*, 1999) (Figure 2.13).

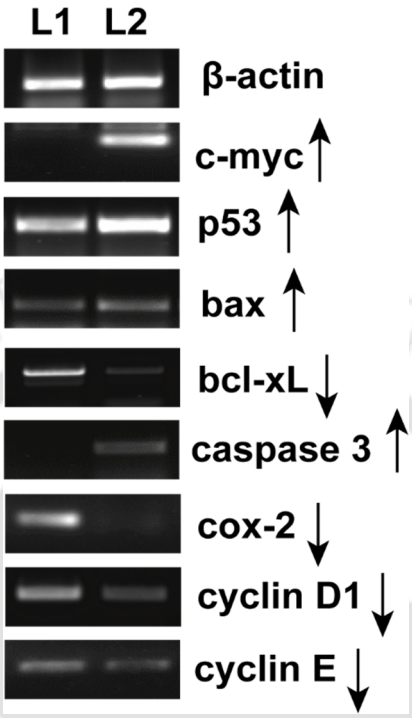

Figure 2.13 Expression analysis of proapoptotic genes (bax, c-myc, p53 and caspase-3) and antiapoptotic genes (bcl-xl, cox-2, cyclin D1, cyclin-E) with housekeeping gene β-actin. L1- untreated U87MG cells, L2- U87MG cells treated with recombinant IκBα loaded curcumin NPs.

The entire molecular pathway involving possible regulatory genes is depicted in the scheme (Figure 2.14). The scheme depicted that upon inhibition of NFκB by IκBα induces modulation in expression of several genes directly regulated by NFκB which include bcl-xL, cox-2, cyclin D1 and cyclin E. Down regulation of these genes elicits downstream cellular event like arrest of cell cycle and molecular events like upregulation of c-myc, p53 and bax, which further initiate different signaling cascade including upregulation of caspase-3, followed by apoptosis.

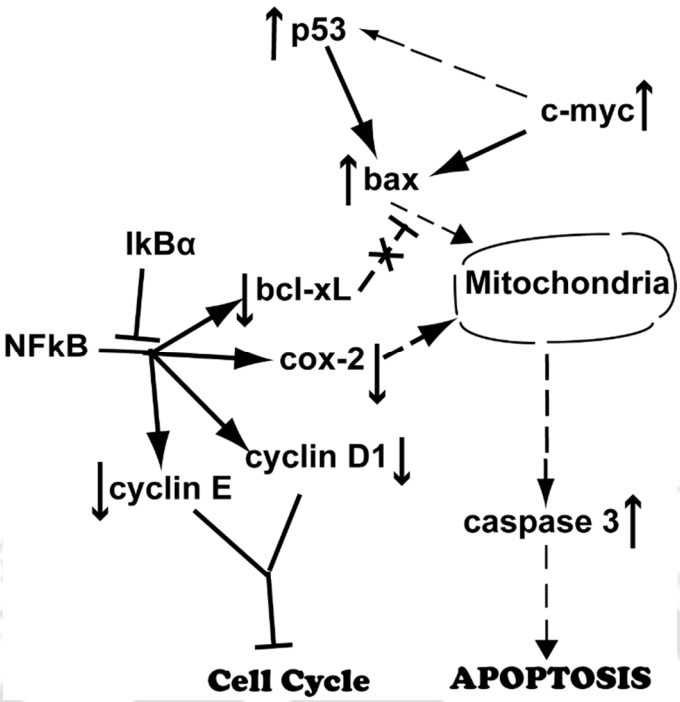

Figure 2.14 Key genes involved in IκBα loaded curcumin NPs mediated cell killing.

Conclusions of part 2

The therapeutic module designed by the recombinant IκBα loaded curcumin NPs showed strong therapeutic efficacy against HeLa and U87MG cells. The augmented effect of recombinant IκBα loaded curcumin NPs was prominent on drug resistant U87MG cells. In this module, recombinant IκBα and curcumin together affected the function of NFκB and thus, down-regulated cyclin D1, cyclin E, bcl-xL and cox-2 genes which are known to be modulated by NFκB, which in turn inducted cell cycle arrest and apoptosis. On the other hand, curcumin, a known inhibitor of NFκB and cellular ROS generator, played a crucial role in induction of apoptosis via caspase-3 upregulation. Thus, taken together individual components in the module had induced pro-apoptotic genes p53, bax, c-myc to initiate apoptotic process. The possible contributory effects of the recombinant IκBα and the curcumin present in the NPs to improve therapeutic efficacy against cancer cells are shown in **Scheme 2.2.** Thus, bioactive agent based combinatorial therapy with recombinant proteins holds great promises for improved cancer therapeutics.

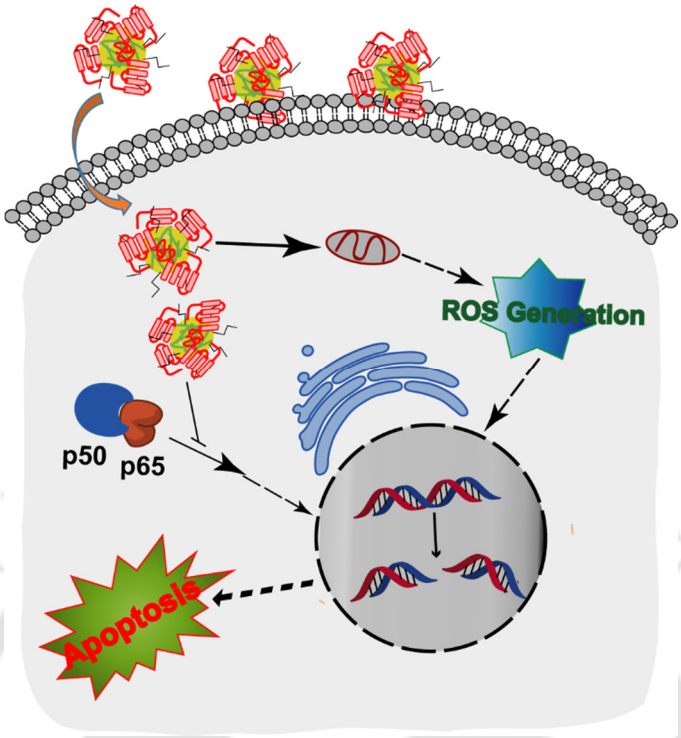

Scheme 2.2. Overall mode of action of IκBα loaded curcumin NPs on the cells.

The effect of GST-IκBα was tested by adding it from outside alone via hydrogel and in combination with 5-FU and curcumin NPs in the previous part. The question that still remains is what happens if the IκBα overexpressing cells are challenged with curcumin NPs and 5-FU. In order to address the question, in the third part of the thesis work, IκBα was transfected in U87MG cells, and IκBα over expressing U87-IκBα cell line was established by G418 selection. The cell line was challenged with BSA coated curcumin NPs and 5-FU alone and in combination. Higher efficacy was observed, which establishes the effect of IκBα on U87MG cells to induce drug sensitivity.

PART 3- *Effect of 5-Fluorouracil and curcumin nanoparticles on IκBα over expressing glioblastoma.*

The work plan is presented by the following scheme-

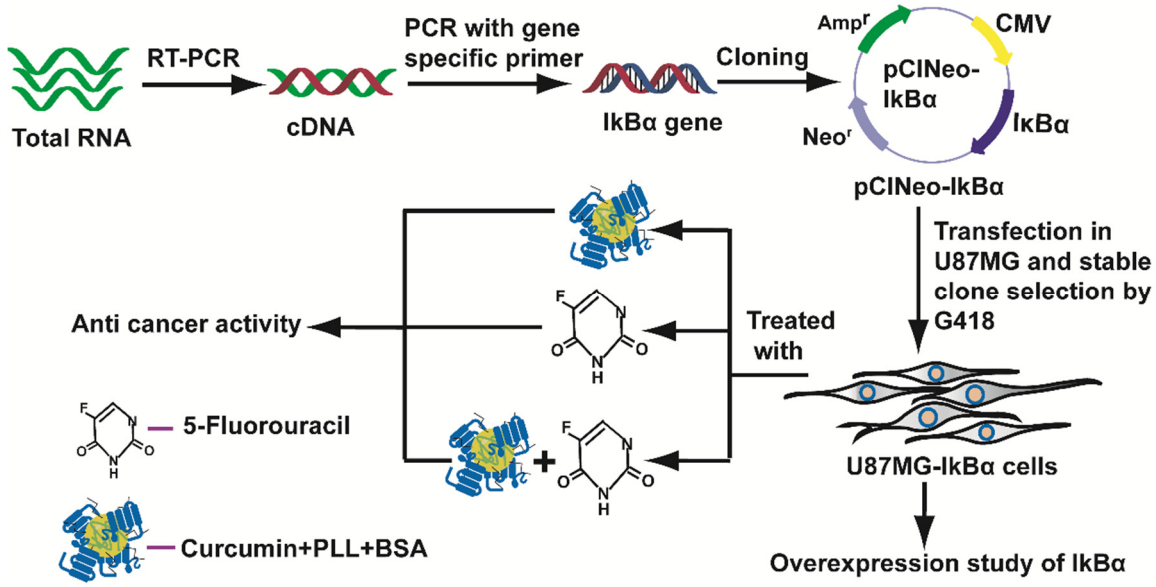

Scheme 3.1 Work plan for part 3

3.1 Cloning of IκBα in pCINeo vector

IκBα gene was cloned into pCINeo vector as mentioned in materials and methods section. In brief, the IκBα gene was released from pGEM T Easy backbone by *Eco* RI and *Spe* I digestions. The pCINeo backbone was also digested by *Eco* RI and *Xba* I. Then the digested insert and vector was ligated. The ligated product was transformed into *E. coli* and plated on agar plate with ampicillin screening. The cloning was checked by digestion with *Eco* RI and *Not* I, which generated a 970 bp fragment. The Not I site was selected at the 3' downstream of *Xba* I in the vector backbone (Figure 3.1).

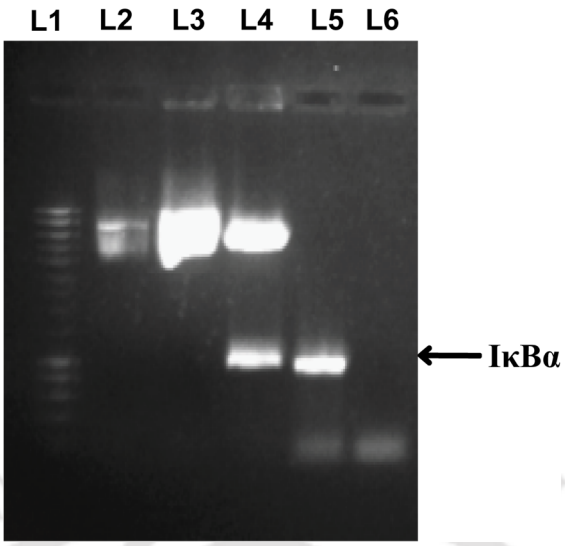

Figure 3.1 Cloning of IκBα in pCINeo vector. L1: marker, L2: control pCINeo, L3: IκBα-pCINeo plasmid, L4: IκBα-pCINeo digested with EcoRI and NotI, L5: IκBα PCR amplicon as positive control, L6: No template control.

3.2 Generation of U87-IκBα cells

IκBα over expressing U87-IκBα cell line was established by lipofectamine based transfection followed by G418 antibiotic selection, as mentioned in the materials and methods section. The RNA was isolated and cDNA was synthesized form U87-IκBα and untransfected U87MG cell lines. The overexpression of full length IκBα was seen after 30 cycles of PCR using gene specific primers compared to the housekeeping β-actin as loading control. Higher expression of IκBα in transfected cell line as compared to untransfected U87MG cells was observed, whereas the β-actin band intensity was unchanged (Figure 3.2).

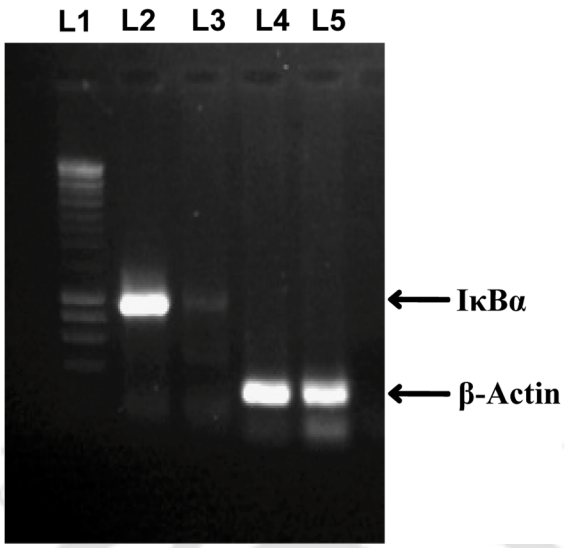

Figure 3.2 Overexpression of IκBα by semiquantitative PCR. L1: Marker, L2: IκBα expression in U87-IκBα cells, L3: Control U87MG, L4: β-actin expression in U87-IκBα cells, L5: β-actin in untransfected U87MG.

Further, the overexpression was probed by the real time PCR using gene specific realtime PCR primers (Table 1). There also, almost three fold higher expression was observed by calculating the over expression from threshold cycle (C_T) by Pfaffle method (Figure 3.3).

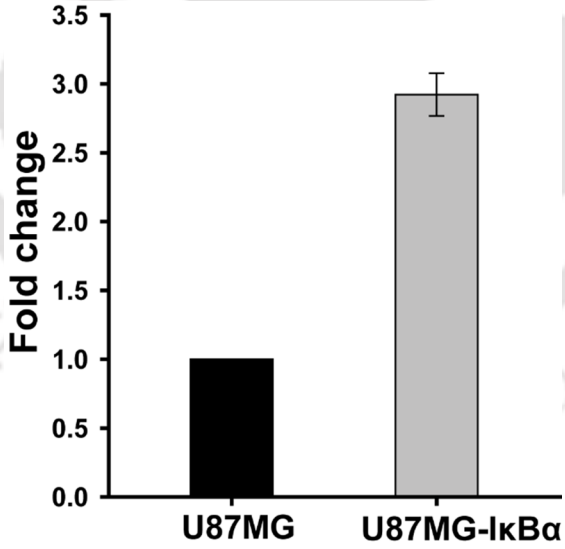

Figure 3.3 Over expression of IκBα in transfected U87MG cells by real time PCR.

The IκBα overexpression was also confirmed at the protein level by immunoblotting method against mouse anti-human IκBα antibody with β-actin as loading control (Figure 3.4). The HRP conjugated goat anti-mouse antibody was used as secondary antibody.

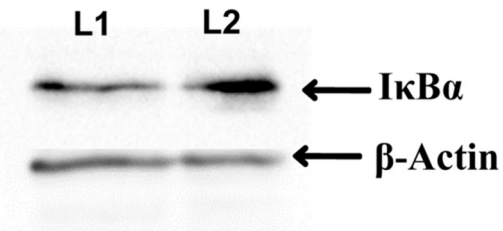

Figure 3.4 Over expression of IκBα by Western blotting method. L1- U87MG cells alone, L2- U87-IκBα cells.

3.3 Expression of p50 and p65 in U87MG and U87-IκBα cells

In cancer cells, the NFκB (p50 and p65 genes) is constitutively expressed. Hence, the expressions of p50 and p65 genes were checked by semiquantitaive PCR of 32 cycles. Upon analysing on 1% agarose gel, both p50 (product length 449 bp) and p65 (product length 630 bp) was found to be expressed in uninduced cancer cells. However, no significant difference in their expressions were seen.

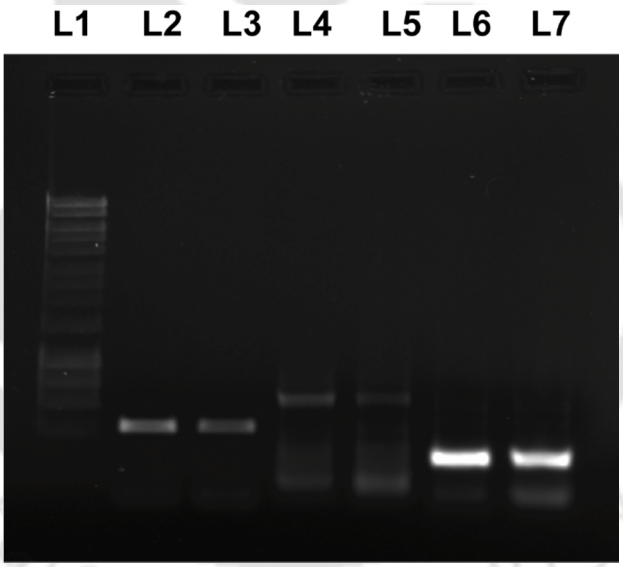

Figure 3.5 Differential expression of p50 and p65 genes in U87MG and IκBα over expressing U87MG cells. L1-DNA hyperladder marker, L2-p50 gene in U87MG cells, L3-p50 gene in IκBα over expressing U87MG cells, L4- p65 gene in U87MG cells, L5- p65 gene in IκBα over expressing U87MG cells, L6- β-actin gene in U87MG cells, L7- β-actin gene in IκBα over expressing U87MG cells.

3.4 5-FU sensitization of U87-IκBα cells

U87MG cells are known to be 5-FU resistant at admissible range. So, 5-FU was chosen to

check whether IκBα over expression has any effect in sensitization of U87MG cells. Also, this experiment reconfirms the previous study conducted in part 1, where U87MG cells showed higher sensitivity towards 5-FU when added in combination with hydrogel mediated recombinant IκBα protein. After treatment with 48 h, the result showed that, U87-IκBα cells were more sensitive towards 5-FU than U87MG cells (Figure 3.6). It is to be mentioned here that U87-IκBα cells showed higher difference in cell viability at elevated range of 5-FU concentration.

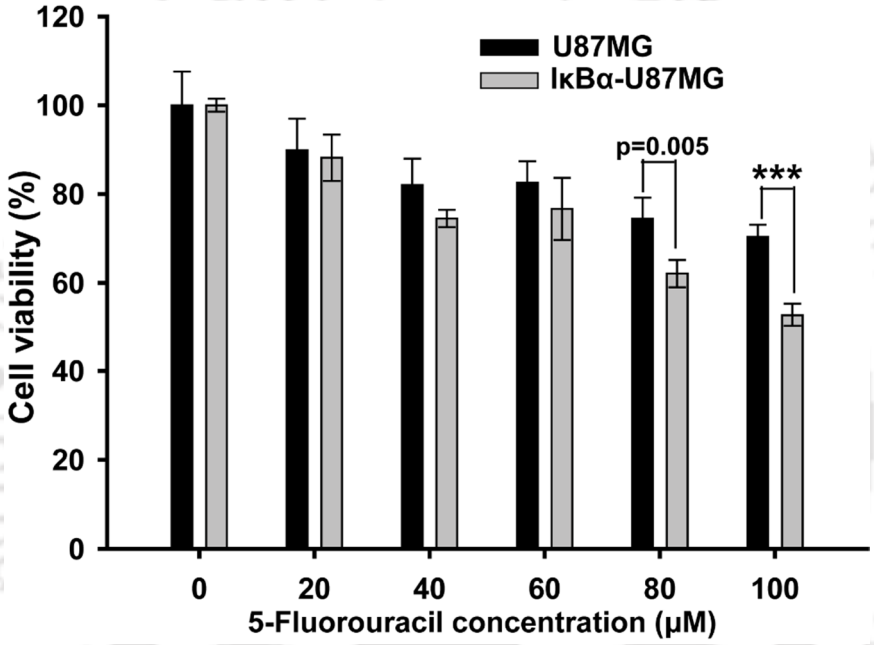

Figure 3.6 Anti-cell proliferative effect of 5-FU on U87MG and U87-IκBα cells. All data are represented as Mean ± S.D. and statistical analysis was done by two way ANOVA in Sigma Plot software. Statistical significance between treated samples with significant p value (<0.05) are mentioned and p<0.001 are denoted by ***.

3.5 5-FU induced reduction in cell proliferation

After the viability assay, the microscopic observation indicated very little or negligible cell death, thus hinted that the difference of cell viability may be due to differential rate of cell proliferation. Hence, cell proliferation was studied by FACS based CFSE staining method. The results showed that in U87MG cells, the cell proliferation rate decreased with time (in 72 h) in 5-FU treated cells (Figure 3.7). In U87-IκBα cells (Figure 3.8), the difference in cell proliferation rate was even more prominent after 72 h of 5-FU (50 μM) treatment, whereas,

both untreated cell lines showed almost no difference in proliferation rate. This experiment confirmed that the difference in viability was due to inhibition of cell proliferation and indicated that 5-FU may have an effect on cell cycle.

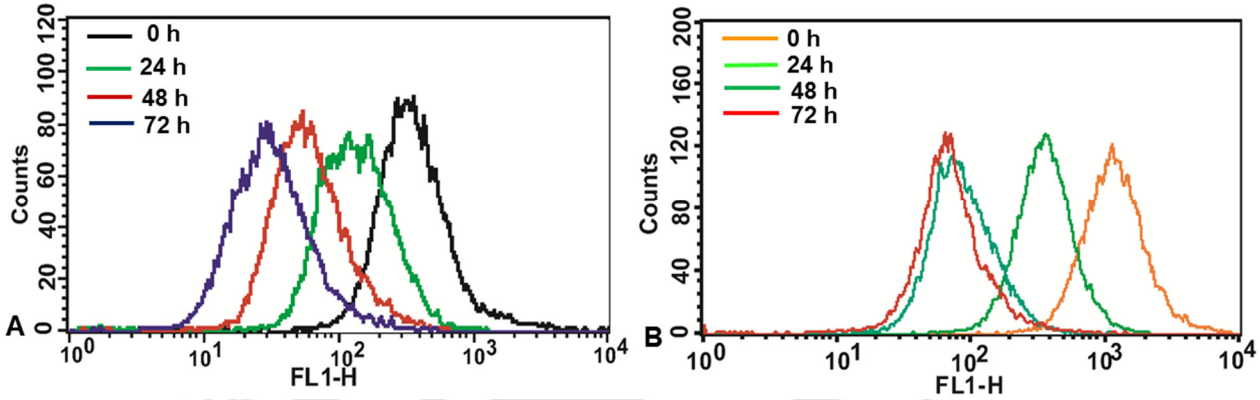

Figure 3.7 Proliferation of U87MG cells studied by CFSE dye based flow cytometry method. (A) Untreated U87MG cells. (B) U87MG cells treated with 50 µM 5-FU.

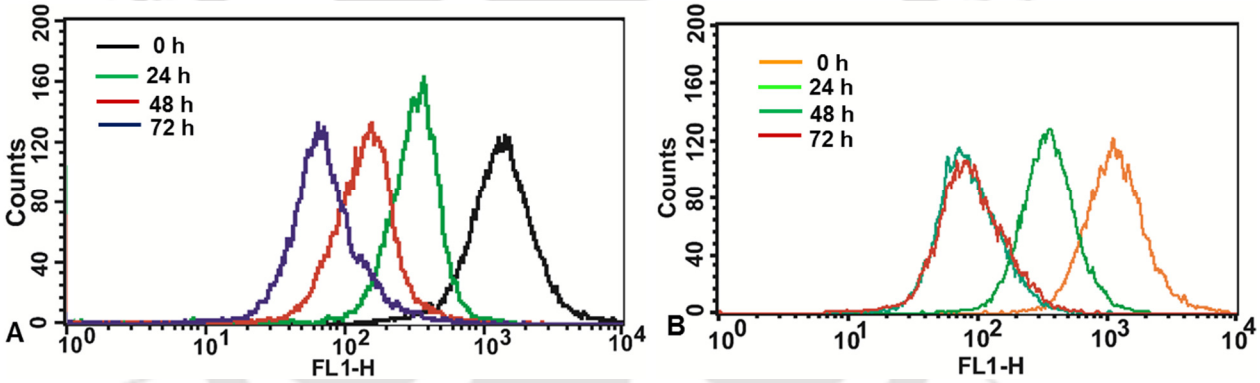

Figure 3.8 Proliferation of U87MG-IκBα cells studied by CFSE dye based flow cytometry method. (A) Untreated U87MG-IκBα cells. (B) U87MG-IκBα cells treated with 50 µM 5-FU.

3.6 Effect of 5-FU on cell cycle

The effect on cell cycle was studied by PI mediated cell cycle analysis with dose dependent manner in 48 h treatment. From the histogram analysis of each phase of cell cycle using ModFit™ software, it was evident that 5-FU has differential effect on U87MG cells and U87-IκBα cells with almost no sub G0 population in both types of cells. But with increase of 5-FU concentration, U87MG cells showed higher number of cells in G1 phase as compared to untreated U87MG cells (Figure 3.9).

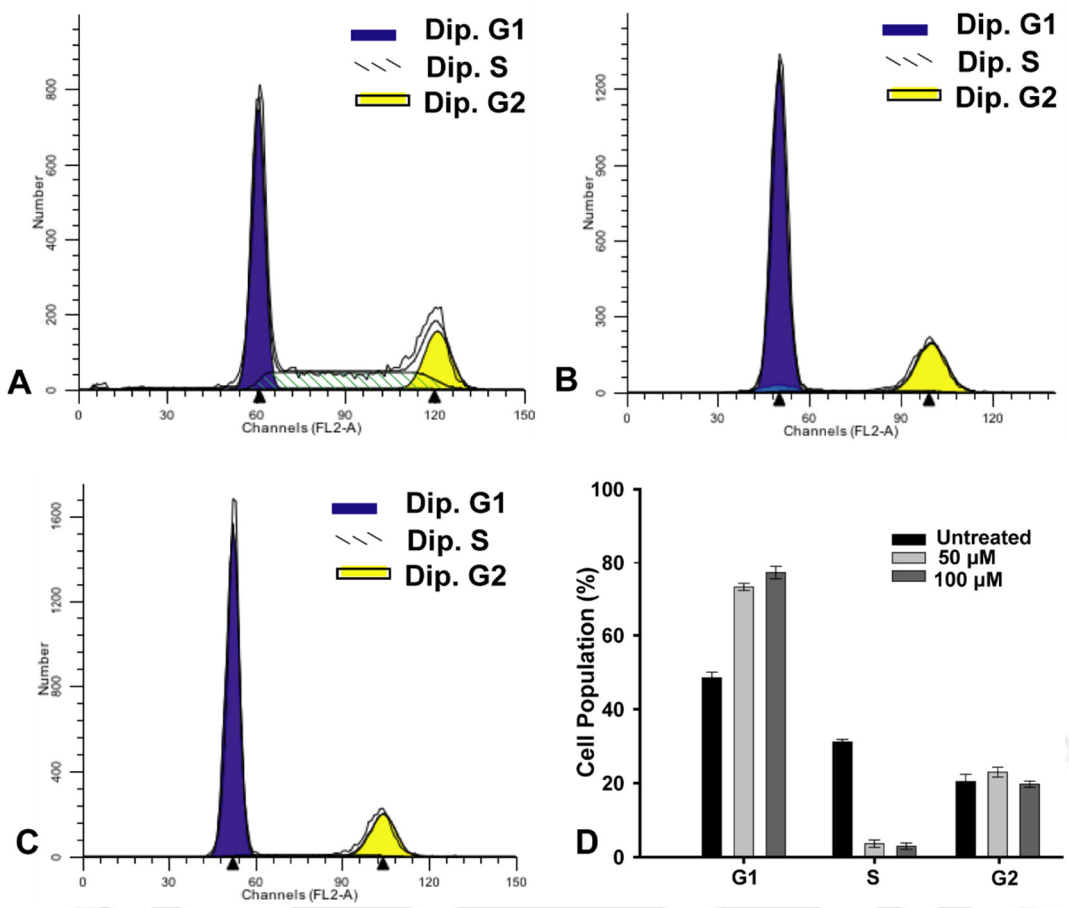

Figure 3.9 Analysis of the effect of 5-Fluorouracil on U87MG upon 48 h treatment by flow cytometry. (A) Untreated (B) 50 µM, (C) 100 µM, (D) Comparative study by bar diagram analysis.

But, interestingly, U87-IκBα cells showed higher number of cells in G1 and S phase with diminishing G2 phase at 50 µM of 5-FU. But at 100 µM 5-FU concentration, cells showed significant G1 phase arrest with reducing number of cells at S phase and G2 phase (Figure 3.10). The result indicated that the overexpression of IκBα changes the cellular response towards 5-FU with its increasing concentrations.

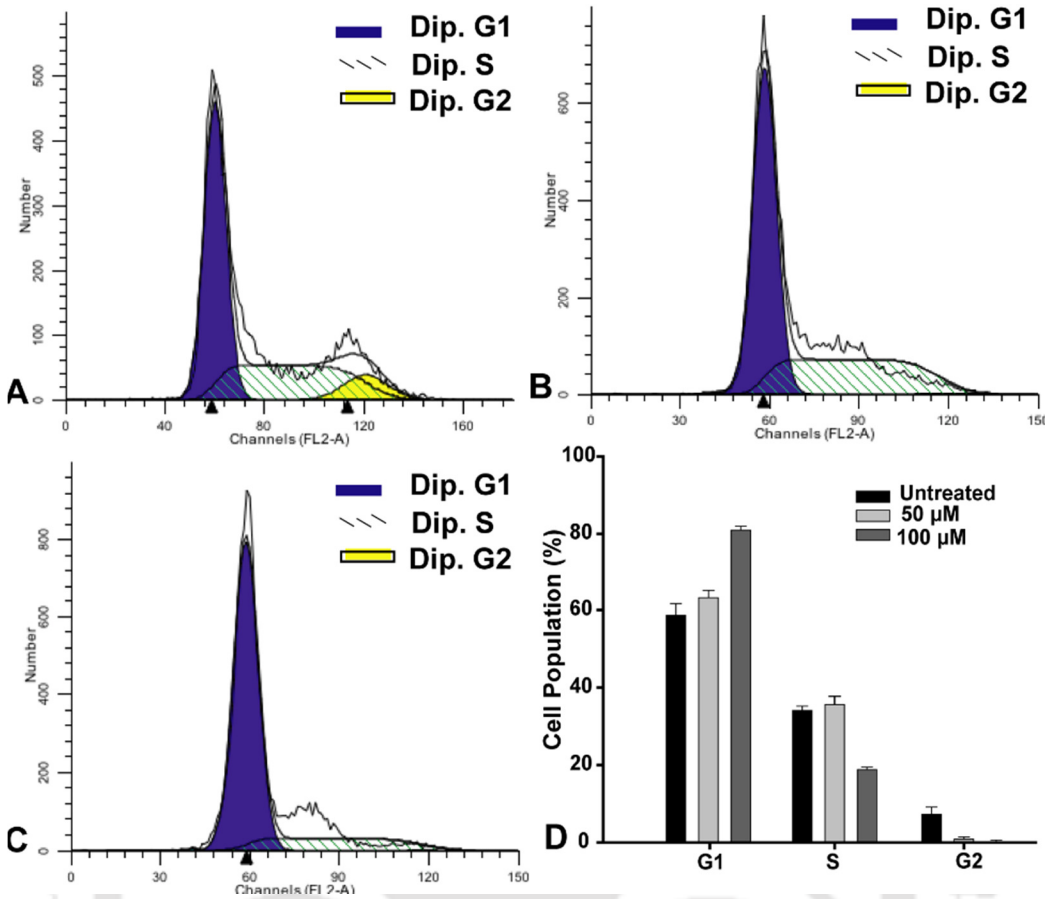

Figure 3.10 Analysis of the effect of 5-Fluorouracil on U87-IκBα upon 48 h treatment by flow cytometry. (A) Untreated (B) 50 µM, (C) 100 µM, (D) Comparative study by bar diagram analysis.

3.7 Effect of BSA loaded curcumin NPs on the cells

In the second part of the work, the impact of IκBα loaded curcumin NPs was tested on U87MG cells along with BSA loaded curcumin NPs to elucidate the effect of curcumin NPs alone as BSA is commonly regarded to be nontoxic to cells. As physicochemical properties (similar molecular weight of the proteins, zeta potential etc.) of BSA curcumin NPs were similar to IκBα curcumin NPs, in this study, BSA curcumin NPs were used, which mimicked the IκBα loaded curcumin NPs module when added to the U87-IκBα cells. Thus, the effect of various concentrations of BSA loaded curcumin NPs were tested on both U87MG and U87-IκBα cells. The higher efficacy was found in U87-IκBα cells (Figure 3.11), which indicated the role of IκBα towards sensitization of U87MG to the curcumin NPs.

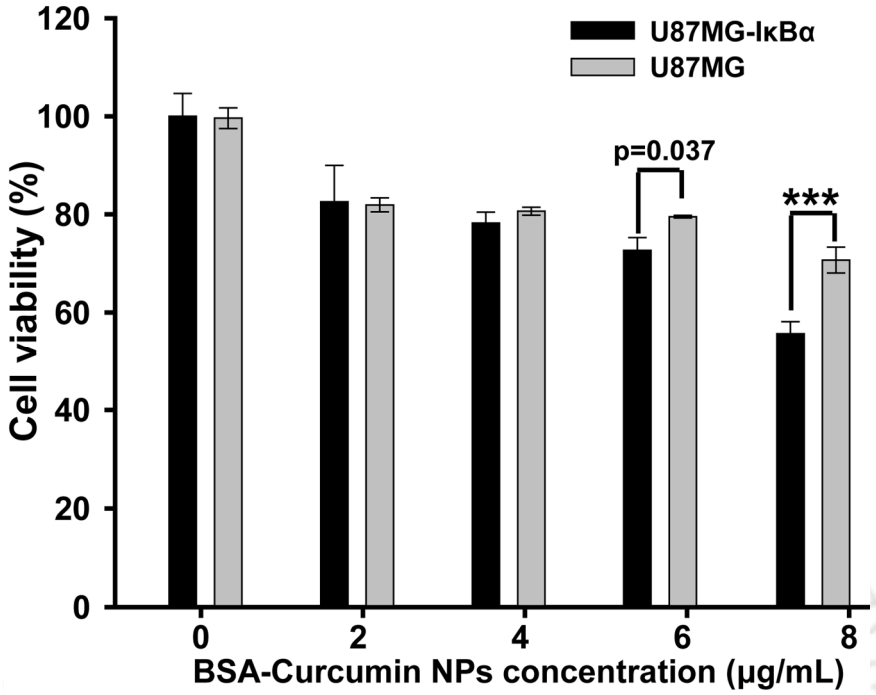

Figure 3.11 Comparative study of anti-cell proliferative effect of BSA loaded curcumin NPs on U87-IκBα and U87MG cells. All data are represented as Mean ± S.D. and the statistical analysis was done by two way ANOVA in Sigma Plot software. Statistical significance between treated samples with significant p value (<0.05) are mentioned and p<0.001 are denoted by ***.

3.8 Effect on cell cycle upon treatment with BSA loaded curcumin NPs

The effect of BSA loaded curcumin NPs on cell cycle was studied following the result obtained by cell viability assay. The U87-IκBα cells were treated with BSA-curcumin NPs for 24 h, and the cells were stained with PI analysed by flow cytometry method with 15000 cells for each sample. Higher number of cells were found in sub G0 population of BSA-curcumin NPs treated IκBα overexpressing U87MG cells as compared to ordinary U87MG cells. Also, for BSA-curcumin NPs treated IκBα overexpressing cells, higher number of cells were found in the G1 phase with a lower number of cells in S and G2 phase, as compared to untreated overexpressing cells, treated and untreated ordinary U87MG cells (Figure 3.12). Thus, the possibility of higher amount of apoptosis of BSA-curcumin NPs treated U87-IκBα cells emerge from the flow cytometry analysis.

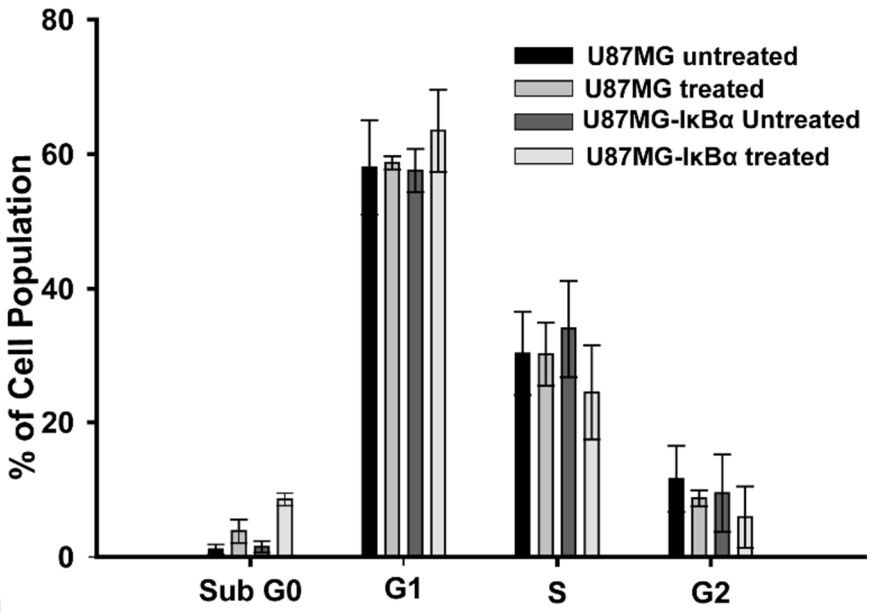

Figure 3.12 Cell cycle analysis of U87MG and U87MG-IκBα cells treated with BSA loaded curcumin NPs for 24 h. All data are represented as Mean ± S.D of three individual experiments.

3.9 Microscopy studies of BSA loaded curcumin NPs treated cells

The microscopic analysis was carried out on both type of cells upon treatment with BSA loaded curcumin NPs for 12 h, and stained with DAPI and ethidium bromide (EB). DAPI readily enters the cell and stain the nucleus, but EB only enters through the membrane compromised cells. The goal of the experiment was to identify the live and dead cells upon treatment with BSA loaded curcumin NPs, as well as the uptake of BSA loaded curcumin NPs against the DAPI staining. Higher number of EB positive cells, which is membrane compromised, was found in IκBα overexpressing U87MG cells as compared to untransfected U87MG cells, which indicates that curcumin played pro-apoptotic function in both types of U87MG cells, but more prominent in U87-IκBα cells.

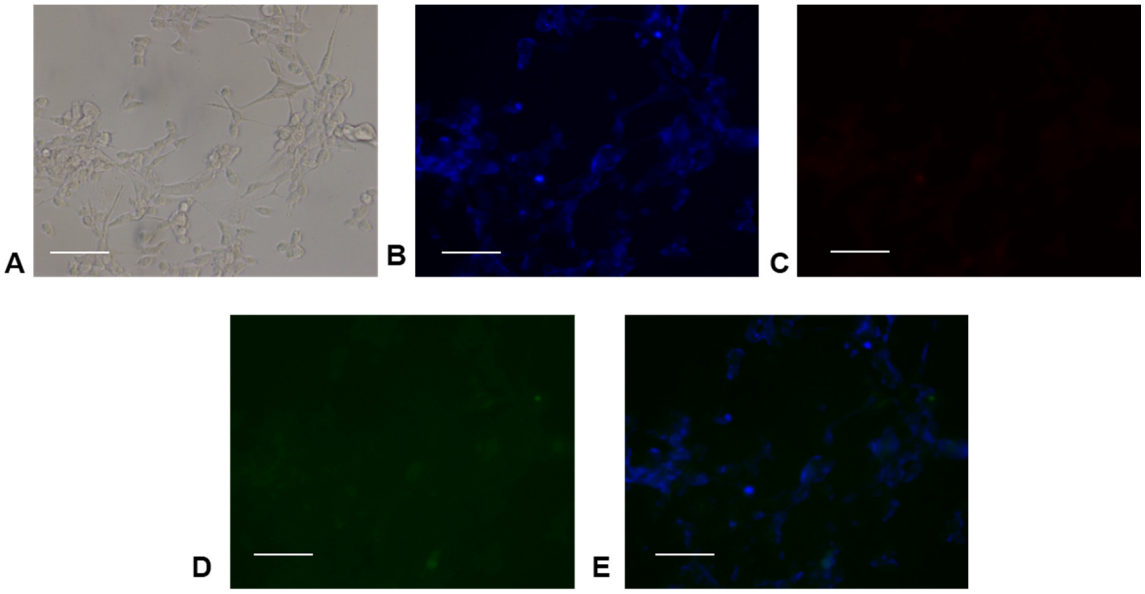

Figure 3.13 Fluorescence microscopy image for U87MG (A) bright field, (B) DAPI staining, (C) EB staining (D) untreated cell by blue excitation, (E) merged image for B and D. Scale bar 100 µM.

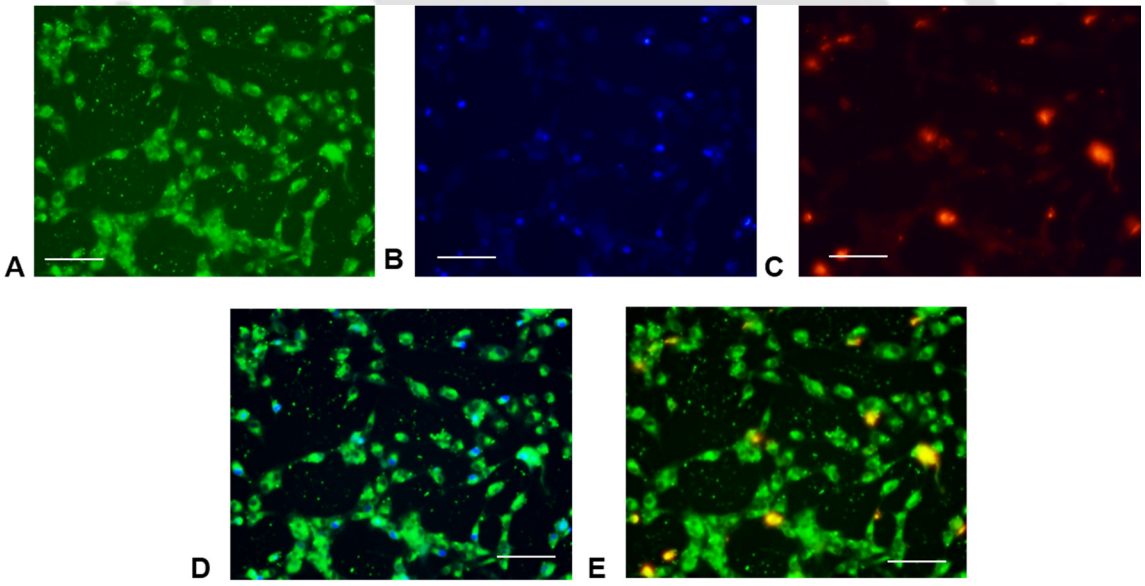

Figure 3.14 Fluorescence microscopy image for U87MG treated with curcumin nanoparticles (A) curcumin treated, (B) DAPI staining, (C) EB staining (D) merged image for A and B, (E) merged image for A and C. Scale bar 100 µM.

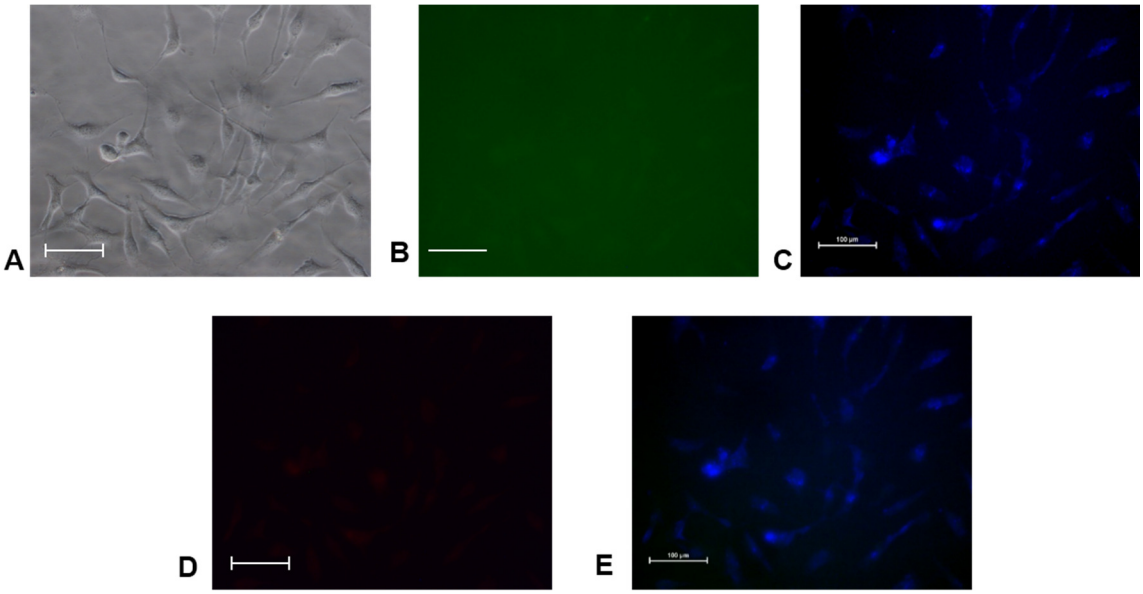

Figure 3.15 Fluorescence microscopy image for U87-IκBα cells (A) bright field, (B) DAPI staining, (C) EB staining (D) untreated cell by blue excitation, (E) merged image for B and D. Scale bar 100 µM.

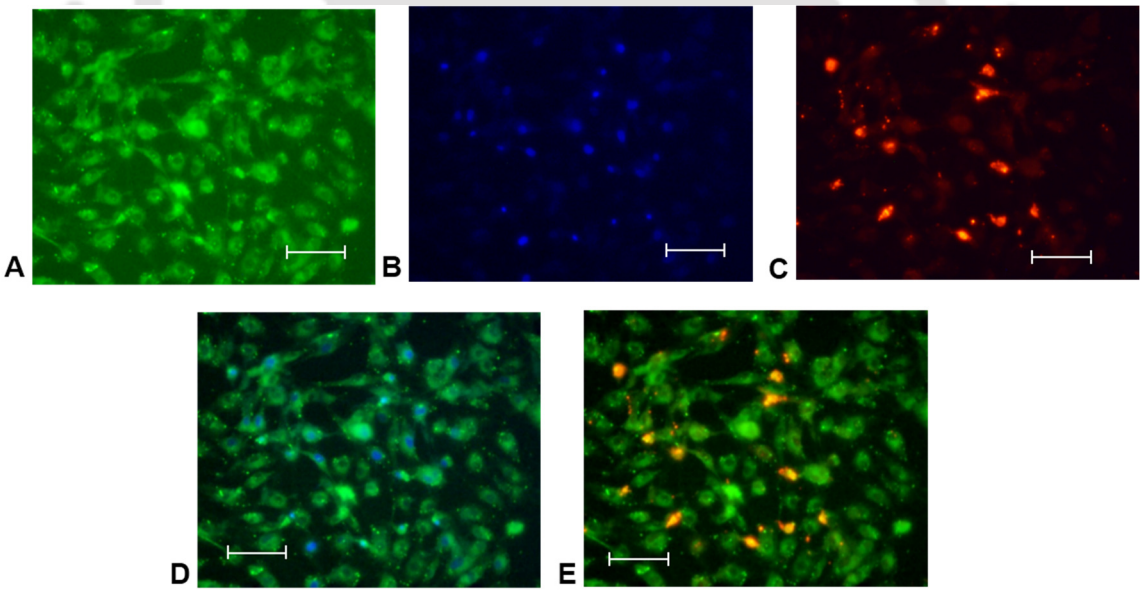

Figure 3.16 Fluorescence microscopy image for U87-IκBα cells treated with curcumin nanoparticles (A) bright field, (B) DAPI staining, (C) EB staining (D) untreated cell by blue excitation, (E) merged image for B and D. Scale bar 100 µM.

3.10 ROS generation study

The generation of reactive oxygen species (ROS) influences the apoptotic event. Induction of apoptosis by protein loaded curcumin nanoparticle was studied in the previous part. Here, the effect of BSA loaded curcumin loaded NPs upon IκBα overexpressing U87MG cells and ordinary U87MG have been studied by flowcytometry based DCFDA based ROS measurement. It was found that upon treatment of BSA loaded curcumin NPs for 3 h, U87-IκBα cells show a higher ROS generation (Figure 3.18) as compared to U87MG (Figure 3.17), which played a pivotal role in the protein loaded curcumin mediated apoptosis.

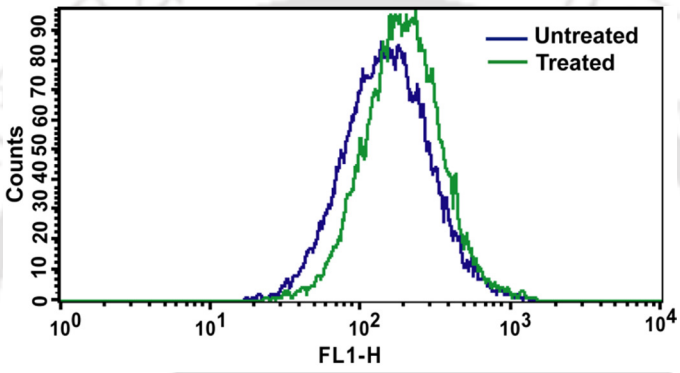

Figure 3.17 ROS generation assay by DCFDA dye for U87MG cells treated with BSA loaded curcumin nanoparticles.

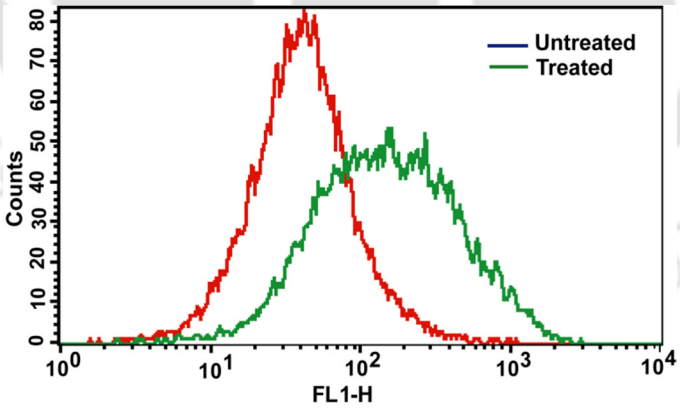

Figure 3.18 ROS generation assay by DCFDA dye for U87-IκBα cells treated with BSA loaded curcumin nanoparticles.

3.11 Detection of apoptotic cells by Annexin V-FITC and PI based double staining method

Following the trail of cell viability assay, PI based flow cytometry and microscopy analysis, the mode of cell death was confirmed by Annexin V-FITC and PI based double staining method by flow cytometry. As mentioned earlier, in the early apoptosis stage, phopsphotidyl serine (PS) of inner membrane exposed outward, which was recognised by FITC tagged Annexin V antibody. Propidium iodide was also used to identify late apoptotic and necrotic cells. In flowcytometry, the BSA loaded curcumin NPs treated (for 12 h) U87- IκBα cells showed greater number of early apoptotic cells (9.12%) (Figure 3.20 B) as compared to the treated U87MG cells (3.17%) (Figure 3.19 A). This result confirmed the mode of cells death was apoptosis.

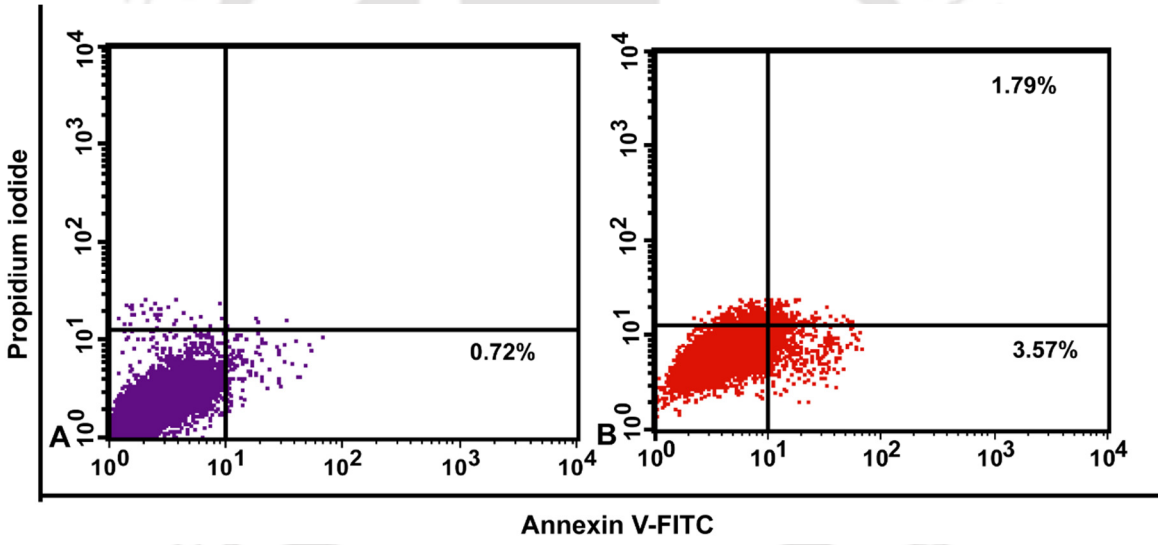

Figure 3.19 Detection of apoptosis in U87MG cells by FITC-Annexin V and PI double staining. (A) Untreated U87MG, (B) U87MG cells treated with BSA loaded curcumin NPs for 12 h.

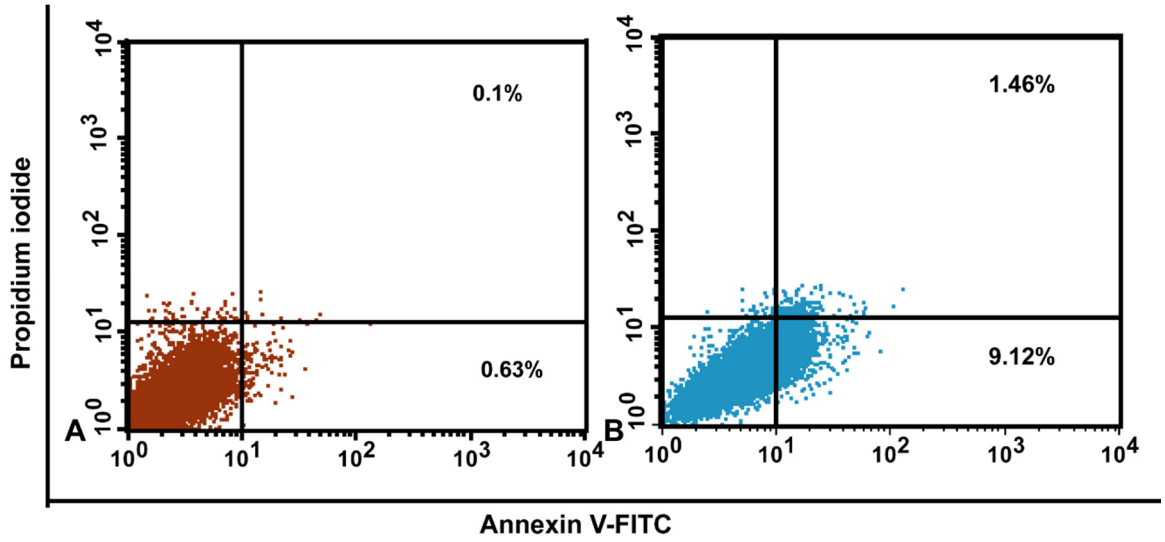

Figure 3.20 Detection of apoptosis in U87-IκBα cells. (A) Untreated U87-IκBα cells and (B) U87-IκBα cells treated with BSA loaded curcumin NPs for 12 h.

3.12 Confirmation of apoptosis by caspase-3 assay

Caspase-3 is called the executioner caspase in apoptosis event. The heightened activity of caspase-3 during the apoptosis is detected by FACS based caspase-3 assay. PE conjugated anticaspase-3 antibody is used for the purpose of studying the apoptosis event. The mode of cell death was reconfirmed by FACS based caspase-3 assay. Among BSA-curcumin NPs treated cells, U87-IκBα cells showed higher number of caspase-3 positive cells (29%) (Figure 3.21 B) than ordinary U87MG cells (12.7%) (Figure 3.22 B) after 16 h of treatment. Thus, the IκBα overexpressing cells showed more sensitivity towards BSA curcumin NPs over ordinary U87MG cells.

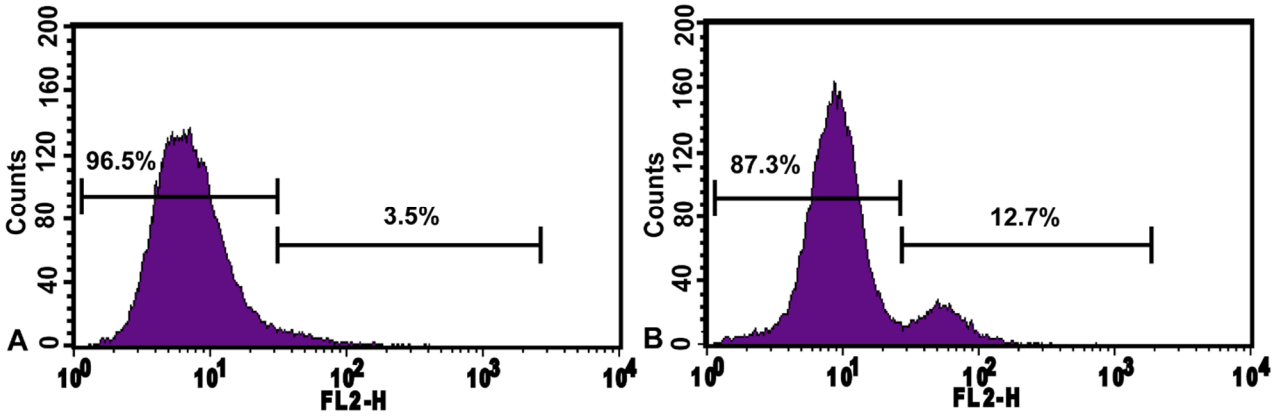

Figure 3.21 Detection of apoptosis in U87MG cells upon treatment with BSA loaded

curcumin NPs for 14 h. (A) untreated U87MG cells and (B) U87MG cells treated with BSA loaded curcumin NPs.

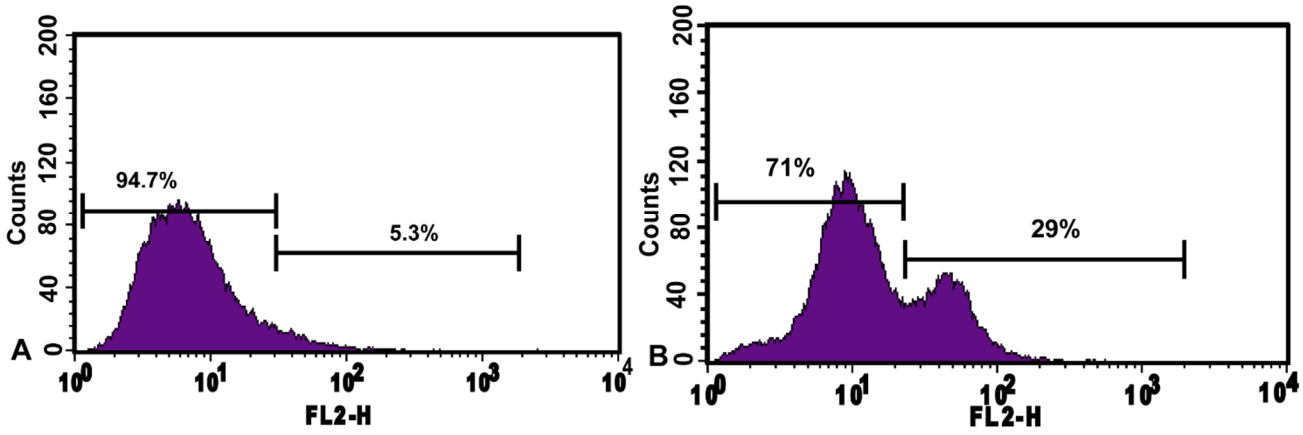

Figure 3.22 Detection of apoptosis in U87MG-IκBα cells upon treatment with BSA loaded curcumin NPs for 16 h. (A) untreated U87MG-IκBα cells and (B) U87MG-IκBα cells treated with BSA loaded curcumin NPs.

3.13 Cell cycle gene expression analysis

The expressions of cell cycle related genes such as, cyclin D1, cyclin D2, p27 and p21 were checked to establish the underlying molecular events. Both curcumin and IκBα are found to modulate the expression of cyclin D1 via inhibition of NFκB (Joyce *et al*, 2001; Mukhopadhyay *et al*, 2002). The expression of cyclin D1 was found to be downregulated in BSA loaded curcumin NPs treated U87MG cells as compared to the untreated cells, which led to G1 phase arrest (Figure 3.23 A). Further, untreated U87- IκBα cells were found to express even lower level of cyclin D1 as a result of IκBα overexpression, which might lead to inhibition of NFκB as compared to ordinary U87MG cells (both treated and untreated). Further, the BSA loaded curcumin NPs treated cells showed low cyclin D1 expression, although not significant when compared to untreated cells (Figure 3.23 A). Cyclin D2 is another D type cyclin critical for G1 to S progression of cell cycle. There is no conclusive report stating that curcumin modulates the expression of cyclin D2 in U87MG cells, although, there is report of activation of cyclin D2 by NFκB in T cells and resting fibroblast (Iwanaga *et al*, 2008). Here, upon treatment with BSA loaded curcumin NPs, more than 4 fold over expression was observed for cyclin D2 in treated ordinary U87MG cells, which indicates that U87MG cells are undergoing proliferation and survival upon treatment, thus

leading to higher expression of cyclin D2. But surprisingly, in U87- IκBα cells, the cyclin D2 expression level was found to be quite less (almost two fold) as compared to untreated ordinary U87MG cells. Upon treatment with BSA loaded curcumin NPs, the cyclin D2 was found to be significantly low, which indicated the there is a synergistic effect of both curcumin and IκBα on the curcumin NPs mediated sensitization. Although no significant differences in expressions have been found in cyclin E (Figure 3.23 C) and cyclin A2 (Figure 3.23 D).

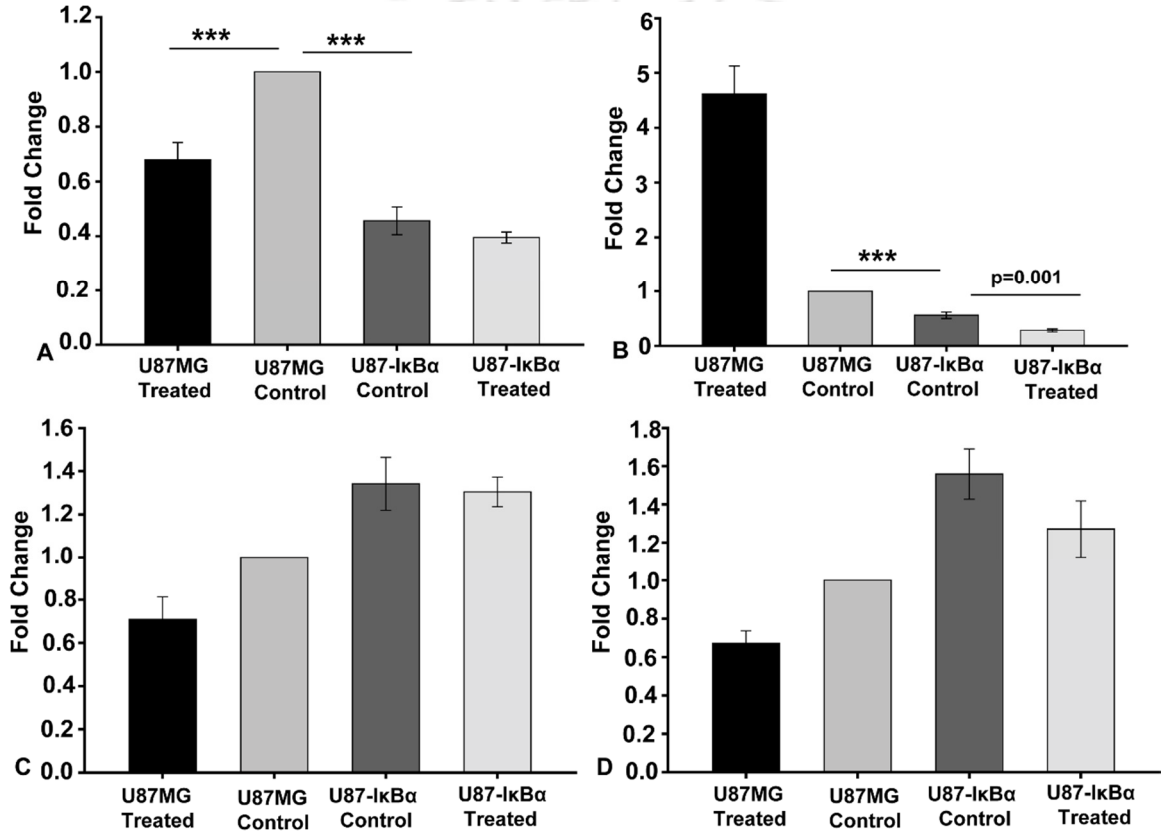

Figure 3.23 Analysis of cell cycle related genes upon treatment with BSA loaded Curcumin NPs by real time PCR. (A) Cyclin D1, (B) Cyclin D2 (C) Cyclin E and (D) Cyclin A2. All data are represented as Mean ± S.D. and the statistical analysis was done by Rank some test followed by Student's t test in Sigma plot software. Statistical significance between untreated control and treated samples were denoted by mentioning p value above the results or by mentioning *** when p<0.001.

The role of p21 and p27 was found in the TNF-α mediated inhibition of human glioma cell proliferation (Kumar *et al*, 2007). The role of NFκB and curcumin mediated upregulation of

p21 and p27 has also been reported (Aggarwal *et* al, 2007; Hasima and Aggarwal, 2013) at the protein level. Here the expression level of p27 (Figure 3.24 A) and p21 (Figure 3.24 B) has been measured upon treatment with BSA loaded curcumin loaded NPs. The p27 expression was found to be higher in treated U87MG cells as compared to the untreated cells. For U87- IκBα cells, p27 expression was found to be higher in untreated cells as compared to the U87MG cells. In treated cells, the p27 expression was found to be significantly higher (almost three fold as compared to untreated U87MG cells and almost two fold as compared to treated U87MG and untreated U87- IκBα cells). Similarly, p21 was also found to be differentially over expressed for both kind of treated cells as compared to their corresponding untreated cells (Figure 3.24 B). The results indicate that the cell cycle arrest in G1 to S phase transition leading to apoptosis (Shishodia *et al*, 2005) is responsible for BSA loaded curcumin NPs mediated sensitization of IκBα over expressing glioma cells, which was found to be much higher as compared to the glioma cells.

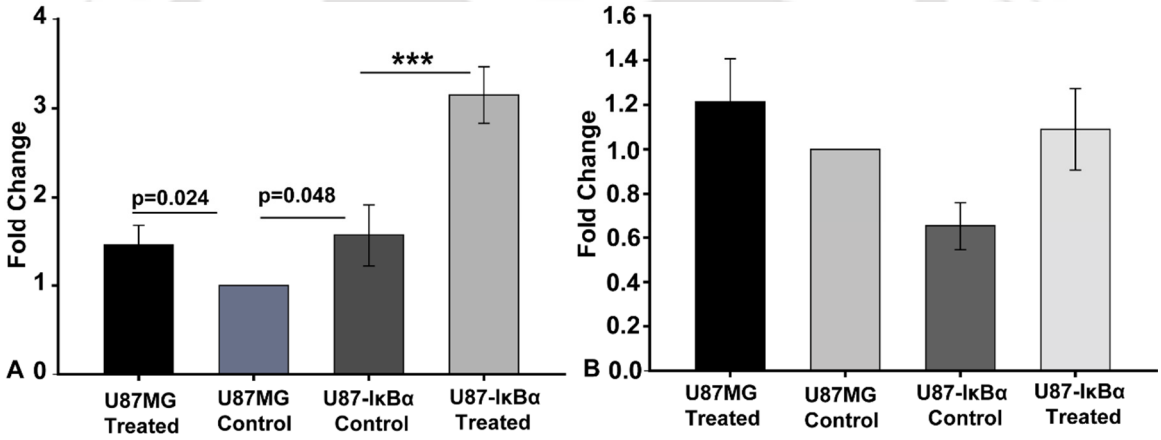

Figure 3.24 Analysis of cell cycle related genes upon treatment with BSA loaded Curcumin NPs by real time PCR. (A) p27 and (B) p21. All data are represented as Mean ± S.D. and the statistical analysis was done by Rank some test followed by Student's t test in Sigma plot software. Statistical significance between untreated control and treated samples were denoted by mentioning p value above the results or by mentioning *** when p<0.001.

3.14 Combination study

The U87MG and U87- IκBα cells were treated in combination with 5-FU and BSA loaded curcumin NPs. This experiment was carried out in two ways- firstly, the cells were treated with different concentrations of 5-FU along with a fixed amount of BSA loaded curcumin

NPs (5 µg/mL). It was found that in the presence of curcumin NPs, the U87- IκBα cells become more sensitized towards 5-FU (Figure 3.25). The result indicates that U87MG confers resistance towards common anticancer drug 5-FU, even in the presence of curcumin NPs. But, IκBα overexpression sensitizes U87MG significantly towards the combination therapy.

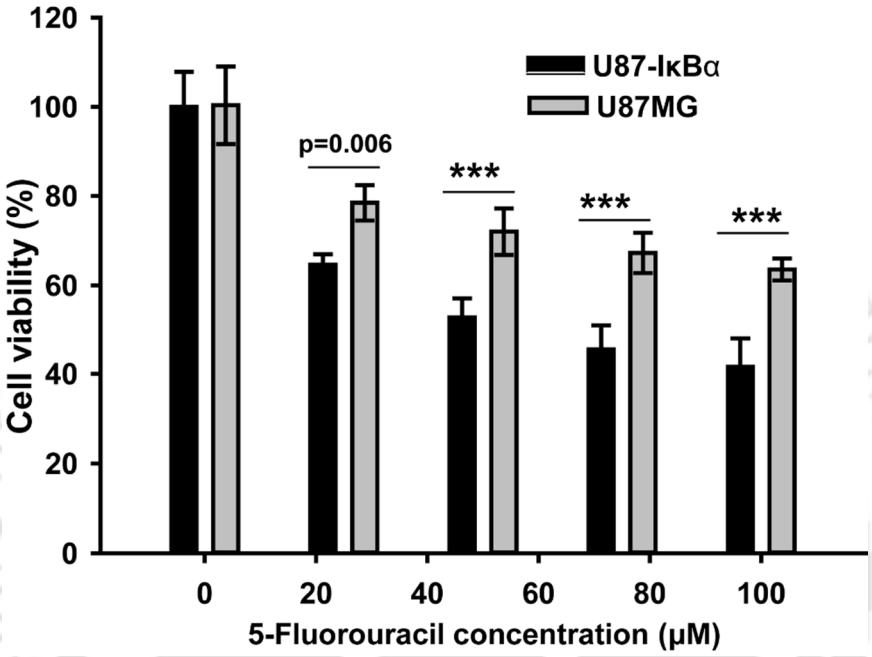

Figure 3.25 Comparative study of anti-cell proliferative effect of 5-FU on U87-IκBα and U87MG cells in combination with BSA loaded curcumin NPs (5 µg/mL). All data are represented as Mean ± S.D. and the statistical analysis was done by two way ANOVA in Sigma Plot software. Statistical significance between treated samples with significant p value (<0.05) are mentioned and p<0.001 are denoted by ***.

In another combination approach, the cells were treated with different concentrations of BSA loaded curcumin NPs with fixed concentration of 5-FU (50 µM). The cell viability decreased steadily in both the cell lines with increasing concentration of BSA loaded curcumin NPs. It was found that both cell lines were equally sensitized by the combination where the effect was more in U87-IκBα cells (Figure 3.26).

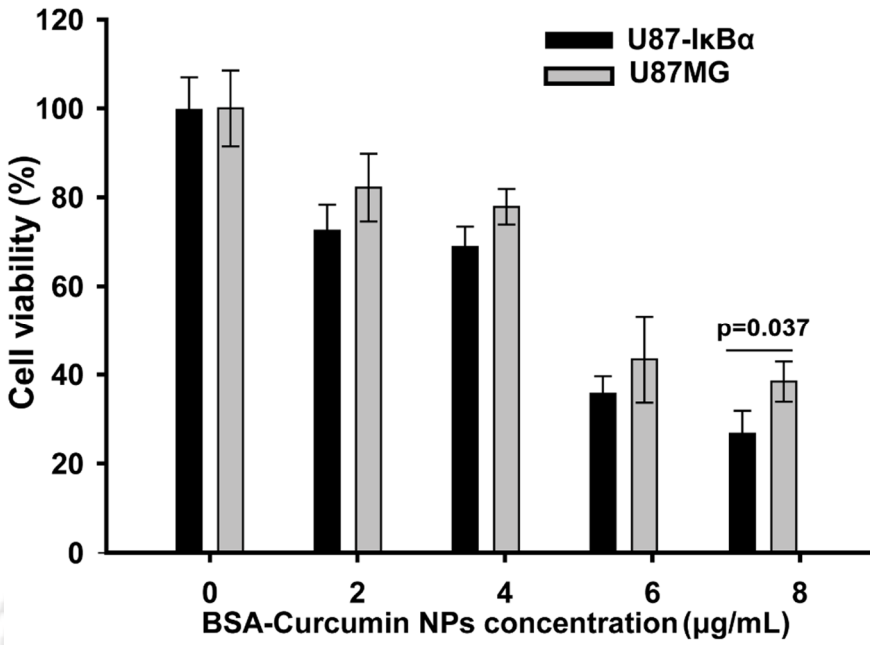

Figure 3.26 Comparative study of anti-cell proliferative effect of BSA loaded curcumin NPs on U87-IκBα and U87MG cells in combination with 5-FU (50 µM). All data are represented as Mean ± S.D. and the statistical analysis was done by two way ANOVA in Sigma Plot software. Statistical significance between treated samples with significant p value (<0.05) are mentioned.

3.15 IκBα stability analysis

U87MG and U87-IκBα cells were treated with BSA loaded curcumin NPs for different time point (0, 40, 100 and 180 min). The cell lysates were collected by lysing the cells with RIPA buffer in presence of cocktail inhibitor. Then the stability of IκBα was checked by immunoblotting method. Here, for U87- IκBα cells, the sustained expression of IκBα was found with respect to U87MG cells. At the beginning (0 min) the IκBα amount was higher in U87- IκBα cells as expected, but in the next time point (40 min) the expression level of IκBα dropped further in U87- IκBα cells than only U87MG cells. Further, at 100 min, the IκBα level in transfected U87MG cells was found to be stable, whereas there was a steady decrease in the amount of IκBα for U87MG cells. After 3h, it was found that the expression level of IκBα diminished to almost zero (Figure 3.27 B), whereas the amount of IκBα remains almost same for U87-IκBα cells (Figure 3.27 A). The result indicated that, upon treatment with BSA loaded curcumin NPs, the NFκB mediated survival mechanism of cells become active resulting in degradation of IκBα, although at a slower rate as curcumin itself is an inhibitor.

But, for IκBα over expressing U87-IκBα cells, the stability of IκBα was found to have increased despite the an initial drop in the amount of IκBα as compared to the U87MG cells, which indicate the higher sensitization of U87- IκBα cells towards BSA loaded curcumin NPs.

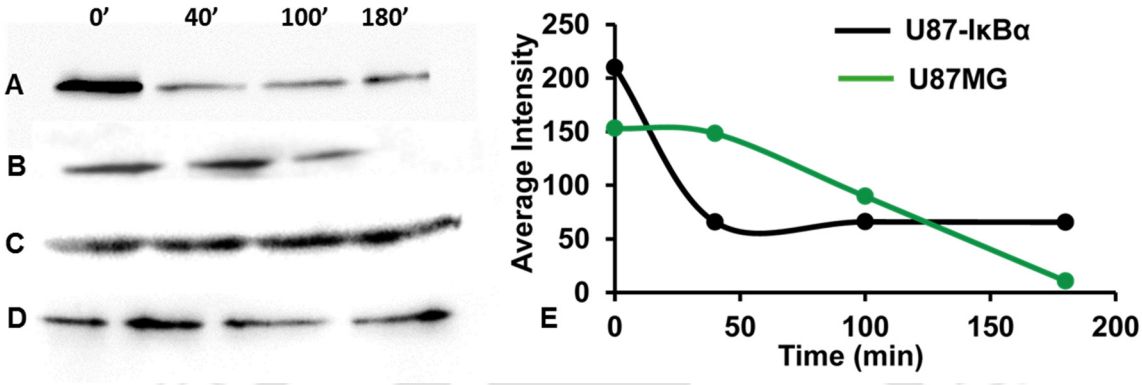

Figure 3.27 Time dependent stability of IκBα in U87MG and U87-IκBα cells after treatment with BSA-curcumin NPs probed by Western blotting. (A) IκBα in U87-IκBα cells, (B) IκBα in U87MG cells, (C) β-Actin as loading control in U87-IκBα cells, (D) β-Actin as loading control in U87MG cells. (E) Change in average intensity of IκBα in U87MG and U87-IκBα cells with time.

Conclusion of part 3

The IκBα overexpressing U87- IκBα stable cell line was established with a purpose to check the role of IκBα in chemosensitization of cells. Anticancer drug, 5-FU to which U87MG is resistant, was administered upon the overexpressing cells, and the anticell proliferative effect was compared with ordinary U87MG cells by MTT assay and CFSE based flow cytometry analysis. Further, the effect of 5-FU on the cell cycle was studied by serum synchronization followed by PI based flowcytometry analysis. The effect of curcumin NPs were checked with BSA loaded curcumin NPs to keep the module almost identical with the previous part. MTT based cell viability assay, fluorescence microscopy and different flowcytometry analysis (PI based cell cycle assay, Caspase-3 and FITC conjugated Annexin V-PI double staining) was employed to study the effect of curcumin NPs over the IκBα over expressing U87-IκBα cells. Higher stability of IκBα protein inside U87-IκBα cells was found out by Western blotting. Further, the combined effect of 5-FU and BSA loaded curcumin NPs was checked on the U87MG and U87-IκBα cells. A higher degree of sensitization was found in U87-IκBα cells.

5

CONCLUSIONS & FUTURE ASPECTS

CONCLUSIONS & FUTURE ASPECTS 5

In conclusion, it may be mentioned here that this thesis work investigated the potential of IκBα as a therapeutic protein. In order to do so, the work was categorized into three different parts.

In *first part*, IκBα was cloned from mammalian cells into bacterial cell and subcloned into expression vector. Then, IκBα was purified from bacterial cells as recombinant GST tagged IκBα protein by glutathione-agarose chromatography. The purified protein was characterized by mass spectrometry, circular dichroism and Western blotting method. In order to deliver the protein inside the cells in its functional form, PVA/PVP based hydrogel nanocarriers (NCs) were synthesized by paraffin oil based green synthesis method with repeated freeze thaw cycle. During synthesis, the protein was encapsulated inside the hydrogel NCs, and the oil was removed by washing it with hexane. The trace amount of hexane was evaporated by air drying. Then, the protein encapsulated hydrogel was characterized by various physical methods. The shape and size were determined by field emission scanning electron microscopy (FESEM) and transmission electron microscopy (TEM). The presence of protein was determined by Fourier transform-infrared (FT-IR) spectrophotometry. The hydrodynamic diameter (z average diameter) of the hydrogel NCs was determined by dynamic light scattering (DLS) method and the surface charge was determined by zeta (ζ) potential measurement. The time dependent protein release profile and pH tenability were also determined at two different pH (pH 7.4 and 4.0). Further, to ensure hydrogel mediated delivery of the protein, FITC conjugated dextran of similar molecular weight was delivered to the cells and determined by microscopy and flow cytometry. Finally, the protein loaded hydrogel NCs were delivered upon two cancer cell lines- cervical carcinoma HeLa and glioblastoma cell line U87MG. HeLa is a cervical cancer cell line to check the efficacy of different drugs and U87MG is resistant to 5-FU and cisplatin. Firstly, the recombinant IκBα encapsulated hydrogel NCs were tested upon HeLa cells and the efficacy was checked by cell viability assay, acridine orange/ethidium bromide based cell staining and identification of live and dead (apoptotic) cells by fluorescence microscopy, flow cytometry based propidium iodide based cell cycle analysis and APO-BrDU antibody based DNA fragmentation analysis as a confirmatory evidence for apoptosis. Further, the

delivery of recombinant IκBα inside the cells was confirmed by anti IκBα antibody based western blotting analysis. The effect of IκBα encapsulated hydrogel was extended to U87MG cells, where it was not found to be as effective as HeLa cells. But, this module was shown to be effective when added in combination with common anticancer drug 5-fluorouracil (5-FU), which is also rendered ineffective against U87MG cells when used alone. Thus, this work indicates the promise of IκBα, the cellular inhibitor of p50/p65 subunit of NFκB as an efficient protien molecule in protein therapeutics domain. Also, this molecule has shown promise in combinatorial therapy towards drug resistant U87MG cells. This observation paved the path for the second part of the thesis work to formulate a combination module of anticancer small molecule with IκBα.

So in *second part*, curcumin nanoparticle was synthesized by stabilizing it with PVP followed by organic to aqueous phase transfer under heating and stirring. Then, the synthesized particles were sonicated and centrifuged to collect the small particles and dispersed in water. During experimentation, IκBα was electrostatically attached to it by poly L lysine. The synthesized NPs were characterized by different methods. Nanoparticles formation was identified by UV-Vis and fluorescence spectroscopy. The shape and size were determined by field emission scanning electron microscopy (FESEM) and transmission electron microscopy (TEM). As the protein is electrostatically attached, the charge upon the NPs at various stage is very important and the surface charge was determined by zeta potential measurement. Exploiting the intrinsic fluorescence property of curcumin, the protein-curcumin NPs module was delivered to HeLa and U87MG cells and determined by fluorescence microscopy. Then the recombinant IκBα loaded curcumin NPs were added upon HeLa and U87MG cells to check its therapeutic efficacy. Curcumin is a well-known bioactive agent with prominent anticancer activities against many types of cancer and also NFκB inhibitor. Thus, higher therapeutic efficacy was determined observed by cell viability assay. Also flow cytometry analysis was carried out to determine the effects of IκBα loaded curcumin NPs and BSA loaded mock curcumin NPs- PI based cell cycle assay, DCFDA dye based ROS detection, FITC tagged Annexin V and PI based apoptosis detection of U87MG and HeLa cells. Further, few key pro apoptotic and antiapoptotic gene expressions were checked by semi quantitative RT PCR. It was found that therapeutic protein and bioactive molecule based combination module may be an attractive agent in natural product based

biopharamaceutical regime. Thus from the obtained results, it was necessary to check the effect of IκBα on a homogenous population and observe the difference in activity when it was expressed inside the cells. This work prompted the third part of the thesis work.

Finally, in the *third part*, IκBα was subcloned into mammalian expression vector pCINeo, transfected into malignant glioblastoma cell line U87MG by lipofectamine based method and IκBα overexpressing U87-IκBα cell line was established by screening with antibiotic G418. The overexpression of IκBα was checked by semiquantitive RT PCR, real time PCR and Western blotting with anti-IκBα antibody. As, U87MG is resistant to 5-FU, and data from first part of the thesis work suggested higher sensitization of U87MG towards 5-FU, the cell viability assay was done by addition of different concentrations of 5-FU. The result indicated greater reduction in cell viability in IκBα over expressing U87-IκBα cells. The flow cytometry based CFSE assay showed that there was a time dependent reduction in cell proliferation in 5-FU treated IκBα over expressing U87-IκBα cells. The effect on cell cycle was checked by FACS based cell cycle study done by PI staining, which revealed differential arrest of cell cycle phases upon treatment with two different concentrations of 5-FU on U87MG cells and U87-IκBα cells. These results revealed that IκBα over expression sensitized the U87MG cells but they did not undergo apoptosis. As in the previous part of the work, the effect of curcumin NPs was checked by coating it with similar molecular weight but nontoxic protein BSA to keep its physicochemical properties relatively identical. The same module was administered upon U87- IκBα cells and ordinary U87MG cells. It was found by cell viability assay that this module has relatively higher anti cell proliferative effect upon transfected U87MG cells. Further, whether the cells are undergoing apoptosis or not was checked by ethidium bromide (EB) based staining method with intrinsic fluorescence of curcumin. A higher number of BSA-curcumin NPs treated cells were found to have stained with EB, which only enters in the membrane compromised cells. Further, the effect was checked by flow cytometry assay with following experiments- PI based cell cycle analysis and determination of sub G0 population (commonly regarded as dead cells), FITC conjugated Annexin V and PI based determination of apoptotic cells and PE conjugated caspase-3 antibody based staining to determine the caspase-3 positive cell population (the cells undergoing apoptosis). Further, the expression of some cell cycle related genes was checked by real time PCR. Then the combinatorial effect of 5-FU and BSA loaded curcumin

NPs was checked upon the U87MG and U87- IκBα cells by cell viability determination, which showed that variable concentrations of BSA loaded curcumin NPs with fixed concentration of 5-FU has higher anticell proliferative effect as compared to different concentrations of 5-FU with fixed concentration of BSA loaded curcumin NPs. But this combinatorial effect was higher than only 5-FU. Thus, this work demonstrated curcumin and IκBα heightened the effect of 5-FU. Further, upon treatment with BSA loaded curcumin NPs for different time points, the half-life of IκBα was found to have increased in IκBα transfected cells as compared to only U87MG cells, which may have an important role in sensitizing the U87MG cells towards 5-FU or curcumin NPs.

Thus, as a whole, this work indicates the potential of IκBα as a therapeutic protein in the growing list of protein based therapeutics and the efficacy of IκBα based therapeutic modules to work in combination with common anticancer drug 5-FU.

The future aspect of this work is the following experiments may be done- .

- Other active form of IκBα (e.g. - super repressor form) may be explored.
- Interaction of recombinant IκBα loaded nanoparticles to be tested with other signaling molecules.

REFERENCES

REFERENCES

Adams, J., Palombella, V.J., Sausville, E.A., Johnson, J., Destree, A., Lazarus, D.D., Maas, J., Pien, C.S., Prakash, S., and Elliott, P.J. (1999). Proteasome inhibitors: a novel class of potent and effective antitumor agents. Cancer Res. *59*, 2615–2622.

Aggarwal, B., Sethi, G., Nair, A., and Ichikawa, H. (2006). Nuclear Factor-κB: A Holy Grail in Cancer Prevention and Therapy. Current Signal Transduction Therapy *1*, 25–52.

Aggarwal, B.B., and Sung, B. (2009). Pharmacological basis for the role of curcumin in chronic diseases: an age-old spice with modern targets. Trends in Pharmacological Sciences *30*, 85–94.

Aggarwal, B.B., Banerjee, S., Bharadwaj, U., Sung, B., Shishodia, S., and Sethi, G. (2007). Curcumin induces the degradation of cyclin E expression through ubiquitin-dependent pathway and up-regulates cyclin-dependent kinase inhibitors p21 and p27 in multiple human tumor cell lines. Biochem. Pharmacol. *73*, 1024–1032.

Aggarwal, B.B., Sundaram, C., Malani, N., and Ichikawa, H. (2007). Curcumin: the Indian solid gold. Adv. Exp. Med. Biol. *595*, 1–75.

Akhtar, F., Rizvi, M.M.A., and Kar, S.K. (2012). Oral delivery of curcumin bound to chitosan nanoparticles cured Plasmodium yoelii infected mice. Biotechnology Advances *30*, 310–320.

Anand, P., Kunnumakkara, A.B., Newman, R.A., and Aggarwal, B.B. (2007). Bioavailability of Curcumin: Problems and Promises. Molecular Pharmaceutics *4*, 807–818.

Anitha, A., Maya, S., Deepa, N., Chennazhi, K.P., Nair, S.V., Tamura, H., and Jayakumar, R. (2011). Efficient water soluble O-carboxymethyl chitosan nanocarrier for the delivery of curcumin to cancer cells. Carbohydrate Polymers *83*, 452–461.

Arenzana-Seisdedos, F., Turpin, P., Rodriguez, M., Thomas, D., Hay, R.T., Virelizier, J.L., and Dargemont, C. (1997). Nuclear localization of I kappa B alpha promotes active transport of NF-kappa B from the nucleus to the cytoplasm. J. Cell. Sci. *110 (Pt 3)*, 369–378.

Atzpodien, J., Kirchner, H., Lopez Hänninen, E., Deckert, M., Fenner, M., and Poliwoda, H. (1993). Interleukin-2 in combination with interferon-α and 5-fluorouracil for metastatic renal cell cancer. European Journal of Cancer *29*, S6–S8.

Baeuerle, P.A., and Baltimore, D. (1988). I kappa B: a specific inhibitor of the NF-kappa B transcription factor. Science *242*, 540–546.

Baldin, V., Lukas, J., Marcote, M.J., Pagano, M., and Draetta, G. (1993). Cyclin D1 is a nuclear protein required for cell cycle progression in G1. Genes Dev. *7*, 812–821.

Baldwin, A.S. (2001). Series Introduction: The transcription factor NF-κB and human disease. Journal of Clinical Investigation *107*, 3–6.

Baldwin, A.S., Jr (1996). The NF-kappa B and I kappa B proteins: new discoveries and insights. Annu. Rev. Immunol. *14*, 649–683.

Bansal, S.S., Goel, M., Aqil, F., Vadhanam, M.V., and Gupta, R.C. (2011). Advanced Drug Delivery Systems of Curcumin for Cancer Chemoprevention. Cancer Prevention Research *4*, 1158–1171.

Bellas, R.E., FitzGerald, M.J., Fausto, N., and Sonenshein, G.E. (1997). Inhibition of NF-kappa B activity induces apoptosis in murine hepatocytes. Am. J. Pathol. *151*, 891–896.

Bentires-Alj, M., Barbu, V., Fillet, M., Chariot, A., Relic, B., Jacobs, N., Gielen, J., Merville, M.-P., and Bours, V. (2003). NF-kappaB transcription factor induces drug resistance through MDR1 expression in cancer cells. Oncogene *22*, 90–97.

Bertz, A., Wöhl-Bruhn, S., Miethe, S., Tiersch, B., Koetz, J., Hust, M., Bunjes, H., and Menzel, H. (2013). Encapsulation of proteins in hydrogel carrier systems for controlled drug delivery: Influence of network structure and drug size on release rate. Journal of Biotechnology *163*, 243–249.

Bharti, A.C., Donato, N., Singh, S., and Aggarwal, B.B. (2003). Curcumin (diferuloylmethane) down-regulates the constitutive activation of nuclear factor-kappa B and IkappaBalpha kinase in human multiple myeloma cells, leading to suppression of proliferation and induction of apoptosis. Blood *101*, 1053–1062.

Bilotti, E. (2013). Carfilzomib: a next-generation proteasome inhibitor for multiple myeloma treatment. Clin J Oncol Nurs *17*, E35–44.

Bisht, S., Feldmann, G., Soni, S., Ravi, R., Karikar, C., Maitra, A., and Maitra, A. (2007). Polymeric nanoparticle-encapsulated curcumin ("nanocurcumin"): a novel strategy for human cancer therapy. Journal of Nanobiotechnology *5*, 3.

Bours, V., Villalobos, J., Burd, P.R., Kelly, K., and Siebenlist, U. (1990). Cloning of a mitogen-inducible gene encoding a κB DNA-binding protein with homology to the rel oncogene and to cell-cycle motifs. Nature *348*, 76–80.

Chen, H.-W., and Huang, H.-C. (1998). Effect of curcumin on cell cycle progression and apoptosis in vascular smooth muscle cells. British Journal of Pharmacology *124*, 1029–1040.

Chen, Y.-Q., Ghosh, S., and Ghosh, G. (1998). A novel DNA recognition mode by the NF-κB p65 homodimer. Nature Structural Biology *5*, 67–73.

Chen, Z., Hagler, J., Palombella, V.J., Melandri, F., Scherer, D., Ballard, D., and Maniatis, T. (1995). Signal-induced site-specific phosphorylation targets I kappa B alpha to the ubiquitin-proteasome pathway. Genes & Development *9*, 1586–1597.

Chen, Z.J., Parent, L., and Maniatis, T. (1996). Site-specific phosphorylation of IkappaBalpha by a novel ubiquitination-dependent protein kinase activity. Cell *84*, 853–862.

Chignell, C.F., Bilski, P., Reszka, K.J., Motten, A.G., Sik, R.H., and Dahl, T.A. (1994). Spectral and photochemical properties of curcumin. Photochem. Photobiol. *59*, 295–302.

Choudhuri, T., Pal, S., Das, T., and Sa, G. (2005). Curcumin selectively induces apoptosis in deregulated cyclin D1-expressed cells at G2 phase of cell cycle in a p53-dependent manner. J. Biol. Chem. *280*, 20059–20068.

Cleland, J.L., Mac, A., Boyd, B., Yang, J., Duenas, E.T., Yeung, D., Brooks, D., Hsu, C., Chu, H., Mukku, V., et al. (1997). The stability of recombinant human growth hormone in poly (lactic-co-glycolic acid) (PLGA) microspheres. Pharm. Res. *14*, 420–425.

Colleoni, M., Cole, B.F., Viale, G., Regan, M.M., Price, K.N., Maiorano, E., Mastropasqua, M.G., Crivellari, D., Gelber, R.D., Goldhirsch, A., et al. (2010). Classical cyclophosphamide, methotrexate, and fluorouracil chemotherapy is more effective in triple-negative, node-negative breast cancer: results from two randomized trials of adjuvant chemoendocrine therapy for node-negative breast cancer. J. Clin. Oncol. *28*, 2966–2973.

Coviello, T., Matricardi, P., and Alhaique, F. (2006). Drug delivery strategies using polysaccharidic gels. Expert Opin Drug Deliv *3*, 395–404.

Coviello, T., Matricardi, P., Marianecci, C., and Alhaique, F. (2007). Polysaccharide hydrogels for modified release formulations. J Control Release *119*, 5–24.

Creasey, W.A., and Markiw, M.E. (1964). Biochemical effects of the vinca alkaloids II. A comparison of the effects of colchicine, vinblastine and vincristine on the synthesis of ribonucleic acids in Ehrlich ascites carcinoma cells. Biochimica et Biophysica Acta (BBA) - Specialized Section on Nucleic Acids and Related Subjects *87*, 601–609.

Cregan, S.P., MacLaurin, J.G., Craig, C.G., Robertson, G.S., Nicholson, D.W., Park, D.S., and Slack, R.S. (1999). Bax-dependent caspase-3 activation is a key determinant in p53-induced apoptosis in neurons. J. Neurosci. *19*, 7860–7869.

Croy, C.H., Bergqvist, S., Huxford, T., Ghosh, G., and Komives, E.A. (2004). Biophysical characterization of the free IkappaBalpha ankyrin repeat domain in solution. Protein Sci. *13*, 1767–1777.

D'Souza, A.J.M., Schowen, R.L., and Topp, E.M. (2004). Polyvinylpyrrolidone–drug conjugate: synthesis and release mechanism. Journal of Controlled Release *94*, 91–100.

De Paoli Lacerda, S.H., Ingber, B., and Rosenzweig, N. (2005). Structure-release rate correlation in collagen gels containing fluorescent drug analog. Biomaterials *26*, 7164–7172.

Delmas, D., Solary, E., and Latruffe, N. (2011). Resveratrol, a Phytochemical Inducer of Multiple Cell Death Pathways: Apoptosis, Autophagy and Mitotic Catastrophe. Current Medicinal Chemistry *18*, 1100–1121.

Dolan, M.E., Mitchell, R.B., Mummert, C., Moschel, R.C., and Pegg, A.E. (1991). Effect of O6-benzylguanine analogues on sensitivity of human tumor cells to the cytotoxic effects of alkylating agents. Cancer Res. *51*, 3367–3372.

Dolcet, X., Llobet, D., Pallares, J., and Matias-Guiu, X. (2005). NF-kB in development and progression of human cancer. Virchows Archiv *446*, 475–482.

Duan, J., Zhang, Y., Han, S., Chen, Y., Li, B., Liao, M., Chen, W., Deng, X., Zhao, J., and Huang, B. (2010). Synthesis and in vitro/in vivo anti-cancer evaluation of curcumin-loaded chitosan/poly (butyl cyanoacrylate) nanoparticles. Int J Pharm *400*, 211–220.

Duvoix, A., Blasius, R., Delhalle, S., Schnekenburger, M., Morceau, F., Henry, E., Dicato, M., and Diederich, M. (2005). Chemopreventive and therapeutic effects of curcumin. Cancer Lett. *223*, 181–190.

El-Hag Ali, A., Shawky, H.A., Abd El Rehim, H.A., and Hegazy, E.A. (2003). Synthesis and characterization of PVP/AAc copolymer hydrogel and its applications in the removal of heavy metals from aqueous solution. European Polymer Journal *39*, 2337–2344.

Emmerich, F., Meiser, M., Hummel, M., Demel, G., Foss, H.D., Jundt, F., Mathas, S., Krappmann, D., Scheidereit, C., Stein, H., et al. (1999). Overexpression of I kappa B alpha without inhibition of NF-kappaB activity and mutations in the Ikappa B alpha gene in Reed-Sternberg cells. Blood *94*, 3129–3134.

Ernst, M.K., Dunn, L.L., and Rice, N.R. (1995). The PEST-like sequence of I kappa B alpha is responsible for inhibition of DNA binding but not for cytoplasmic retention of c-Rel or RelA homodimers. Mol. Cell. Biol. *15*, 872–882.

Finucane, D.M., Bossy-Wetzel, E., Waterhouse, N.J., Cotter, T.G., and Green, D.R. (1999). Bax-induced Caspase Activation and Apoptosis via Cytochrome c Release from Mitochondria Is Inhibitable by Bcl-xL. Journal of Biological Chemistry *274*, 2225–2233.

Folprecht, G., Lutz, M.P., Schöffski, P., Seufferlein, T., Nolting, A., Pollert, P., and Köhne, C.-H. (2006). Cetuximab and irinotecan/5-fluorouracil/folinic acid is a safe combination for the first-line treatment of patients with epidermal growth factor receptor expressing metastatic colorectal carcinoma. Ann. Oncol. *17*, 450–456.

Foxwell, B., Browne, K., Bondeson, J., Clarke, C., de Martin, R., Brennan, F., and Feldmann, M. (1998). Efficient adenoviral infection with IkappaB alpha reveals that macrophage tumor necrosis factor alpha production in rheumatoid arthritis is NF-kappaB dependent. Proc. Natl. Acad. Sci. U.S.A. *95*, 8211–8215.

Galm, U., Hager, M.H., Van Lanen, S.G., Ju, J., Thorson, J.S., and Shen, B. (2005). Antitumor antibiotics: bleomycin, enediynes, and mitomycin. Chem. Rev. *105*, 739–758.

Gandapu, U., Chaitanya, R.K., Kishore, G., Reddy, R.C., and Kondapi, A.K. (2011). Curcumin-loaded apotransferrin nanoparticles provide efficient cellular uptake and effectively inhibit HIV-1 replication in vitro. PLoS ONE *6*, e23388.

George, M., and Abraham, T.E. (2006). Polyionic hydrocolloids for the intestinal delivery of protein drugs: alginate and chitosan--a review. J Control Release *114*, 1–14.

Gerondakis, S., and Siebenlist, U. (2009). Roles of the NF- B Pathway in Lymphocyte Development and Function. Cold Spring Harbor Perspectives in Biology *2*, a000182–a000182.

Gerondakis, S., Grumont, R., Gugasyan, R., Wong, L., Isomura, I., Ho, W., and Banerjee, A. (2006). Unravelling the complexities of the NF-kappaB signalling pathway using mouse knockout and transgenic models. Oncogene *25*, 6781–6799.

Ghosh, G., van Duyne, G., Ghosh, S., and Sigler, P.B. (1995). Structure of NF-kappa B p50 homodimer bound to a kappa B site. Nature *373*, 303–310.

Ghosh, S., May, M.J., and Kopp, E.B. (1998). NF-kappa B and Rel proteins: evolutionarily conserved mediators of immune responses. Annu. Rev. Immunol. *16*, 225–260.

Gilmore, T., Gapuzan, M.-E., Kalaitzidis, D., and Starczynowski, D. (2002). Rel/NF-kappa B/I kappa B signal transduction in the generation and treatment of human cancer. Cancer Lett. *181*, 1–9.

Gopinath, P., Gogoi, S.K., Chattopadhyay, A., and Ghosh, S.S. (2008). Implications of silver nanoparticle induced cell apoptosis for in vitro gene therapy. Nanotechnology *19*, 075104.

Greenfield, N., and Fasman, G.D. (1969). Computed circular dichroism spectra for the evaluation of protein conformation. Biochemistry *8*, 4108–4116.

Greenfield, N.J. (2006). Using circular dichroism spectra to estimate protein secondary structure. Nat Protoc *1*, 2876–2890.

Grem, J.L. (2000). 5-Fluorouracil: forty-plus and still ticking. A review of its preclinical and clinical development. Invest New Drugs *18*, 299–313.

Grumont, R.J., and Gerondakis, S. (1989). Structure of a mammalian c-rel protein deduced from the nucleotide sequence of murine cDNA clones. Oncogene Res. *4*, 1–8.

Gupta, V., Aseh, A., Ríos, C.N., Aggarwal, B.B., and Mathur, A.B. (2009). Fabrication and characterization of silk fibroin-derived curcumin nanoparticles for cancer therapy. Int J Nanomedicine *4*, 115–122.

Hamaguchi, T., Ono, K., and Yamada, M. (2010). REVIEW: Curcumin and Alzheimer's Disease: Curcumin and AD. CNS Neuroscience & Therapeutics *16*, 285–297.

Hamidi, M., Azadi, A., and Rafiei, P. (2008). Hydrogel nanoparticles in drug delivery. Advanced Drug Delivery Reviews *60*, 1638–1649.

Hasima, N., and Aggarwal, B.B. (2013). Targeting Proteasomal Pathways by Dietary Curcumin for Cancer Prevention and Treatment. Curr. Med. Chem.

Hassan, C.M. and Peppas, N.A. (2000). Structure and applications of poly (vinyl alcohol) hydrogels produced by conventional crosslinking or by freeze/thawing methods, in: J.Y. Chang, D.Y. Godovsky, M.J. Han, C.M. Hassan, J. Kim, B. Lee, Y. Lee, N.A. Peppas, R.P. Quirk, T. Yoo (Eds.), Biopolymers PVA Hydrogels, Anionic Polymerisation Nanocomposites, Advances in Polymer Science, vol. 153, Springer, Berlin, , pp. 37–65.

Hassan, C.M., and Peppas, N.A.(2000) Structure and Applications of Poly (vinyl alcohol) Hydrogels Produced by Conventional Crosslinking or by Freezing/Thawing Methods. In Biopolymers · PVA Hydrogels, Anionic Polymerisation Nanocomposites, (Berlin, Heidelberg: Springer Berlin Heidelberg), pp. 37–65.

Hatada, E.N., Nieters, A., Wulczyn, F.G., Naumann, M., Meyer, R., Nucifora, G., McKeithan, T.W., and Scheidereit, C. (1992). The ankyrin repeat domains of the NF-kappa

B precursor p105 and the protooncogene bcl-3 act as specific inhibitors of NF-kappa B DNA binding. Proc. Natl. Acad. Sci. U.S.A. *89*, 2489–2493.

Hayden, M.S., and Ghosh, S. (2004). Signaling to NF- B. Genes & Development *18*, 2195–2224.

Hayden, M.S., and Ghosh, S. (2008). Shared Principles in NF-κB Signaling. Cell *132*, 344–362.

Helleday, T., Petermann, E., Lundin, C., Hodgson, B., and Sharma, R.A. (2008). DNA repair pathways as targets for cancer therapy. Nat. Rev. Cancer *8*, 193–204.

Hideshima, T., Chauhan, D., Podar, K., Schlossman, R.L., Richardson, P., and Anderson, K.C. (2001). Novel therapies targeting the myeloma cell and its bone marrow microenvironment. Semin. Oncol. *28*, 607–612.

Hoffman, B., and Liebermann, D.A. (2008). Apoptotic signaling by c-MYC. Oncogene *27*, 6462–6472.

Hoffmann, A., and Baltimore, D. (2006). Circuitry of nuclear factor kappaB signaling. Immunol. Rev. *210*, 171–186.

Holzwarth, G., and Doty, P. (1965). The ultraviolet circular dichroism of polypeptides. J. Am. Chem. Soc. *87*, 218–228.

Hu, B.-H., Su, J., and Messersmith, P.B. (2009). Hydrogels Cross-Linked by Native Chemical Ligation. Biomacromolecules *10*, 2194–2200.

Huang, T.T., Kudo, N., Yoshida, M., and Miyamoto, S. (2000). A nuclear export signal in the N-terminal regulatory domain of IkappaBalpha controls cytoplasmic localization of inactive NF-kappaB/IkappaBalpha complexes. Proc. Natl. Acad. Sci. U.S.A. *97*, 1014–1019.

Hurley, L.H. (2002). DNA and its associated processes as targets for cancer therapy. Nat. Rev. Cancer *2*, 188–200.

Hyon, S.H., Cha, W.I., Ikada, Y., Kita, M., Ogura, Y., and Honda, Y. (1994). Poly(vinyl alcohol) hydrogels as soft contact lens material. J Biomater Sci Polym Ed *5*, 397–406.

Ikada, Y., Jamshidi, K., Tsuji, H., and Hyon, S.H. (1987). Stereocomplex formation between enantiomeric poly (lactides). Macromolecules *20*, 904–906.

Iwanaga, R., Ozono, E., Fujisawa, J., Ikeda, M.A., Okamura, N., Huang, Y., and Ohtani, K. (2008). Activation of the cyclin D2 and cdk6 genes through NF-kappaB is critical for cell-cycle progression induced by HTLV-I Tax. Oncogene *27*, 5635–5642.

Jaklenec, A., Hinckfuss, A., Bilgen, B., Ciombor, D.M., Aaron, R., and Mathiowitz, E. (2008). Sequential release of bioactive IGF-I and TGF-beta 1 from PLGA microsphere-based scaffolds. Biomaterials *29*, 1518–1525.

Joyce, D., Albanese, C., Steer, J., Fu, M., Bouzahzah, B., and Pestell, R.G. (2001). NF-kappaB and cell-cycle regulation: the cyclin connection. Cytokine Growth Factor Rev. *12*, 73–90.

Kaltschmidt, B., Kaltschmidt, C., Hehner, S.P., Dröge, W., and Schmitz, M.L. (1999). Repression of NF-kappaB impairs HeLa cell proliferation by functional interference with cell cycle checkpoint regulators. Oncogene *18*, 3213–3225.

Kamei, N., Morishita, M., Chiba, H., Kavimandan, N.J., Peppas, N.A., and Takayama, K. (2009). Complexation hydrogels for intestinal delivery of interferon beta and calcitonin. J Control Release *134*, 98–102.

Kanai, F., Kawakami, T., Hamada, H., Sadata, A., Yoshida, Y., Tanaka, T., Ohashi, M., Tateishi, K., Shiratori, Y., and Omata, M. (1998). Adenovirus-mediated transduction of Escherichia coli uracil phosphoribosyltransferase gene sensitizes cancer cells to low concentrations of 5-fluorouracil. Cancer Res. *58*, 1946–1951.

Karin, M., and Ben-Neriah, Y. (2000). Phosphorylation Meets Ubiquitination: The Control of NF-κB Activity. Annual Review of Immunology *18*, 621–663.

Karmakar, S., Banik, N.L., and Ray, S.K. (2007). Curcumin suppressed anti-apoptotic signals and activated cysteine proteases for apoptosis in human malignant glioblastoma U87MG cells. Neurochem. Res. *32*, 2103–2113.

Kawamura, K., Tasaki, K., Hamada, H., Takenaga, K., Sakiyama, S., and Tagawa, M. (2000). Expression of Escherichia coli uracil phosphoribosyltransferase gene in murine

colon carcinoma cells augments the antitumoral effect of 5-fluorouracil and induces protective immunity. Cancer Gene Ther. *7*, 637–643.

Kern, M.A., Haugg, A.M., Koch, A.F., Schilling, T., Breuhahn, K., Walczak, H., Fleischer, B., Trautwein, C., Michalski, C., Schulze-Bergkamen, H., et al. (2006). Cyclooxygenase-2 inhibition induces apoptosis signaling via death receptors and mitochondria in hepatocellular carcinoma. Cancer Res. *66*, 7059–7066.

Khan, M.A., Gahlot, S., and Majumdar, S. (2012). Oxidative stress induced by curcumin promotes the death of Cutaneous T-cell Lymphoma (HuT-78) by disrupting the function of several molecular targets. Molecular Cancer Therapeutics *11*, 1873–1883.

Kieran, M., Blank, V., Logeat, F., Vandekerckhove, J., Lottspeich, F., Le Bail, O., Urban, M.B., Kourilsky, P., Baeuerle, P.A., and Israël, A. (1990). The DNA binding subunit of NF-kappa B is identical to factor KBF1 and homologous to the rel oncogene product. Cell *62*, 1007–1018.

Kim, T.H., Jiang, H.H., Youn, Y.S., Park, C.W., Tak, K.K., Lee, S., Kim, H., Jon, S., Chen, X., and Lee, K.C. (2011). Preparation and characterization of water-soluble albumin-bound curcumin nanoparticles with improved antitumor activity. Int J Pharm *403*, 285–291.

Kobayashi, H., Minatoguchi, S., Yasuda, S., Bao, N., Kawamura, I., Iwasa, M., Yamaki, T., Sumi, S., Misao, Y., Ushikoshi, H., et al. (2008). Post-infarct treatment with an erythropoietin-gelatin hydrogel drug delivery system for cardiac repair. Cardiovasc. Res. *79*, 611–620.

Kong, J., and Yu, S. (2007). Fourier transform infrared spectroscopic analysis of protein secondary structures. Acta Biochim. Biophys. Sin. (Shanghai) *39*, 549–559.

Koo, J.Y., Kim, H.J., Jung, K.-O., and Park, K.-Y. (2004). Curcumin inhibits the growth of AGS human gastric carcinoma cells in vitro and shows synergism with 5-fluorouracil. J Med Food *7*, 117–121.

Kumar, A., Takada, Y., Boriek, A., and Aggarwal, B. (2004). Nuclear factor-κB: its role in health and disease. Journal of Molecular Medicine *82*.

Kumar, P., Shiras, A., Das, G., Jagtap, J.C., Prasad, V., and Shastry, P. (2007). Differential expression and role of p21cip/waf1 and p27kip1 in TNF-α-induced inhibition of proliferation in human glioma cells. Molecular Cancer *6*, 42.

Kunnumakkara, A.B., Anand, P., and Aggarwal, B.B. (2008). Curcumin inhibits proliferation, invasion, angiogenesis and metastasis of different cancers through interaction with multiple cell signaling proteins. Cancer Letters *269*, 199–225.

Langer, R., and Peppas, N.A. (2003). Advances in biomaterials, drug delivery, and bionanotechnology. AIChE Journal *49*, 2990–3006.

Lawrence, T. (2009). The nuclear factor NF-kappaB pathway in inflammation. Cold Spring Harb Perspect Biol *1*, a001651.

Lee, D.S., Lee, M.K., and Kim, J.H. (2009). Curcumin induces cell cycle arrest and apoptosis in human osteosarcoma (HOS) cells. Anticancer Res. *29*, 5039–5044.

Lee, K.Y., Peters, M.C., Anderson, K.W., and Mooney, D.J. (2000). Controlled growth factor release from synthetic extracellular matrices. Nature *408*, 998–1000.

Leeman, J.R., Weniger, M.A., Barth, T.F., and Gilmore, T.D. (2008). Deletion analysis and alternative splicing define a transactivation inhibitory domain in human oncoprotein REL. Oncogene *27*, 6770–6781.

Li, J.K., Wang, N., and Wu, X.S. (1998). Poly (vinyl alcohol) nanoparticles prepared by freezing–thawing process for protein/peptide drug delivery. Journal of Controlled Release *56*, 117–126.

Li, L., Braiteh, F.S., and Kurzrock, R. (2005). Liposome-encapsulated curcumin: In vitro and in vivo effects on proliferation, apoptosis, signaling, and angiogenesis. Cancer *104*, 1322–1331.

Li, M.-H., Ito, D., Sanada, M., Odani, T., Hatori, M., Iwase, M., and Nagumo, M. (2004). Effect of 5-fluorouracil on G1 phase cell cycle regulation in oral cancer cell lines. Oral Oncol. *40*, 63–70.

Lin, Z.P., Boller, Y.C., Amer, S.M., Russell, R.L., Pacelli, K.A., Patierno, S.R., and Kennedy, K.A. (1998). Prevention of brefeldin A-induced resistance to teniposide by the

proteasome inhibitor MG-132: involvement of NF-kappaB activation in drug resistance. Cancer Res. *58*, 3059–3065.

Longley, D.B., Harkin, D.P., and Johnston, P.G. (2003). 5-fluorouracil: mechanisms of action and clinical strategies. Nat. Rev. Cancer *3*, 330–338.

Luque, I., and Gélinas, C. (1998). Distinct domains of IkappaBalpha regulate c-Rel in the cytoplasm and in the nucleus. Mol. Cell. Biol. *18*, 1213–1224.

Magné, N., Toillon, R.-A., Bottero, V., Didelot, C., Houtte, P.V., Gérard, J.-P., and Peyron, J.-F. (2006). NF-kappaB modulation and ionizing radiation: mechanisms and future directions for cancer treatment. Cancer Lett. *231*, 158–168.

Mahady, G.B., Pendland, S.L., Yun, G., and Lu, Z.Z. (2002). Turmeric (Curcuma longa) and curcumin inhibit the growth of Helicobacter pylori, a group 1 carcinogen. Anticancer Res. *22*, 4179–4181.

Malek, S., Huang, D.-B., Huxford, T., Ghosh, S., and Ghosh, G. (2003). X-ray crystal structure of an IkappaBbeta x NF-kappaB p65 homodimer complex. J. Biol. Chem. *278*, 23094–23100.

Malkoch, M., Vestberg, R., Gupta, N., Mespouille, L., Dubois, P., Mason, A.F., Hedrick, J.L., Liao, Q., Frank, C.W., Kingsbury, K., et al. (2006). Synthesis of well-defined hydrogel networks using click chemistry. Chem. Commun. (Camb.) 2774–2776.

Mansur, H.S., Sadahira, C.M., Souza, A.N., and Mansur, A.A.P. (2008). FTIR spectroscopy characterization of poly (vinyl alcohol) hydrogel with different hydrolysis degree and chemically crosslinked with glutaraldehyde. Materials Science and Engineering: C *28*, 539–548.

Marienfeld, R., Neumann, M., Chuvpilo, S., Escher, C., Kneitz, B., Avots, A., Schimpl, A., and Serfling, E. (1997). Cyclosporin A interferes with the inducible degradation of NF-kappa B inhibitors, but not with the processing of p105/NF-kappa B1 in T cells. Eur. J. Immunol. *27*, 1601–1609.

Meyer, S., Kohler, N.G., and Joly, A. (1997). Cyclosporine A is an uncompetitive inhibitor of proteasome activity and prevents NF-kappaB activation. FEBS Lett. *413*, 354–358.

Milo, L.J., Jr, Lai, J.H., Wu, W., Liu, Y., Maw, H., Li, Y., Jin, Z., Shu, Y., Poplawski, S.E., Wu, Y., et al. (2011). Chemical and biological evaluation of dipeptidyl boronic acid proteasome inhibitors for use in prodrugs and pro-soft drugs targeting solid tumors. J. Med. Chem. *54*, 4365–4377.

Mitsiades, C.S., Mitsiades, N., Poulaki, V., Schlossman, R., Akiyama, M., Chauhan, D., Hideshima, T., Treon, S.P., Munshi, N.C., Richardson, P.G., et al. (2002). Activation of NF-kappaB and upregulation of intracellular anti-apoptotic proteins via the IGF-1/Akt signaling in human multiple myeloma cells: therapeutic implications. Oncogene *21*, 5673–5683.

Moiseeva, E.P., Almeida, G.M., Jones, G.D.D., and Manson, M.M. (2007). Extended treatment with physiologic concentrations of dietary phytochemicals results in altered gene expression, reduced growth, and apoptosis of cancer cells. Mol. Cancer Ther. *6*, 3071–3079.

Muenchen, H.J., Lin, D.L., Walsh, M.A., Keller, E.T., and Pienta, K.J. (2000). Tumor necrosis factor-alpha-induced apoptosis in prostate cancer cells through inhibition of nuclear factor-kappaB by an IkappaBalpha "super-repressor."Clin. Cancer Res. *6*, 1969–1977.

Mukhopadhyay, A., Banerjee, S., Stafford, L.J., Xia, C., Liu, M., and Aggarwal, B.B. (2002). Curcumin-induced suppression of cell proliferation correlates with down-regulation of cyclin D1 expression and CDK4-mediated retinoblastoma protein phosphorylation. Oncogene *21*, 8852–8861.

Müller, C.W., Rey, F.A., Sodeoka, M., Verdine, G.L., and Harrison, S.C. (1995). Structure of the NF-κB p50 homodimer bound to DNA. Nature *373*, 311–317.

Nakase, H., Okazaki, K., Tabata, Y., Ozeki, M., Watanabe, N., Ohana, M., Uose, S., Uchida, K., Nishi, T., Mastuura, M., et al. (2002). New cytokine delivery system using gelatin microspheres containing interleukin-10 for experimental inflammatory bowel disease. J. Pharmacol. Exp. Ther. *301*, 59–65

Nam, N.-H. (2006). Naturally occurring NF-kappaB inhibitors. Mini Rev Med Chem *6*, 945–951.

Nguyen, K.T., and West, J.L. (2002). Photopolymerizable hydrogels for tissue engineering applications. Biomaterials *23*, 4307–4314.

Nolan, G.P., Ghosh, S., Liou, H.C., Tempst, P., and Baltimore, D. (1991). DNA binding and I kappa B inhibition of the cloned p65 subunit of NF-kappa B, a rel-related polypeptide. Cell *64*, 961–969.

Oh, H.I., Hoff, J.E., Armstrong, G.S., and Haff, L.A. (1980). Hydrophobic interaction in tannin-protein complexes. Journal of Agricultural and Food Chemistry *28*, 394–398.

Ohno, H., Takimoto, G, and McKeithan, TW (1990). The candidate proto-oncogene bcl-3 is related to genes implicated in cell lineage determination and cell cycle control. Cell *60*, 991–997.

Ohya, Y., Takei, T., Kobayashi, H., and Ouchi, T. (1993). Release behaviour of 5-fluorouracil from chitosan-gel microspheres immobilizing 5-fluorouracil derivative coated with polysaccharides and their cell specific recognition. J Microencapsul *10*, 1–9.

Ota, H., Nagano, H., Sakon, M., Eguchi, H., Kondo, M., Yamamoto, T., Nakamura, M., Damdinsuren, B., Wada, H., Marubashi, S., et al. (2005). Treatment of hepatocellular carcinoma with major portal vein thrombosis by combined therapy with subcutaneous interferon-alpha and intra-arterial 5-fluorouracil; role of type 1 interferon receptor expression. Br. J. Cancer *93*, 557–564.

Ouaaz, F., Arron, J., Zheng, Y., Choi, Y., and Beg, A.A. (2002). Dendritic Cell Development and Survival Require Distinct NF-κB Subunits. Immunity *16*, 257–270.

Owellen, R.J., Owens, A.H., and Donigian, D.W. (1972). The binding of vincristine, vinblastine and colchicine to tubulin. Biochemical and Biophysical Research Communications *47*, 685–691.

Paluszczak, J., Krajka-Kuźniak, V., and Baer-Dubowska, W. (2010). The effect of dietary polyphenols on the epigenetic regulation of gene expression in MCF7 breast cancer cells. Toxicology Letters *192*, 119–125.

Parker, W.B., and Cheng, Y.C. (1990). Metabolism and mechanism of action of 5-fluorouracil. Pharmacology & Therapeutics *48*, 381–395.

Patel, P.N., Gobin, A.S., West, J.L., and Patrick, C.W., Jr (2005). Poly(ethylene glycol) hydrogel system supports preadipocyte viability, adhesion, and proliferation. Tissue Eng. *11*, 1498–1505.

Pfaffl, M.W. (2001). A new mathematical model for relative quantification in real-time RT-PCR. Nucleic Acids Res. *29*, e45.

Pierce, J.W., Read, M.A., Ding, H., Luscinskas, F.W., and Collins, T. (1996). Salicylates inhibit I kappa B-alpha phosphorylation, endothelial-leukocyte adhesion molecule expression, and neutrophil transmigration. J. Immunol. *156*, 3961–3969.

Rajendran, P., Ho, E., Williams, D.E., and Dashwood, R.H. (2011). Dietary phytochemicals, HDAC inhibition, and DNA damage/repair defects in cancer cells. Clinical Epigenetics *3*, 4.

Rawat, S., Raman Suri, C., and Sahoo, D.K. (2010). Molecular mechanism of polyethylene glycol mediated stabilization of protein. Biochem. Biophys. Res. Commun. *392*, 561–566.

Razzak, M.T., Zainuddin, Erizal, Dewi, S.P., Lely, H., Taty, E., and Sukirno (1999). The characterization of dressing component materials and radiation formation of PVA–PVP hydrogel. Radiation Physics and Chemistry *55*, 153–165.

Reimer, R.R., Hoover, R., Fraumeni, J.F., and Young, R.C. (1977). Acute Leukemia after Alkylating-Agent Therapy of Ovarian Cancer. New England Journal of Medicine *297*, 177–181.

Rejman, J., Oberle, V., Zuhorn, I.S., and Hoekstra, D. (2004). Size-dependent internalization of particles via the pathways of clathrin- and caveolae-mediated endocytosis. Biochem. J. *377*, 159–169.

Ricciardi, R., Auriemma, F., De Rosa, C., and Lauprêtre, F. (2004). X-ray Diffraction Analysis of Poly (vinyl alcohol) Hydrogels, Obtained by Freezing and Thawing Techniques. Macromolecules *37*, 1921–1927.

Rottjakob, E.M., Sachdev, S., Leanna, C.A., McKinsey, T.A., and Hannink, M. (1996). PEST-dependent cytoplasmic retention of v-Rel by I (kappa) B-alpha: evidence that I (kappa) B-alpha regulates cellular localization of c-Rel and v-Rel by distinct mechanisms. J. Virol. *70*, 3176–3188.

Rushlow, C., and Warrior, R. (1992). The rel family of proteins. Bioessays *14*, 89–95.

Scherer, D.C., Brockman, J.A., Chen, Z., Maniatis, T., and Ballard, D.W. (1995). Signal-induced degradation of I kappa B alpha requires site-specific ubiquitination. Proceedings of the National Academy of Sciences *92*, 11259–11263.

Schrama, D., Reisfeld, R.A., Becker, J.C., (2006). Antibody targeted drugs as cancer therapeutics. Nature Reviews Drug Discovery *5 (2)*, 147–159.

Scott, J.D., and Williams, R.M. (2002). Chemistry and biology of the tetrahydroisoquinoline antitumor antibiotics. Chem. Rev. *102*, 1669–1730.

Scudiero, D.A., Shoemaker, R.H., Paull, K.D., Monks, A., Tierney, S., Nofziger, T.H., Currens, M.J., Seniff, D., and Boyd, M.R. (1988). Evaluation of a soluble tetrazolium/formazan assay for cell growth and drug sensitivity in culture using human and other tumor cell lines. Cancer Res. *48*, 4827–4833.

Seliktar, D., Zisch, A.H., Lutolf, M.P., Wrana, J.L., and Hubbell, J.A. (2004). MMP-2 sensitive, VEGF-bearing bioactive hydrogels for promotion of vascular healing. J Biomed Mater Res A *68*, 704–716.

Sen, R. (2006). Control of B lymphocyte apoptosis by the transcription factor NF-kappaB. Immunity *25*, 871–883.

Sen, R., and Baltimore, D. (1986). Inducibility of κ immunoglobulin enhancer-binding protein NF-κB by a posttranslational mechanism. Cell *47*, 921–928.

Sengchanthalangsy, L.L., Datta, S., Huang, D.-B., Anderson, E., Braswell, E.H., and Ghosh, G. (1999). Characterization of the Dimer Interface of Transcription Factor NFκB p50 Homodimer. Journal of Molecular Biology *289*, 1029–1040.

Seo, S.H., Han, H.D., Noh, K.H., Kim, T.W., and Son, S.W. (2009). Chitosan hydrogel containing GMCSF and a cancer drug exerts synergistic anti-tumor effects via the induction of CD8+ T cell-mediated anti-tumor immunity. Clin. Exp. Metastasis *26*, 179–187.

Shehzad, A., and Lee, Y.S. (2013). Molecular mechanisms of curcumin action: signal transduction. Biofactors *39*, 27–36.

Shishodia, S. (2013). Molecular mechanisms of curcumin action: gene expression. Biofactors *39*, 37–55.

Shishodia, S., Amin, H.M., Lai, R., and Aggarwal, B.B. (2005). Curcumin (diferuloylmethane) inhibits constitutive NF-κB activation, induces G1/S arrest, suppresses proliferation, and induces apoptosis in mantle cell lymphoma. Biochemical Pharmacology *70*, 700–713.

Shishodia, S., Potdar, P., Gairola, C.G., and Aggarwal, B.B. (2003). Curcumin (diferuloylmethane) down-regulates cigarette smoke-induced NF-kappaB activation through inhibition of IkappaBalpha kinase in human lung epithelial cells: correlation with suppression of COX-2, MMP-9 and cyclin D1. Carcinogenesis *24*, 1269–1279.

Simmonds, R.E., and Foxwell, B.M. (2008). Signalling, inflammation and arthritis: NF-kappaB and its relevance to arthritis and inflammation. Rheumatology (Oxford) *47*, 584–590.

Simon, H.U., Haj-Yehia, A., and Levi-Schaffer, F. (2000). Role of reactive oxygen species (ROS) in apoptosis induction. Apoptosis *5*, 415–418.

Singh, H., Sen, R., Baltimore, D., and Sharp, P.A. (1986). A nuclear factor that binds to a conserved sequence motif in transcriptional control elements of immunoglobulin genes. Nature *319*, 154–158.

Singh, S., and Aggarwal, B.B. (1995). Activation of transcription factor NF-kappa B is suppressed by curcumin (diferuloylmethane) [corrected]. J. Biol. Chem. *270*, 24995–25000.

Singh, S., and Khar, A. (2006). Biological Effects of Curcumin and Its Role in Cancer Chemoprevention and Therapy. Anti-Cancer Agents in Medicinal Chemistry *6*, 259–270.

Sreedhar, B., Chattopadhyay, D.K., Karunakar, M.S.H., and Sastry, A.R.K. (2006). Thermal and surface characterization of plasticized starch polyvinyl alcohol blends crosslinked with epichlorohydrin. Journal of Applied Polymer Science *101*, 25–34.

Srimal, R.C., and Dhawan, B.N. (1973). Pharmacology of diferuloyl methane (curcumin), a non-steroidal anti-inflammatory agent*. Journal of Pharmacy and Pharmacology *25*, 447–452.

Srivastava, R., Dikshit, M., Srimal, R.C., and Dhawan, B.N. (1985). Anti-thrombotic effect of curcumin. Thrombosis Research *40*, 413–417.

Srivastava, R.K., Chen, Q., Siddiqui, I., Sarva, K., and Shankar, S. (2007). Linkage of curcumin-induced cell cycle arrest and apoptosis by cyclin-dependent kinase inhibitor p21(/WAF1/CIP1). Cell Cycle *6*, 2953–2961.

Surh, Y.-J., Chun, K.-S., Cha, H.-H., Han, S.S., Keum, Y.-S., Park, K.-K., and Lee, S.S. (2001). Molecular mechanisms underlying chemopreventive activities of anti-inflammatory phytochemicals: down-regulation of COX-2 and iNOS through suppression of NF-κB activation. Mutation Research/Fundamental and Molecular Mechanisms of Mutagenesis *480-481*, 243–268.

Tak, P.P., and Firestein, G.S. (2001). NF-κB: a key role in inflammatory diseases. Journal of Clinical Investigation *107*, 7–11.

Tam, W.F., Wang, W., and Sen, R. (2001). Cell-Specific Association and Shuttling of I B Provides a Mechanism for Nuclear NF- B in B Lymphocytes. Molecular and Cellular Biology *21*, 4837–4846.

Thayyullathil, F., Chathoth, S., Hago, A., Patel, M., and Galadari, S. (2008). Rapid reactive oxygen species (ROS) generation induced by curcumin leads to caspase-dependent and -independent apoptosis in L929 cells. Free Radical Biology and Medicine *45*, 1403–1412.

Thomasset, S.C., Berry, D.P., Garcea, G., Marczylo, T., Steward, W.P., and Gescher, A.J. (2007). Dietary polyphenolic phytochemicals—promising cancer chemopreventive agents in humans- A review of their clinical properties. International Journal of Cancer *120*, 451–458.

Traenckner, E.B., Pahl, H.L., Henkel, T., Schmidt, K.N., Wilk, S., and Baeuerle, P.A. (1995). Phosphorylation of human I kappa B-alpha on serines 32 and 36 controls I kappa B-alpha proteolysis and NF-kappa B activation in response to diverse stimuli. EMBO J. *14*, 2876–2883.

Trinh, D.V., Zhu, N., Farhang, G., Kim, B.J., and Huxford, T. (2008). The Nuclear IκB Protein IκBζ Specifically Binds NF-κB p50 Homodimers and Forms a Ternary Complex on κB DNA. Journal of Molecular Biology *379*, 122–135.

Van Antwerp, D.J., Martin, S.J., Kafri, T., Green, D.R., and Verma, I.M. (1996). Suppression of TNF-alpha-induced apoptosis by NF-kappaB. Science *274*, 787–789.

Van de Manakker, F., van der Pot, M., Vermonden, T., van Nostrum, C.F., and Hennink, W.E. (2008). Self-Assembling Hydrogels Based on β-Cyclodextrin/Cholesterol Inclusion Complexes. Macromolecules *41*, 1766–1773.

Van Dijk, M., Rijkers, D.T.S., Liskamp, R.M.J., van Nostrum, C.F., and Hennink, W.E. (2009). Synthesis and applications of biomedical and pharmaceutical polymers via click chemistry methodologies. Bioconjug. Chem. *20*, 2001–2016.

Van Tomme, S.R., Storm, G., and Hennink, W.E. (2008). In situ gelling hydrogels for pharmaceutical and biomedical applications. Int J Pharm *355*, 1–18.

Vermonden, T., Censi, R., and Hennink, W.E. (2012). Hydrogels for Protein Delivery. Chemical Reviews *112*, 2853–2888.

Vinogradov, S.V., Bronich, T.K., and Kabanov, A.V. (2002). Nanosized cationic hydrogels for drug delivery: preparation, properties and interactions with cells. Adv. Drug Deliv. Rev. *54*, 135–147.

Wang, C.Y., Mayo, M.W., and Baldwin, A.S., Jr (1996). TNF- and cancer therapy-induced apoptosis: potentiation by inhibition of NF-kappaB. Science *274*, 784–787.

Wang, D., Veena, M.S., Stevenson, K., Tang, C., Ho, B., Suh, J.D., Duarte, V.M., Faull, K.F., Mehta, K., Srivatsan, E.S., et al. (2008). Liposome-encapsulated curcumin suppresses growth of head and neck squamous cell carcinoma in vitro and in xenografts through the inhibition of nuclear factor kappaB by an AKT-independent pathway. Clin. Cancer Res. *14*, 6228–6236.

Wigmore, P.M., Mustafa, S., El-Beltagy, M., Lyons, L., Umka, J., and Bennett, G. (2010). Effects of 5-FU. Adv. Exp. Med. Biol. *678*, 157–164.

Wu, M., Lee, H., Bellas, R.E., Schauer, S.L., Arsura, M., Katz, D., FitzGerald, M.J., Rothstein, T.L., Sherr, D.H., and Sonenshein, G.E. (1996). Inhibition of NF-kappaB/Rel induces apoptosis of murine B cells. EMBO J. *15*, 4682–4690.

Yallapu, M.M., Gupta, B.K., Jaggi, M., and Chauhan, S.C. (2010). Fabrication of curcumin encapsulated PLGA nanoparticles for improved therapeutic effects in metastatic cancer cells. Journal of Colloid and Interface Science *351*, 19–29.

Yamamoto, Y., and Gaynor, R. (2001). Role of the NF-kB Pathway in the Pathogenesis of Human Disease States. Current Molecular Medicine *1*, 287–296.

Yin, M.J., Yamamoto, Y., and Gaynor, R.B. (1998). The anti-inflammatory agent aspirin and salicylate inhibit the activity of I (kappa) B kinase-beta. Nature *396*, 77–80.

Yoo, J.-W., Irvine, D.J., Discher, D.E., and Mitragotri, S. (2011). Bio-inspired, bioengineered and biomimetic drug delivery carriers. Nat Rev Drug Discov *10*, 521–535.

Zhou, Y., Ma, G., Shi, S., Yang, D., and Nie, J. (2011). Photopolymerized water-soluble chitosan-based hydrogel as potential use in tissue engineering. Int. J. Biol. Macromol. *48*, 408–413.

LIST OF PUBLICATIONS

1. Subhamoy Banerjee, Amaresh Kumar Sahoo, Arun Chattopadhyay, Siddhartha Sankar Ghosh (2013). Hydrogel nanocarrier encapsulated recombinant IκBα as a novel anticancer protein therapeutics. ***RSC Advances*** 2013, **3**, 14123-14131 DOI:10.1039/C3RA23181J).

2. Subhamoy Banerjee, Amaresh Kumar Sahoo, Arun Chattopadhyay, Siddhartha Sankar Ghosh (2013). Recombinant IκBα loaded curcumin nanoparticles for improved cancer therapeutics. ***Manuscript Communicated.***

3. Subhamoy Banerjee, Siddhartha Sankar Ghosh (2013). Effect of 5-Fluorouracil and curcumin nanoparticles on IκBα overexpressing glioblastoma. ***Manuscript under preparation.***

Collaborative Research Work:

4. Amaresh Kumar Sahoo, **Subhamoy Banerjee**, Siddhartha Sankar Ghosh, Arun Chattopadhyay (2013). Simultaneous RGB Emitting Au Nanoclusters in Chitosan Nanoparticles for Anticancer Gene Theranostic. Accepted in ***ACS Applied Materials & Interfaces*** (DOI: 10.1021/am4051266).

5. Vinod Kumar Yata**, Subhamoy Banerjee,** Siddhartha Sankar Ghosh (2013). Nanocarrier mediated targeted delivery of *E. coli* cytosine deaminase into cancer cells for enzyme dependent prodrug therapy. ***Advanced Science, Engineering and Medicine*** (**Accepted**).

6. Amaresh Kumar Sahoo, **Subhamoy Banerjee**, Siddhartha Sankar Ghosh, Arun Chattopadhyay (2014). Single cycle PCR based synthesis of highly fluorescent Au nanoclusters for determination of the gene expression. ***Manuscript under preparation.***

7. Sourav Majumdar, Biplob Sarmah, Debananda Gogoi, **Subhamoy Banerjee**, Siddhartha S. Ghosh, Pronobesh Chattopadhyay, Ashis K. Mukherjee (2014). Purification and characterization of a novel nontoxic extracellular fibrinolytic protease with anticoagulant property from rice beer borne Brevibacillus sp. strain FF02B. ***Manuscript under preparation.***

Conferences:

1. **Subhamoy Banerjee**, Amaresh Kumar Sahoo, Siddhartha Sankar Ghosh. pH sensitive biodegradable hydrogel nanoparticles for functional delivery of GST-tagged IκBα as therapeutic protein. World Congress on Biotechnology 04-06 May, 2012, Hyderabad, India.

2. Subhamoy Banerjee, Amaresh Kumar Sahoo, Arun Chattopadhyay, Siddhartha Sankar Ghosh. "Hydrogel Nanoparticle mediated functional delivery of recombinant IκBα protein for cancer therapy". Accepted in FICS, 03-04 December, 2012, IIT Guwahati, India.

Workshops attended:

1. Workshop 6th-7th November, 2012 "Analysis of Biological Networks", IIT Guwahati, India.

2. Workshop 20th-22nd March, 2013 "Science & communication workshop" held by DBT-Wellcome trust alliance, Hyderabad, India.